CRANFIELD UNIVERSITY

YIFEI LIU

OPTIMUM DESIGN OF A COMPOSITE OUTER WING SUBJECT TO STIFFNESS AND STRENGTH CONSTRAINTS

SCHOOL OF ENGINEERING
MSc by Research Thesis

MSc THESIS
Academic Year: 2010 - 2011

Supervisor: Dr. Shijun Guo
January 2011

CRANFIELD UNIVERSITY

SCHOOL OF ENGINEERING

MSc by Research Thesis

Academic Year 2010 - 2011

YIFEI LIU

Optimum Design of a Composite Outer Wing Subject to Stiffness and Strength Constraints

Supervisor: Dr. Shijun Guo

January 2011

ABSTRACT

Composite materials have been more and more used in aircraft primary structures such as wing and fuselage. The aim of this thesis is to identify an effective way to optimize composite wing structure, especially the stiffened skin panels for minimum weight subject to stiffness and strength constraints.

Many design variables (geometrical dimensions, ply angle proportion and stacking sequence) are involved in the optimum design of a composite stiffened panel. Moreover, in order to meet practical design, manufacturability and maintainability requirements should be taken into account as well, which makes the optimum design problem more complicated.

In this thesis, the research work consists of three steps:

Firstly, attention is paid to metallic stiffened panels. Based on the study of Emero's optimum design method and buckling analysis, a VB program IPO, which employs closed form equations to obtain buckling load, is developed to facilitate the optimization process. The IPO extends the application of Emero's method to an optimum solution based on user defined panel dimensional range to satisfy practical design constraints.

Secondly, the optimum design of a composite stiffened panel is studied. Based on the research of laminate layup effects on buckling load and case study of bucking analysis methods, a practical laminate database (PLDB) concept is presented, upon which the optimum design procedure is established. By employing the PLDB, laminate equivalent modulus and closed form equations, a VB program CPO is developed to achieve the optimum design of a composite stiffened panel. A multi-level and step-length-adjustable optimization strategy is applied in CPO, which makes the optimization process efficient and effective.

Lastly, a composite outer wing box, which is related to the author's GDP work, is optimized by CPO. Both theoretical and practical optimum solutions are obtained and the results are validated by FE analysis.

Keywords:

Stiffened panel, Buckling, Compressive load, Optimization

ACKNOWLEDGEMENTS

I would like to express my sincere appreciation to my supervisor Dr. Shijun Guo for his thoughtful suggestions and guidance throughout the research project.

I would also like to give my gratitude to my company, Aviation Industry Corporation of China (AVIC) and the First Aircraft Institute (FAI) of AVIC, who have provided the opportunity and sponsored me to study at Cranfield University.

Lastly, I am grateful to my wife and my parents for their understanding and entirely support during the period of my research. I dedicate this work to them.

TABLE OF CONTENTS

LIST OF FIGURES

LIST OF TABLES

LIST OF EQUATIONS

NOTATIONS

Symbols

$[\bar{Q}]$	Ply stiffness matrix
[A]	Laminate in-plane stiffness matrix
[B]	Laminate in-plane-out-of-plane coupling stiffness matrix
[D]	Laminate out-of-plane bending stiffness matrix
A_{sk}	Skin cross section area
A_{st}	Stringer cross section area
b, B	Panel width
b_a	Stringer lower flange width
b_f	Stringer upper flange width
b_s	Stringer pitch
b_w	Stringer height
E	Modulus of elasticity
E_1	Young's Modulus, Longitude Direction
E_2	Young's Modulus, Transverse Direction
E_t	Tangent modulus of elasticity
E_x,E_y,G_{xy}	Laminate equivalent elastic modulus
F_{cc}	Crippling stress
F_{cr}	Johnson-Euler overall buckling stress
F_{cy}	Compression yield stress
G_{12}	Shear Modulus
G_{xy}^{sw}	Stringer web equivalent shear modulus
K	Non dimensional local buckling coefficient that depend on conditions of edge restraint and shape of plate
K_s	Column shape factor
k_x, k_y, k_{xy}	Laminate curvatures caused by bending moment
L	Panel length
M_x, M_y, M_{xy}	Bending moment applied on laminate
N_x	Axial distributed load
N_x, N_y, N_{xy}	Force applied on laminate

P_e	Euler column buckling load
S	Shear Strength
t	Plate thickness
T	Torque
t_a	Stringer lower flange thickness
t_{av}	Average panel thickness which has the same cross-section area as the skin-stringer panel
t_f	Stringer upper flange thickness
t_s	Skin thickness
t_w	Stringer web thickness
XC	Longitudinal Compressive strength
XT	Longitudinal Tensile Strength
YC	Transverse Compressive Strength
YT	Transverse Tensile Strength
Z_k	Distances from the reference plane to the k^{th} ply
α, β, γ	Non dimensional coefficients
β_g	Non dimensional factor related to stringer section
γ_{xy}	Shear strain
ε_x, ε_y	Normal strain in x, y direction
η_L	Plastic correction
λ	Eigenvalue
μ	Poisson's ratio
ρ	Radius of gyration
σ_b	Allowable proof stress
σ_{cr}	Critical overall buckling stress
σ_{crL}	Critical local buckling stress
σ_s	Allowable shear stress
σ_x , σ_y	Normal stress in x, y direction
τ_{xy}	Shear stress

Acronyms

BC	Boundary Condition
CF	Closed Form
F.I.	Failure Index
FE	Finite Element
FEA	Finite Element Analysis
FEM	Finite Element Method
FSM	Finite Strip Method
GA	Genetic Algorithm
MDO	Multidisciplinary Design Optimization
MP	Mathematical Programming
RF	Reserve Factor

1 Introduction

1.1 Background

China's commercial aircraft transport market is growing at a high rate in recent years. There is a three-year cooperative program between Cranfield University and Aviation Industry Corporation of China (AVIC). Part of the training program is to design a new generation 130-seat airliner called Flying Crane. It mainly focuses on China's domestic market. The design targets of Flying Crane are [1]: more comfortable, more economical and environmental friendly. From 2008 to 2010, the conceptual, preliminary, and detail design of Flying Crane are performed by a group of students from AVIC each year consequently. As a member of the third cohort from AVIC, the author's MSc research work at Cranfield University consists of two phases. Firstly, the author worked as a structure designer in the Group Design Project (GDP) to carry out Flying Crane central and inner wing detail design. Then the second phase is Individual Research Project (IRP) which aims to obtain the optimum design of a composite wing box subject to stiffness and strength constraints. The GDP work will be the background of IRP study.

The application of advanced composite materials in aviation industry has been significantly increasing over the past decades. The development work with composite materials started in the mid of 1960s [2]. At the beginning, the applications of composite materials in aircraft design were only in secondary structures, for example rudder and ailerons. However, with the development of design research and manufacture technology, advanced composite materials have been more and more used as heavily loaded primary structures such as wing, fuselage and empennage component. Especially, the composite wing box is becoming a hot research interest. The newest generation airliners Airbus A350 and Boeing 787 are the outstanding representatives where composite materials play a major role in the wing box design. Compared to conventional isotropic metal materials such as steel, aluminum, and titanium, composite materials have the remarkable advantages as listed below:

- High strength-to-weight ratio
- Good fatigue and corrosion resistance
- Fiber orientation can be designed to meet different requirement
- Reduce machining process

As a next generation airliner, composite materials are employed in the wing box structure design for Flying Crane. The design philosophy of the wing box is a combination of strength, stiffness, weight, cost, reliability and maintainability. According to analysis in GDP, the wing box initial design satisfies all the strength and stiffness requirements, namely the maximum strain remains below 3500 micro strains, the maximum laminate failure index (F.I.) is less than 1.0, and the buckling reserve factors (RF) are greater than 1.0. However, it also indicates that the initial design is a bit conservative, which can be further optimized to obtain higher structure efficiency.

Modern aircraft wings are thin walled structures. The application of stiffened panels is a notable characteristic in wing box design for their high structural efficiency. The load carried by the upper skin of wing is mainly compressive load, thus one major issue should be considered in the design of an upper skin panel is buckling stability.

Many design variables are involved in the optimum design of a composite stiffened panel, such as geometrical dimensions, laminate layup ply angle proportion, and ply stacking sequence. Additionally, in order to achieve a practical design, some design requirements related to manufacturability and maintainability are also to be considered, which makes the optimum design problem more difficult. Thus it is meaningful work to find an effective way to obtain the optimum design of a stiffened panel under buckling and strength constraints.

1.2 Design Aim and Objectives

The aim of this thesis is to identify an effective way to optimize composite wing structure, especially the stiffened skin panels for minimum weight subject to

stiffness and strength constraints. The approach will be a mixture of analytical and numerical methods by using in-house developed codes and commercial programs such as NASTRAN.

In order to achieve this aim, the research work is divided into three stages with objectives listed below:

Firstly, isotropic stiffened panels are selected as the starting point. Optimum design methods will be studied and an effective optimization procedure should be established. Additionally, a computer program should be developed to facilitate the optimum design process.

In the second stage, analytical and numerical research work will be performed to find out whether the optimization procedure for isotropic stiffened panels is capable to solve composite panel problems. Then identify an effective and efficient way to achieve the optimum design of a composite stiffened panel, some computer programs are to be developed.

Lastly, apply the developed procedure (or programs) to the initial design of the author's GDP outer wing box to obtain the optimum design, and then validate the results by FE analysis.

2 Literature Review

2.1 Optimum Design of Isotropic Stiffened Panels

Timoshenko [3] established the elastic bending theory for the analysis of isotropic plates in 1850. This theory is regarded as the foundation of the stress, deformation and buckling analysis for both isotropic and laminated thin plates.

Gerard and Becker [4-6] studied the stability of flat and curved plates, a comprehensive review of the local buckling of stiffener sections and the buckling of plates with stiffeners was given. The instability of stiffened curved plates and general instability of stiffened cylinders were discussed, and numerical values of buckling coefficients for longitudinally compressed stiffener sections of various shapes under compression and shear condition were given in charts and tables.

Many researchers performed study work on the buckling of different stringer section stiffened panels. For example, Rothwell [7] gave the coupled modes in buckling panels with Z-section stringers in compression, and addressed that the buckling stress decreased with the reduction of the flange, which indicated an effect of torsion buckling mode; Boughan and Baab [8] studied the critical local buckling compressive stress of T-section panels and summarized them in charts for calculation; and Catchpole [9] presented the optimum design method for compressive panels with integrated blade stiffeners.

Wittrick [10] presented a general method for the determination of initial buckling of stiffened panels. The deformation of the panel was considered sinusoidal in the spanwise direction.

Emero and Spunt [11] conducted a study of the optimization of stiffened panels based on the assumption that the panel behaved as a column between ribs. The effect of spar support at the unloaded edges of the column was ignored. Based on Euler general stability expression, a total of 23 optimized panel

concepts were presented with appropriate design charts and formulas for desired structural efficiency.

By taking wing flutter and fuselage pressurization requirements into consideration, Niu [12] presented a practical design guideline for stiffened panel preliminary sizing, and the advised ratios of panel geometrical dimensions were listed in a table to facilitate the optimum design.

2.2 Optimum Design of Composite Stiffened Panels

With the development of research and technology, composite materials have played an important role in the structure design of both commercial and military aircrafts. Compared to metallic panels, composite stiffened panels have more variables, such as ply thickness, ply orientations and stacking sequences. Due to these aspects, the optimization of composite panels is more complicated.

Optimum design methods for composites have been investigated ranging from simple plates to stiffened panels. Early in the 1970s, some optimization work on homogeneous and orthotropic property laminated composites were performed by Schmit and Farshi [13-14], who considered the ply thicknesses as continuous variables, and regarded the optimization a sequence of linear problems.

Based on orthotropic plate theory, Nemeth [15-16] carried out some parametric studies and produced generic buckling design charts in terms of useful non dimensional parameters for non-stiffened composite panels subjected to compression and shear loads.

Agarwal and Davis [17] studied hat stiffened composite panels under compression, and presented a nonlinear mathematical method to obtain the minimum weight. They chose a simplified maximum strain criterion as strength limitations, and local buckling was described by orthotropic plate theory, while overall buckling was using wide-column theory.

Grosset et al [18] proposed a new evolutionary algorithm for composite laminate optimization, named Double Distribution Optimization Algorithm (DDOA). They

demonstrated the efficiency of this method on two laminate optimization problems of which the design variables were the fibre angles or the laminate stacking parameters.

Liu et al [19] carried out a two-level method to optimize a composite panel. At global wing level, continuous optimization of 0, 45,-45 and 90 ply thicknesses was performed to achieve weight minimization subject to strain and buckling constraints. Based on the obtained laminate thickness, a response surface was applied at local panel level to search for the optimum stacking sequences to maximize the critical buckling load.

Due to practical manufacturing considerations, laminated composite panels are usually restricted to symmetric or balanced laminates with ply orientations of 0, 90, 45 and -45 degrees [20]. Some research work has been carried out by Liu and Bulter [21] to get the optimum design of composite wing stiffened panels under manufacturing constraints. They employed a bi-level method. At panel level, the cross sectional panel dimensions were optimized. Then at laminate level, the optimum design of stacking sequence of plies was performed by using Genetic Algorithm (GA). Similarly, a bi-level composite optimization procedure was investigated by Liu et al [22], and two approaches were examined for seeking the best stacking sequence of laminated composite wing structures with blending and manufacturing constraints.

2.3 Optimum Design of a Wing box

The optimum design of a wing box is more complicated than that of a stiffened panel because more design requirements need to be considered.

Emero and Spunt [23] presented a method for determining the optimum proportions of a minimum weight multi-rib or multi-web wing box structure subject to vertical shear and unidirectional bending moment. Based on general weight equations, optimum rib (or web) placement and weight minimization expressions were given. Total 23 optimized wide column and compression

panel cover concepts were provided, from which analytical means for determining the optimum design of wing box structure could be achieved.

Seresta et al [24] decomposed the wing box design problem into several independent local panel design problems, and then imposed the blending constraints globally by using a guide based design methodology within the genetic algorithm. The guide was a basic template laminate stacking sequence which was applicable to all the designated panels. Thus a certain number of contiguous plies were kept to represent a particular panel which ensures complete blending.

Butler [25] used VICONOPT to find the optimum designs of a selection of wing panels of various rib pitch, stiffener spacing and stiffener type which were subject to a range of practical loadings and were constrained with buckling and material strength. This parametric study presented optimum design plots to direct the designer's choice of stiffener shape, rib pitch and stiffener spacing with a good approximation of panel mass. But laminate design rules and manufacturing constraints were not considered.

Schuhmacher et al [26] successfully applied the technique of multidisciplinary design optimization (MDO) in sizing Fairchild Dornier regional jet wing boxes. Over 800,000 constraints were applied under all loading conditions to meet the requirements of structural strength, aero elastic behaviour and manufacturing.

2.4 Current Optimization Methods

2.4.1 Multidisciplinary Design Optimization

Aircraft design is governed by more than one discipline such as aerodynamics, structure, strength, control etc, thus Multidisciplinary Design Optimization (MDO) is an ideal candidate for dealing with such complicated problems. In MDO, each disciplinary objective is treated as an independent objective function on an optimizer to obtain knowledge in the design space directly.

A brief development and future trends in MDO was reviewed by Weck et al [27]. In the report, a wing MDO example at Cranfield University was highlighted. In the optimization process, a VIVACE geometry generator was developed to build the parametric wing geometry automatically, and then it was integrated into a wing MDO workflow to obtain optimum design results.

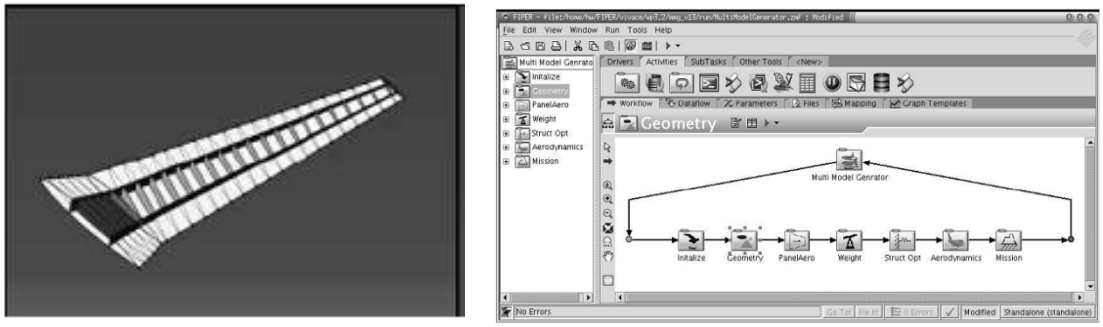

Figure 2-1 Wing MDO at Cranfield University [27]

Many published cases have proved that MDO is an effective way to solve wing box optimization problems. For example, Rajagopal et al [28] optimized a UAV wing box based on the methods of Multi-Objective Genetic Algorithm and MDO; Chiba et al [29] applied MDO method on a design of transonic regional jet wing; and as mentioned before, Schuhmacher et al [26] applied MDO in sizing Fairchild Dornier regional jet wing boxes successfully.

2.4.2 Gradient Methods

Gradient methods are first order optimization algorithms. According to different iterative functions, the gradient methods can be subdivided into natural gradient descent algorithm, steepest descent algorithm, conjugate gradient algorithm and so on [30-31].

The steepest descent algorithm is the simplest to implement, but the slowest to converge; the natural gradient descent algorithm provides improved convergence speed; while conjugate gradient algorithm is a powerful method, which has fast convergence rate and is easy to implement.

The gradient methods are efficient to solve the optimization problems with continuous design variables, however when the design variables fall into discrete problems, genetic algorithm (GA) is more effective.

2.4.3 Genetic Algorithm Optimization

The genetic algorithm (GA) is a “search heuristic that mimics the process of natural evolution. This heuristic is routinely used to generate useful solutions to optimization and search problems”. [32] GA is suitable to deal with the discrete layup optimization problems in composite material structures, due to their ability to simultaneously search from numerous points in the design space.

Nagendra et al [33] employed genetic algorithms to solve the integer stacking sequence problem, and investigated the application of GA method on the blade-stiffened composite panel optimization design.

Adams et al [34] performed a guide based GA to deal with the laminate layup blending problem. A basic laminate stacking sequence which is applicable to all the panels was used as design layup, then individual local panel layup optimization was carried out from the top or bottom of the guide GA based on the assumption that loads on individual panels were constant during the design process. By using this method, 100% blending could be achieved.

Herencia et al [20] applied a two step procedure to optimize long anisotropic laminated composite panels with T-section stiffeners. At the first step, optimization was carried out on parameterized skin and a super stiffener by using mathematical programming (MP) techniques subjected to strength, buckling as well as practical design rules to obtain the minimum weight, and then the composite layup was determined in the second level by using a GA code to optimize the values of lamination parameters coming from the top level, considering ply contiguity.

2.4.4 Commercial Software Optimization

The development of high performance computers makes it convenient to run large finite element analysis and optimization problems. Many kinds of commercial software, for example, MSC.NASTRAN, Hyper Sizer, PASCO, PANDA2, VICONOPT and Hyper Works, have provided modules for composite optimization. These programs provide friendly interface to facilitate the users to define design variables, design targets and constraint parameters, then the optimum design process will be performed automatically.

At a higher level, some framework programs, such as ISIGHT and FIPER, can integrate different kinds of commercial software discussed above into one work flow, thus it will combine the advantages of different commercial software together to solve a complicated optimum design problem.

3 Optimum Design of Isotropic Stiffened Panels

3.1 Buckling Modes of Stiffened Panels

The buckling modes of stiffened panels can be separated into two distinct classes: local buckling and overall buckling.

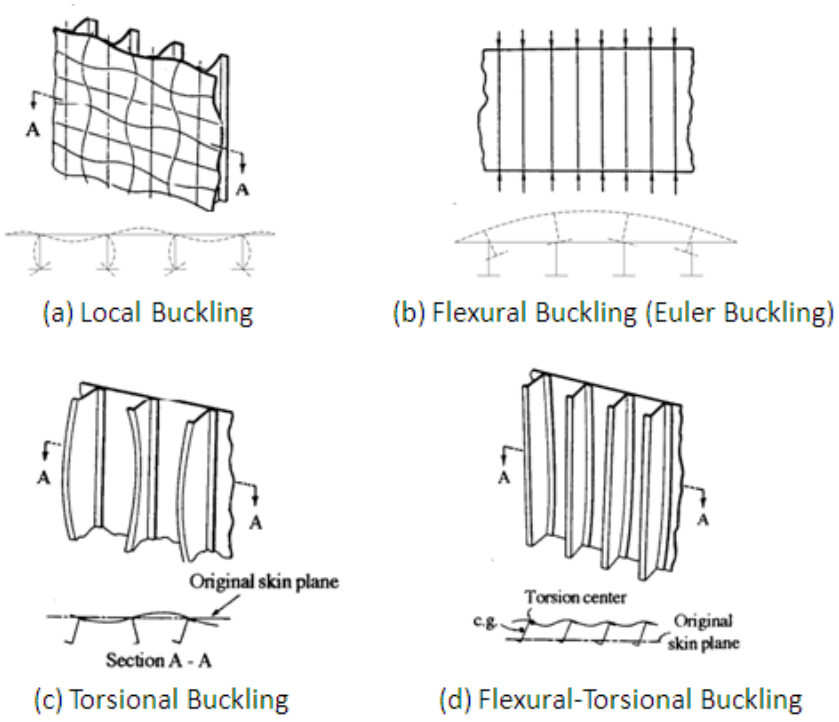

Figure 3-1 Stiffened panel buckling modes [12]

(1) Local Buckling

In local buckling, the buckling half wavelength is comparable with the stringer cross-sectional dimensions or pitch, and may include some degree of stringer torsion [35]. The rotation occurs at the junction of the stringer webs with the sheet. In the case of thin walled stringers, the cross section of the stringers will also distort. See Figure 3-1(a).

(2) Overall Buckling

Buckling modes whose half wavelength is comparable with the frame spacing or rib spacing are usually called overall buckling [35], and it has two extreme forms.

The more common of these is flexural buckling or called Euler buckling, in which the panel translates normal to the original plane of the sheet and no rotation occurs, see Figure 3-1(b). The other is torsional buckling, in which rotation occurs about axes in the sheet at, or close to, the junctions of the stringer webs with the sheet, see Figure 3-1(c). Since the wavelengths of these two forms are similar, a combined mode termed flexural-torsional buckling generally occurs. In this general mode rotation takes place about a series of axes in the plane of the sheet which are away from the stringer web to sheet junctions, see Figure 3-1(d).

3.2 Isotropic Panel Sizing Methods

3.2.1 Emero's Method

3.2.1.1 Introduction of Emero's Method

Emero and Spunt [11] conducted a study of the optimization of stiffened panels subject to a given axial load over a given panel length. They regarded the panel behaved as a column between ribs, and ignored the effect of spar support at the unloaded edges of the column. The principle to obtain the optimum design is that the panel's local and overall buckling modes occur simultaneously, and the optimum panel geometry parameters are derived from Euler general stability expression.

The overall buckling stress of a stiffened panel is:

$$\sigma_{cr} = \frac{N_x}{t_{av}} = \frac{\pi^2 E_t}{\left(L/\rho\right)^2} \qquad \textbf{Equation 3-1}$$

Where,

σ_{cr} = Overall buckling stress (MPa)

N_x = Axial distributed load (N/mm)

t_{av} = Average panel thickness which has the same cross-section area as the

skin-stringer panel (mm)

E = Modulus of elasticity (MPa)

E_t = Tangent modulus of elasticity, E_t=E when in elastic range (MPa)

L = Panel length (mm)

ρ = Radius of gyration

The expression for predicting the local buckling stress is:

$$\sigma_{crL} = \frac{K\pi^2\eta_L E}{12(1-\mu^2)}\left(\frac{t}{b}\right)^2 \qquad \textbf{Equation 3-2}$$

Where,

σ_{crL}= Local buckling stress (MPa)

K = Non dimensional local buckling coefficient that depend on conditions of edge restraint and shape of plate

η_L = Plastic correction

μ = Material Poisson's ratio

t = Plate thickness (mm)

b = Plate width (mm)

Introduce a new factor Ks, which is called a column shape factor,

$$K_s = \frac{\rho}{t_{av}}\left(\frac{t}{b}\right) \qquad \textbf{Equation 3-3}$$

Letting $\sigma_{cr} = \sigma_{crL}$, the above equations can be transformed into the following fomation:

$$\frac{N_x}{L} = \frac{\pi^2}{\sqrt{12(1-\mu^2)}} K_s K^{0.5} (\eta_L E E_t)^{0.5} \left(\frac{t_{av}}{L}\right)^2 \qquad \textbf{Equation 3-4}$$

Equation 3-4 indicates that the highest stress is attained when the multiply result of the local buckling coefficient K and the shape factor Ks for a particular structural concept is a maximum. Letting

$$\frac{N_x}{L} = \frac{\pi^2}{\sqrt{12(1-\mu^2)}} K_s K^{0.5} (\eta_L E E_t)^{0.5} \left(\frac{t_{av}}{L}\right)^2 \qquad \textbf{Equation 3-5}$$

And $$\epsilon = \frac{\pi^2}{\sqrt{12(1-\mu^2)}} K_s K^{0.5} \qquad \textbf{Equation 3-6}$$

Equation 3-4 becomes:

$$\frac{N_x}{L\bar{\eta}E} = \epsilon \left(\frac{t_{av}}{L}\right)^2 \qquad \textbf{Equation 3-7}$$

In this general form, various cross sections can be compared for structural efficiency by inspection of their relative efficiency factors ϵ.

A table of 23 optimized panel concepts is presented in Emero's paper with appropriate design charts and formulations for structural efficiency. In order to develop a general equation to present Ks for different panel cross sections, three non dimensional coefficients α, β and γ are introduced, which can be calculated by configuration ratios of panel's geometrical dimensions.

$$Ks = \frac{(\alpha\gamma - \beta^2)^{0.5}}{\alpha^2} \qquad \textbf{Equation 3-8}$$

3.2.1.2 Study of Emero's Method

Integral blade stiffened panels are widely used in aircraft design for their good manufacturing characteristics. In this thesis, this panel configuration is selected as a representative to demonstrate the optimum design study. The geometrical dimensional design variables of a blade stiffened panel are shown in Figure 3-2.

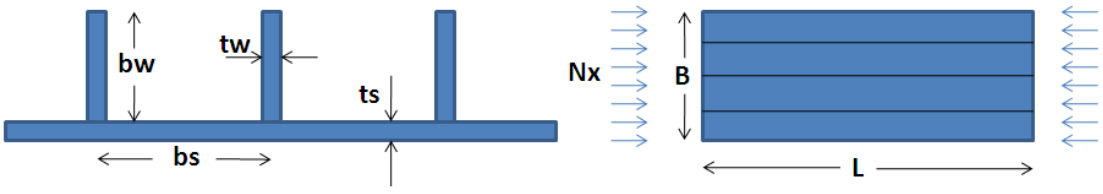

Figure 3-2 Blade stiffened panel geometrical variables

According to Emero's paper, the highest efficiency of a blade stiffened panel is 0.656. In order to achieve this efficiency, a set of equations and dimension ratios are directly provided by Emero to facilitate the optimum design. These optimum expressions are listed in Table 3-1.

Table 3-1 Optimum expressions for blade stiffened panels [11]

Optimum Values	Non Dimensional Geometry Expressions
$\in_{max}$=0.656	α=1+Rbw×Rtw
Rbw=bw/bs=0.65	β=0.5×Rbw^2×Rtw
Rtw=tw/ts=2.25	γ=0.333×Rbw^3×Rtw

Based on Emero's equations, an EXCEL spreadsheet is developed by the author to optimize a metallic blade stiffened panel. A case study is performed to obtain the optimum design of a blade stiffened panel under different compressive load. The length of the panel is 600 mm, and the width is 1200 mm. The axial distributed load applied on this panel varies from 2000 N/mm to 100 N/mm. The material of the panel is aluminium alloy 7050-T7451, and the properties are listed below:

E=72000 MPa (Young's Modulus)
Fcy=400 MPa (Compression Yield Stress)
μ=0.3 (Poisson's Ratio)

The optimum design results are presented in Table 3-2. The change of skin thickness and stringer pitch under different compressive load is plotted in Figure 3-3, and the movement of stringer height and stringer thickness under different compressive load is illustrated in Figure 3-4.

Table 3-2 Emero's optimization results under different loads

Nx (N/mm)	ts (mm)	bs (mm)	bw (mm)	tw (mm)	t-av (mm)	σ_{cr} (MPa)	A_{st}/A_{sk}
2000	2.05	65.89	42.83	4.61	5.04	396.79	1.46
1900	2.00	65.05	42.28	4.49	4.91	386.74	1.46
1800	1.94	64.18	41.71	4.37	4.78	376.42	1.46
1700	1.89	63.27	41.12	4.25	4.65	365.82	1.46
1600	1.83	62.31	40.50	4.12	4.51	354.90	1.46
1500	1.77	61.32	39.86	3.99	4.37	343.63	1.46
1400	1.71	60.27	39.17	3.85	4.22	331.98	1.46
1300	1.65	59.16	38.46	3.71	4.06	319.90	1.46
1200	1.59	57.99	37.69	3.57	3.90	307.35	1.46
1100	1.52	56.74	36.88	3.42	3.74	294.26	1.46
1000	1.45	55.41	36.01	3.26	3.56	280.57	1.46
900	1.37	53.97	35.08	3.09	3.38	266.17	1.46
800	1.29	52.40	34.06	2.91	3.19	250.95	1.46
700	1.21	50.68	32.94	2.72	2.98	234.74	1.46
600	1.12	48.76	31.70	2.52	2.76	217.33	1.46
500	1.02	46.59	30.28	2.30	2.52	198.39	1.46
400	0.92	44.06	28.64	2.06	2.25	177.45	1.46
300	0.79	41.01	26.65	1.78	1.95	153.67	1.46
200	0.65	37.05	24.08	1.46	1.59	125.47	1.46
100	0.46	31.16	20.25	1.03	1.13	88.72	1.46

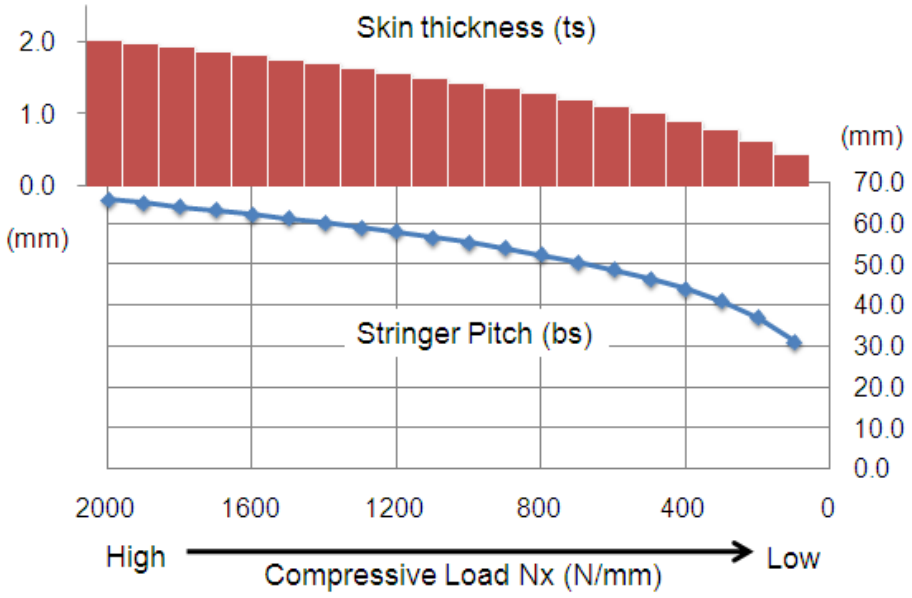

Figure 3-3 Skin thickness-stinger pitch vs. axial load

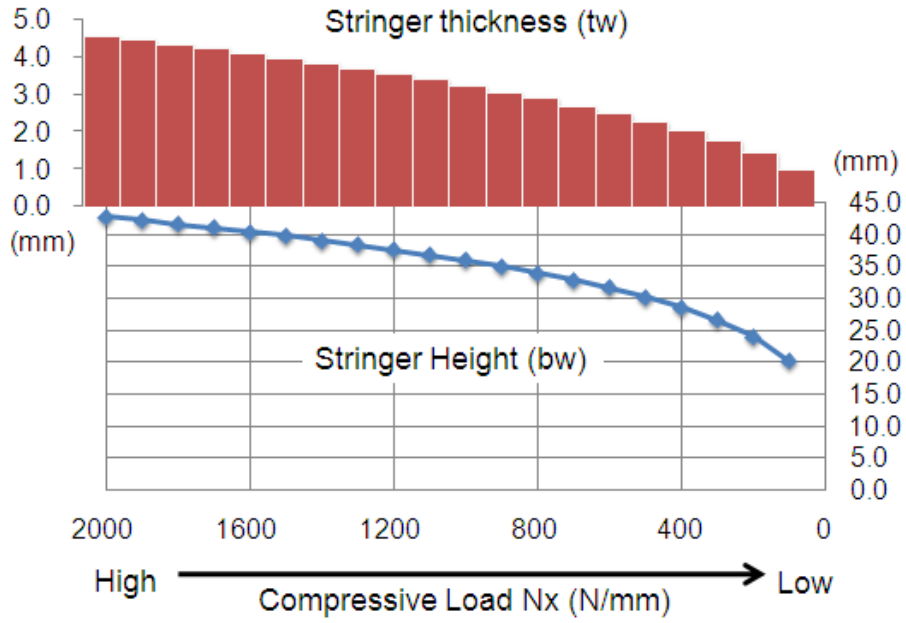

Figure 3-4 Stringer height-stringer thickness vs. axial load

The optimum design results show that for a stiffened panel with a given length, with the reduction of the applied compressive load, all the optimum geometrical dimensions (bs, ts, bw and tw) decrease gradually, which means that if the length of the panel is fixed, thin skin and close stringer configuration is good for achieving high efficiency when the load is at low level, while when the load is high, thick skin and large stringer pitch configuration is better.

This trend is reasonable because when the load is low, thin skin is abundant to carry the load. But thin skin may easily fall into local buckling or overall buckling, thus close stringer layout is needed to enhance skin's stability, and vice versa.

As a common sense, the panel's efficiency can be defined as the load carrying ability of per unit volume (or weight):

Efficiency = Load (N) / Panel Volume (mm^3)

By substitution,

Efficiency = Load (N) / {Cross Section Area (mm^2) ×Panel Length (mm)}

= Stress (N/mm^2) / Panel Length (mm)

The panel's length doesn't change in this case study, thus high critical buckling stress is equivalent to high efficiency. This statement is understandable

because when a panel reaches a high stress level, it means that it uses the material to a sufficient extent.

From the “stress” point of view, an interesting discussion needs to be proposed here. From Table 3-2 we can see that, when the applied load is 2000 N/mm, the panel’s critical buckling stress is 396.78 MPa; while the load reduces to 100 N/mm, the panel’s critical buckling stress drops to 88.724 MPa. It seems like that high compressive load may help the optimum design to achieve a high efficiency, or we can say that when sizing a panel with a fixed length, the optimum design obtained under low axial load is not as efficient as that achieved under high axial load.

The reason for this situation is that the length of the panel is fixed (In this case study, L=600 mm). When the compressive load is at low level, a small cross section area (thin skin and thin stringer) can be used in the optimum design, but this cross section area cannot be smaller than some certain value, in order to ensure that the panel will not fall into overall buckling at the given panel length L=600mm. In other words, the buckling design requirement determines the panel’s final optimum cross section area. To make it clear, some examples are demonstrated in Table 3-3, where the panels with different lengths under the same load are optimized.

Table 3-3 Emero’s optimization results under different panel lengths

Panel Size (L×B)	Nx (N/mm)	Optimum Design Result					
		ts (mm)	bs (mm)	bw (mm)	tw (mm)	t-av (mm)	σ_{cr} (MPa)
600×1200	100	0.46	31.16	20.25	1.03	1.13	88.72
300×1200	100	0.32	18.53	12.04	0.73	0.80	125.47
200×1200	100	0.26	13.67	8.88	0.59	0.65	153.67

From Table 3-3 we can see that when the panel’s length becomes shorter, the optimum design will achieve a higher critical buckling stress (higher efficiency).

Then another question arising here is: In Figure 3-5, which is the best design for a 600×1200 mm panel subject to 100 N/mm compressive loads?

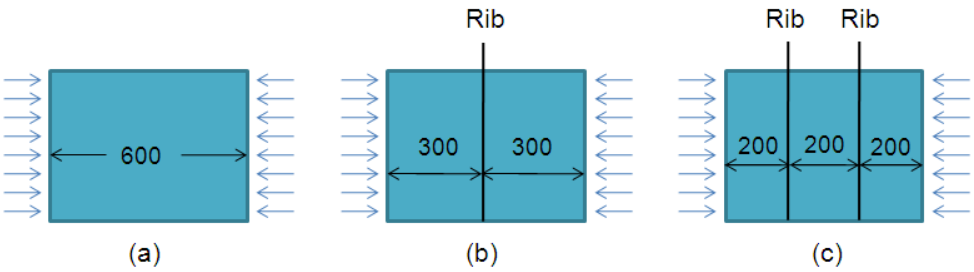

Figure 3-5 Optimum design options

The comparison of these three options is listed below:

Table 3-4 Comparison of design options

		(a)	(b)		(c)		
Emero's Optimum Design	ts(mm)	0.46	0.32	0.32	0.26	0.26	0.26
	bs(mm)	31.16	18.53	18.53	13.67	13.67	13.67
	bw(mm)	20.25	12.04	12.04	8.88	8.88	8.88
	tw(mm)	1.03	0.73	0.73	0.59	0.59	0.59
Total Volume(mm^3)*		813600	576000		468000		
Critical Stress(MPa)		88.72	125.47		153.67		
* Only the panels' volume, ribs' volume NOT included							

From Table 3-4 we can see that, by introducing some ribs into the design, one panel can be divided into several sections along its length, the optimum design of each small panel may achieve a higher buckling stress than the original one piece panel, which will help the panel to achieve a higher efficiency and obtain some weight saving. However, the panel's efficiency improvement is realised at the cost in taking additional rib's weight into design. Thus from a local point of view (only panel), Option C is definitely a better design than A and B, but from a global perspective (panel and ribs), whether Option C is still the best design needs to be further studied.

3.2.1.3 Limitations of Emero's Method

With Emero's equations, the optimum design of an isotropic stiffened panel can be easily achieved. However, there are some limitations in this method.

Firstly, when using Emero's method to optimize a panel, three parameters should be obtained in advance: the efficiency, Rbw (Rbw=bw/bs) and Rtw (Rtw=tw/ts). However, these three parameters cannot be determined arbitrarily because they are not independent: the efficiency is dominated by Rbw and Rtw. Thus, Emero provided a set of efficiency-Rbw-Rtw charts for different stringer shape panels. Figure 3-6 is the chart for blade stiffened panel, but this chart contains only six tw/ts curves which cannot cover all the design space.

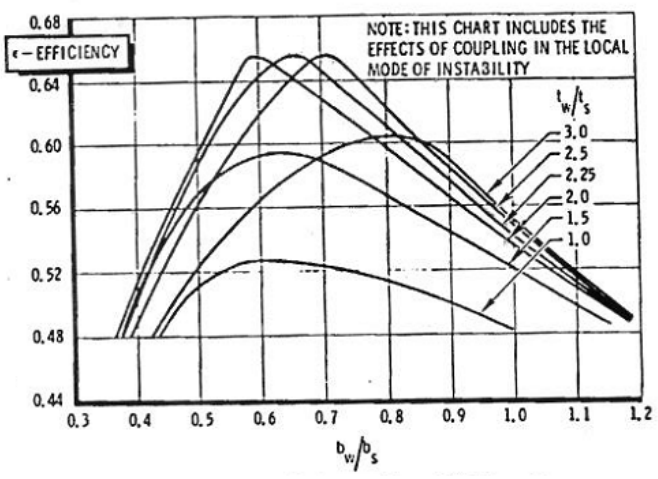

Figure 3-6 Efficiency-Rbw-Rtw curves for blade stiffened panels [11]

Secondly, from Table 3-2 we can see that the optimum stringer pitch (bs) is very small, even when the load reaches a high level of 2000N/mm, the optimum stringer pitch is only 65.89 mm. From a practical design point of view, such a small pitch is not suitable in a real wing box design for it may lead to some difficulties in manufacturing and maintenance. Generally speaking, the average upper skin stinger pitch of large commercial aircrafts is about 150-200 mm.

Thirdly, the optimum design given by Emero's method is a free sizing result from the whole design space, which does not account in any design variable boundary limits. Usually, such a theoretical optimum result cannot be directly

applied in a practical design, because some negotiations have to be made to satisfy other design requirements. For example, due to some reasons the stringer pitch has to be constrained into the range between 180 - 200 mm, but Emero's method is not able to solve this kind of problems.

Lastly, Emero employs Euler expression to predict overall buckling. Euler buckling equation is suitable for long columns; however when the panel is in short to intermediate column range, where the failure mode is dominated by the interaction between the primary flexural instability mode and local crippling mode [12], Euler equation is not accurate enough. A chart from Niu's book demonstrates this effect clearly, see Figure 3-7.

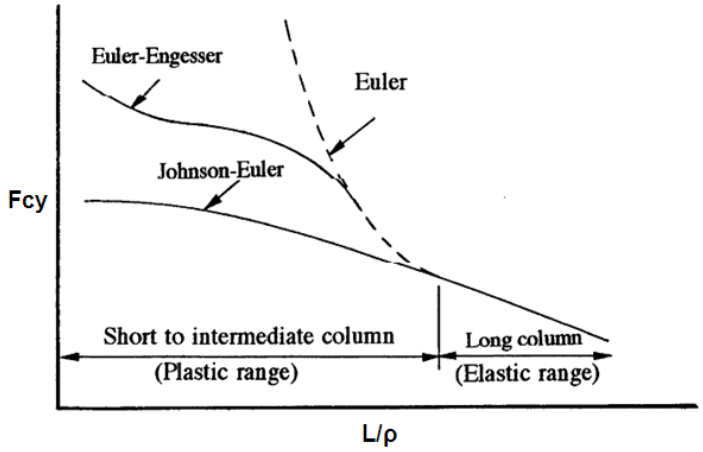

Figure 3-7 Column failure vs. slenderness ratio (L/ ρ) [12]

3.2.2 Niu's Method

Emero's method is able to obtain the highest theoretical efficiency of a stiffened panel, however in practical design, this efficiency cannot be realized. Niu exerts [12] that in practical wing box design, wing flutter requirements dictate a thicker skin than that dictated only by compression load. A stiffening ratio Ast/Ask=0.5 is recommended for practical preliminary design, and the ratio less than 0.5 should not be used for panel damage tolerance considerations. Thus in practical design, the highest efficiency can be only obtained at about 80% of Emero's theoretical efficiency.

Niu also provided a set of practical design guidelines for compressive panel sizing, which is summarized as below:

Table 3-5 Niu's practical guidelines [12]

Element	Design Practice
ba/ta	10 or less
bw/tw	18-22
bf/tf	6-8
Ast/Ask	0.5
ta	0.7ts
bf/bw	0.4

With Niu's guidelines, a more practical design can be realized. However, Niu's guidelines just provide a range of feasible solutions, among which the optimum one is not pointed out. Moreover, the result obtained from Niu's method seems to be approximate and very conservative.

3.3 Isotropic Panel Buckling Analysis

In the optimum design of a stiffened panel under compressive load, attention should be paid to buckling. Thus the methods of calculating panel's buckling loads need to be studied firstly. Based on review work, the author divides the methods into three categories, which are:

- Closed Form Equations (including empirical or semi-empirical formulas)
- Finite Strip Method (FSM)
- Finite Element Method (FEM)

3.3.1 Closed Form Equations

Substantial research work on panel buckling analysis has been performed by previous researchers. Many closed form equations have been developed from tests to predict metallic panel buckling load.

The drawbacks of Euler equation in calculating overall buckling load have been discussed in Section 3.2.1.3. Some closed form formulas have been developed

to take account of the local crippling interaction effects, among which Johnson-Euler equation is recommended by Niu to predict the short to intermediate range failure. The Johnson-Euler formula is:

$$F_{cr} = F_{cc} - \frac{{F_{cc}}^2 \left(L/\rho\right)^2}{4\pi^2 E} \qquad \textbf{Equation 3-9}$$

Where,

F_{cr} = Johnson-Euler overall buckling stress (MPa)

F_{cc} = Crippling stress (MPa)

L = Column (or panel) length (mm)

E = Elastic modulus (MPa)

ρ = Radius of gyration

A new parameter F_{cc} (crippling stress) is invloved in Johnson-Euler equation. Compressive crippling is defined as an inelasticity of the cross section of a structural member in its own plane. The maximum crippling stress of a member is a function of its cross section rather than its length. The crippling stress for a given section is calculated as if the stress are uniform over the entire section. However in reality, the stress is not uniform: some parts of the section will buckle at a stress below crippling stress, but some stable areas, such as intersections and corners of a stringer may reach a higher stress. The crippling stress is the whole section's failure stress [12].

A semi-empirical formula to determine the crippling stress in a sriffened panel is presented by Gerard [5].

$$F_{cc} = F_{cy} \cdot \beta_g \cdot \left[\frac{g t_s t_w}{A}\left(\frac{E}{F_{cy}}\right)^{0.5}\right]^m \qquad \textbf{Equation 3-10}$$

Where,

βg, m, g = Non dimensional factor related to stringer section. For panel sections with straight unloaded edges such as blade, tee, and H stringers, βg

=0.67 and m=0.85.

F_{cy} = Material compressive yield stress

ts = Skin thickness (mm)

tw = Stringer thickness (mm)

A = One stringer pitch bay area (mm^2)

By employing Equation 3-9 and 3-10, the overall buckling stress of a stiffened panel can be calculated by Johnson-Euler formula. Figure 3-7 shows that Johnson-Euler result coincides with Euler result in long column range. Thus Johnson-Euler equation is suitable for all range of panel length.

3.3.2 Finite Strip Method

FSM treats the stiffened panel as an assemblage of plates consisting of narrow strips. This method is a generalised variant of the approach used by Timoshenko for solving various plate buckling problems.

Due to the periodicity of a panel's buckling mode, the displacements u, v and w can be expressed as product functions of two factors: the first one represents the respective displacement modes in x direction, and the second one describes the deformation of the strip in y-z plane, see Figure 3-8. Thus, FSM reduces the 3D numerical problem into 2D, and this is the basic advantage of FSM compared to full-scale FE analysis which will cost great computational effort to solve eigenvalue problems to predict the buckling load.

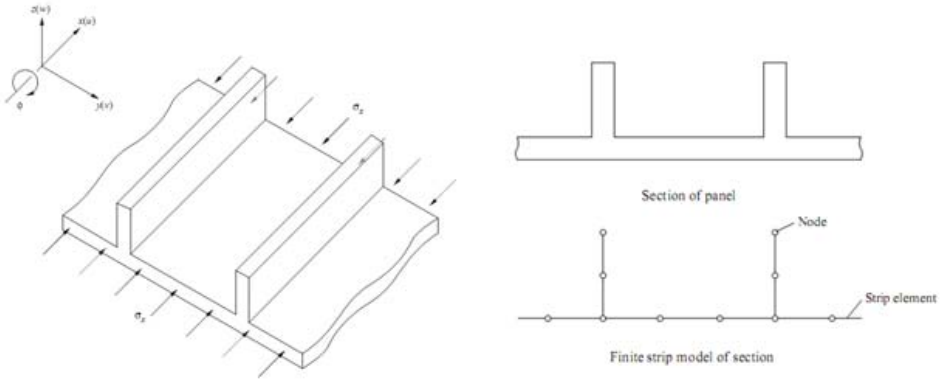

Figure 3-8 Basic coordinate system and strip model [36]

Based on FSM, ESDU 98016 provides a FORTRAN program A9816 to facilitate the calculation of the elastic buckling load of stiffened panels. A9816 has 10 types of predefined stringer sections. With two input files *.mat (define the material attributes) and *.pgd (describe the panel geometry parameters), the program can give local and overall buckling load by choosing different run types. A typical *.pgd input file is shown below.

```
Buckling of Blade-stiffened Panel
Stringer type 1
in.in                                [PGD File Name]
                                     [STO File Name]
mat.mat                              [MAT File Name]
N                                    [Force: Newton]
mm                                   [Length: mm]
1         7                          [IDtype     StringerNumber ]
0.0       0.0       0.0              [No adhesive layer ]
0.0       0.0       0.0              [No rivets ]
40.0      2.0       2                [Blade:  bw  tw   Material]
100       0.5       2                [Skin:   bs  ts   Material]
50        1                          [LeftSideSkinWidth , Support 0=free 1=simple 2=clamp]
50        1                          [RightSideSkinWidth , Support 0=free 1=simple 2=clamp]
600.0     20.0       1.0             [PanelLength, L0, R (dummy) ]
3         0                          [Runtype 1=overall 3=local, Output 0=minimal 1=extended ]
```

Figure 3-9 ESDU A9816 input file example

3.3.3 Finite Element Method

3.3.3.1 Introduction of FEM

Finite element buckling analysis is the most powerful but high cost solution. It can deal with complex structure configurations, and perform either linear or nonlinear buckling analysis, however the preparation of the FE models and the buckling calculation process are time consuming.

In linear FE buckling analysis, the effect of differential stiffness is simply added to the linear stiffness. The differential stiffness is part of the stiffness matrix which is a function of the applied load. The attribution of the differential stiffness can cause the total stiffness matrix to become non positive definite, and that is when the structure buckles. The eigenvalue problem is solved in FE linear analysis, and the critical buckling load is predicted as the eigenvalue λ times the applied load:

$$\{P\}_{cr} = \lambda\{P\} \qquad \textbf{Equation 3-11}$$

MSC.NASTRAN is able to perform linear buckling analysis in SOL105. When using NASTRAN to carry out buckling analysis, the input deck needs two subcases. The first subcase is a standard linear static subcase, which is used to determine the differential stiffness matrix, and the second subcase extracts the eigenvalues. Generally, more attention will be paid to the first mode eigenvalue, which is going to predict the lowest critical buckling stress.

Three methods, named inverse power, enhanced inverse power and Lanczos, can be selected in NASTRAN to perform a linear buckling analysis. Usually, Lanczos method is recommended because it takes full advantage of sparse matrix methods which can substantially increase computational speed.

3.3.3.2 Boundary Condition Case Study

The boundary conditions (BCs) of FE models exert significant influence on analysis accuracy. A case study is carried out to identify a suitable boundary condition for FE buckling analysis. A 600mm×700mm stiffened panel with 7 stringers is selected arbitrarily, which will be modelled under four different BCs, then the FEA results will be compared with ESDU 98016 results. The stiffened panel is shown in Figure 3-10, and Point M is the central point of the skin.

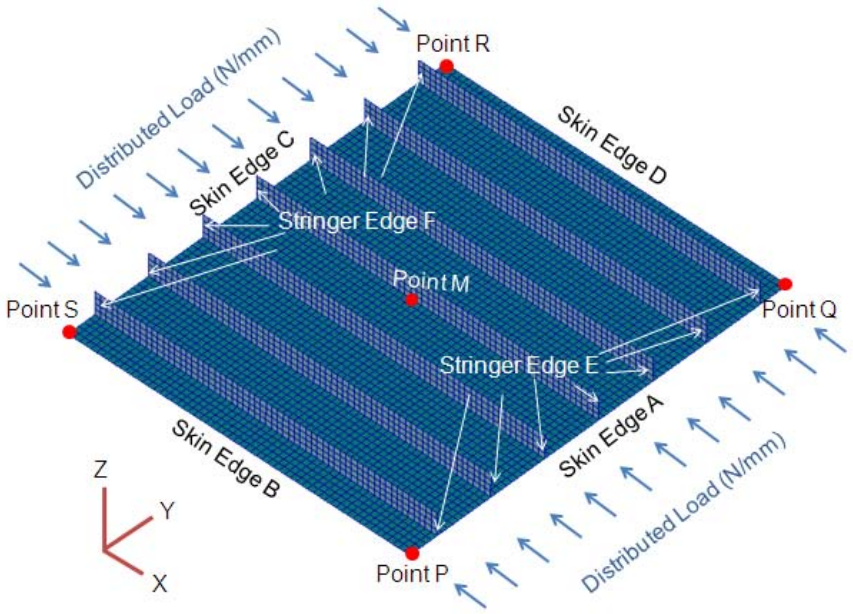

Figure 3-10 Panel FE model

Boundary conditions define:

1: X direction displacement is constrained
2: Y direction displacement is constrained
3: Z direction displacement is constrained
4: X axial rotation is constrained
5: Y axial rotation is constrained
6: Z axial rotation is constrained

Four different boundary conditions are listed below:

Table 3-6 Boundary conditions list

BCs Name	Constrain		Load Applied on
Case A	Edge A,B,C,D : 3 Point P,Q,R,S : 2,3 Point M: : 1	Edge E,F : 2,3	Edge A, C
Case B		Edge E,F : 2,3	Edge A, C, E, F
Case C		Edge E,F : free	Edge A, C
Case D		Edge E,F : free	Edge A, C, E, F

In order to cover both local and overall buckling modes and easy to modify FE model, in each BCs case, the author keeps the dimensions of bs, tw and bw constant, only changes the skin thickness ts from 0.5 mm to 6mm with a increase step of 0.5mm. Thus for each boundary condition, 12 cases are calculated. The panel's material and dimensions are listed below:

Table 3-7 Case study panel properties

Material	Panel Dimension
E = 71000 MPa	L = 600 mm, B = 700 mm
u = 0.3	bs=100mm, bw=40mm, tw=2mm
Fcy = 400 MPa	ts=0.5, 1, 1.5, 2, 2.5, 3, 3.5, 4, 4.5, 5, 5.5, 6 mm

All the 12×4=48 cases FEA post process pictures are shown in Appendix A. The results comparison of ESDU 98016 and FEA are listed in Table 3-8. It is worth mentioning here that ESDU 98016 can give local and overall buckling stress respectively, however FEA will only give the eigenvalues, and the 1st

mode eigenvalue is the most critical one, based on which the critical buckling stress can be calculated by the following equation:

Critical Stress = Load / Panel Cross Section Area

= (Load intensity Nx × 1st Eigenvalue × Load Applied Length) / Panel Cross Section Area

For Case A and Case C:

Load applied length (only on skin) = 700 (mm)

Load intensity = 1(N/mm)

Total load = 1× 700 = 700 (N)

For Case B and Case D:

Load Applied Length (on skin and stringers) = 700 + 7× 40 = 980 (mm)

Load intensity = 1(N/mm)

Total load = 1× 980 = 980 (N)

Table 3-8 ESDU 98016 and FEA buckling stress results

ts (mm)	σ_{cr} (MPa) 98016		σ_{cr} (Mpa) FEA			
	Local	Overall	Case A	Case B	Case C	Case D
0.5	11.07	67.83	4.75	6.41	4.39	5.97
1.0	39.99	164.50	23.86	31.41	21.59	28.69
1.5	68.68	253.59	52.63	63.80	48.92	61.55
2.0	100.60	231.92	89.43	96.95	85.98	96.26
2.5	137.19	211.86	136.65	124.52	133.93	103.25
3.0	165.96	195.17	174.85	123.91	174.33	92.93
3.5	177.98	181.65	160.55	112.24	160.04	83.17
4.0	180.75	170.80	148.90	100.67	148.42	74.96
4.5	180.70	162.15	139.50	91.17	139.04	68.11
5.0	179.92	155.34	131.97	83.04	131.54	62.39
5.5	178.76	150.05	126.02	76.47	125.62	57.56
6.0	177.38	146.06	121.41	71.22	121.03	53.45

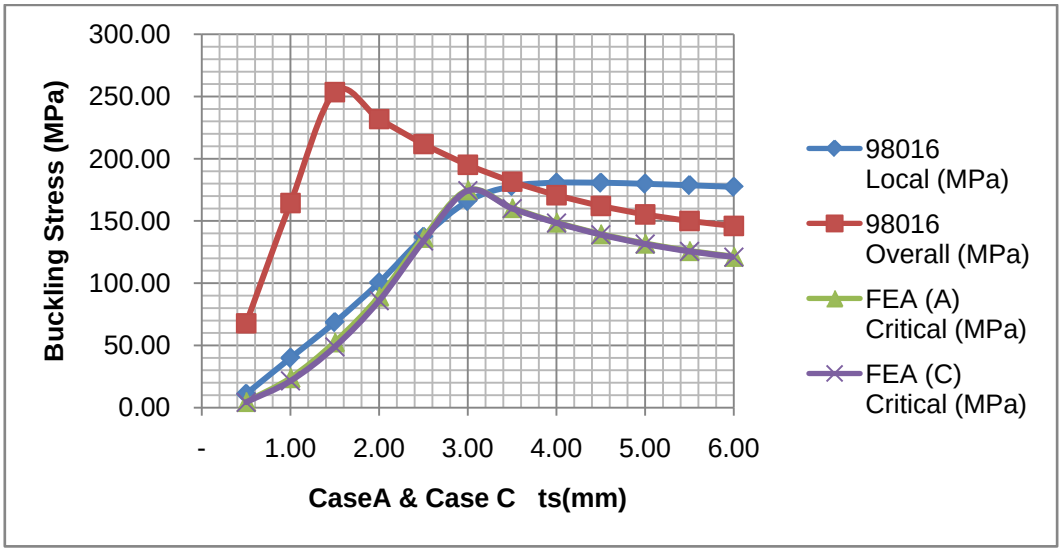

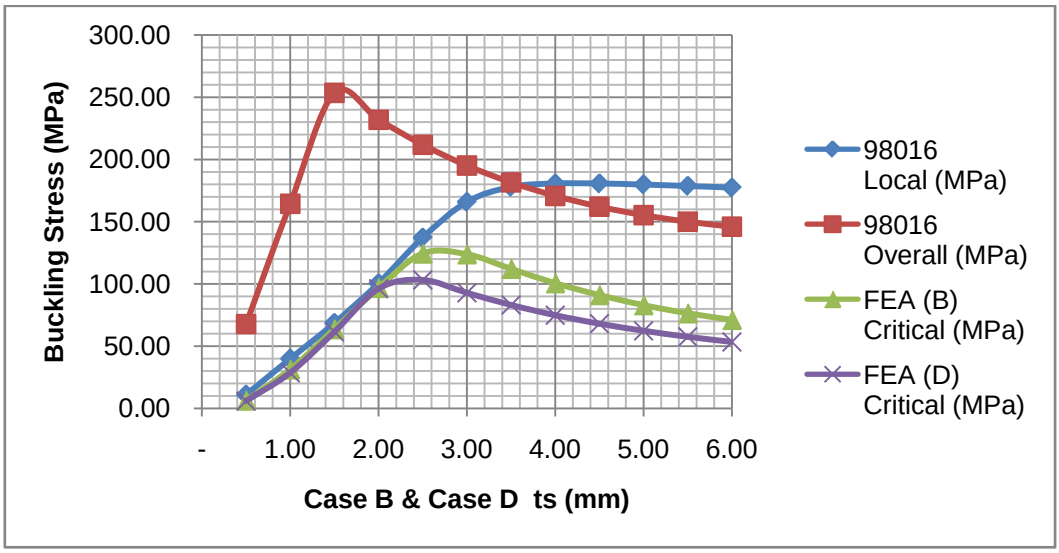

Figure 3-11 ESDU 98016 and FEA results comparison

In Case A and C, load is applied only on skin edges. The FEA results of Case A and C are very close, which means that under this loading condition, the constraint of stringer edges will not affect the results too much. From Appendix A we can see that for Case A and C, the critical buckling modes obtained by FEA coincide with ESDU results very well. The FEA critical buckling stress is almost equal to the smaller one of ESDU's local buckling stress and overall buckling stress. This is meaningful because the smaller one is more critical. Between Case A and C, the results show that Case A is more close to the condition set in the ESDU method, especially at the maximum σ_{cr} design point.

In Case B and D, load is applied on both skin and stringer edges, which means that the stringer will take load directly. Due to this reason, all the buckling modes in case B and D are local buckling (either in skin or in stringer). When they fall into stringer local buckling, the critical buckling stress of Case D is lower than that of Case B, because stringer edges in Case D is free. The FEA results variation trends of Case B and D do not agree with ESDU.

Thus, boundary condition Case A is chosen by the author and the relationship between ESDU's local buckling stress, overall buckling stress, and FEA's critical buckling stress is:

Critical buckling stress = MIN (Local buckling stress, Overall buckling stress)

From Figure 3-11 Case A, it is obvious that the highest critical buckling stress locates at where the local buckling stress equals to overall buckling stress, which means that the panel's highest efficiency can be achieved when local buckling stress is the same with overall buckling stress. In fact, this statement has already been used in Emero's optimum design method, in which it claimed that "The optimization of a given structural cross section is that local and general instability failure modes occur simultaneously." [11]

3.3.4 IPBA Program Development

A Visual Basic program named IPBA (Isotropic Panel Buckling Analysis) is developed to perform buckling analysis for integral blade stiffened panels.

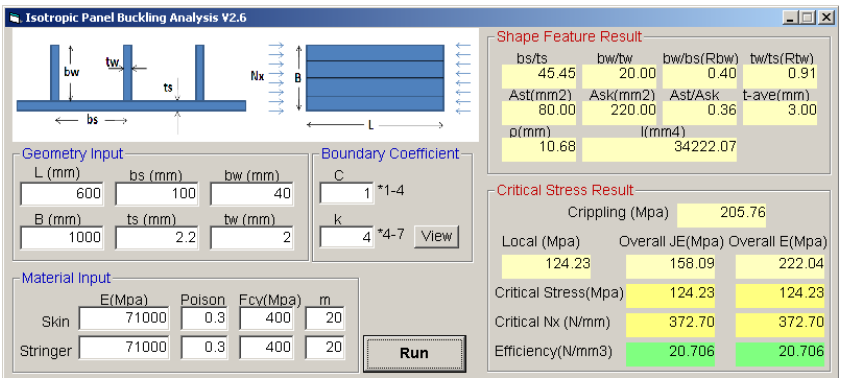

Figure 3-12 IPBA program interface

The interface of IPBA is shown in Figure 3-12. Closed form equations are employed in IPBA. IPBA is able to calculate local buckling stress, crippling stress, and overall buckling stress. The panel efficiency in this program is defined as the load carried by per unit volume of the panel when it buckles.

Cases in Table 3-7 are re-calculated by IPBA, and then the results are compared with ESDU 98016 and FEA. Results in Table 3-9 are summarized in the form of critical buckling stress and their buckling modes, while in Table 3-10 they are compared in the form of critical buckling load.

Table 3-9 Comparison of critical buckling stress

ts (mm)	IPBA (MPa)		98016 (MPa)		FEA (MPa)	
	Stress	Mode	Stress	Mode	Stress	Mode
0.5	6.42	Local	11.07	Local	4.75	Local
1.0	25.67	Local	39.99	Local	23.86	Local
1.5	57.75	Local	68.68	Local	52.63	Local
2.0	102.67	Local	100.60	Local	89.43	Local
2.5	157.40	Overall	137.19	Local	136.65	Local
3.0	154.29	Overall	165.96	Local	174.85	Overall
3.5	149.52	Overall	177.98	Local	160.55	Overall
4.0	143.72	Overall	170.80	Overall	148.90	Overall
4.5	137.26	Overall	162.15	Overall	139.50	Overall
5.0	130.42	Overall	155.34	Overall	131.97	Overall
5.5	123.41	Overall	150.05	Overall	126.02	Overall
6.0	116.38	Overall	146.06	Overall	121.41	Overall

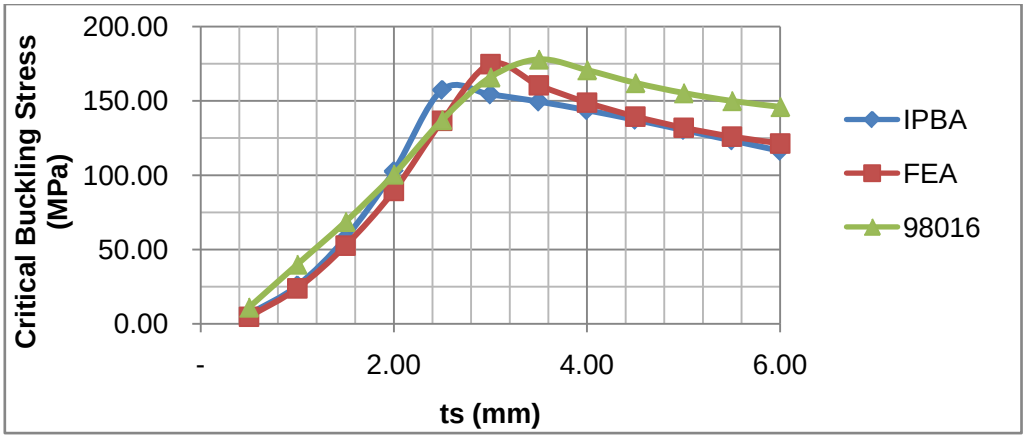

Figure 3-13 Comparison of critical buckling stress

Table 3-10 Comparison of critical buckling load

ts (mm)	IPBA (N/mm)		98016 (N/mm)		FEA (N/mm)	
	Nx	Mode	Nx	Mode	Nx	Mode
0.5	8.35	Local	12.64	Local	6.17	Local
1.0	46.21	Local	63.33	Local	42.96	Local
1.5	132.83	Local	139.11	Local	121.06	Local
2.0	287.48	Local	248.22	Local	250.39	Local
2.5	519.42	Overall	399.14	Local	450.93	Local
3.0	586.30	Overall	556.17	Local	664.42	Overall
3.5	642.94	Overall	675.09	Local	690.35	Overall
4.0	689.86	Overall	723.33	Overall	714.73	Overall
4.5	727.48	Overall	758.37	Overall	739.35	Overall
5.0	756.44	Overall	795.13	Overall	765.45	Overall
5.5	777.48	Overall	834.36	Overall	793.94	Overall
6.0	791.38	Overall	876.70	Overall	825.60	Overall

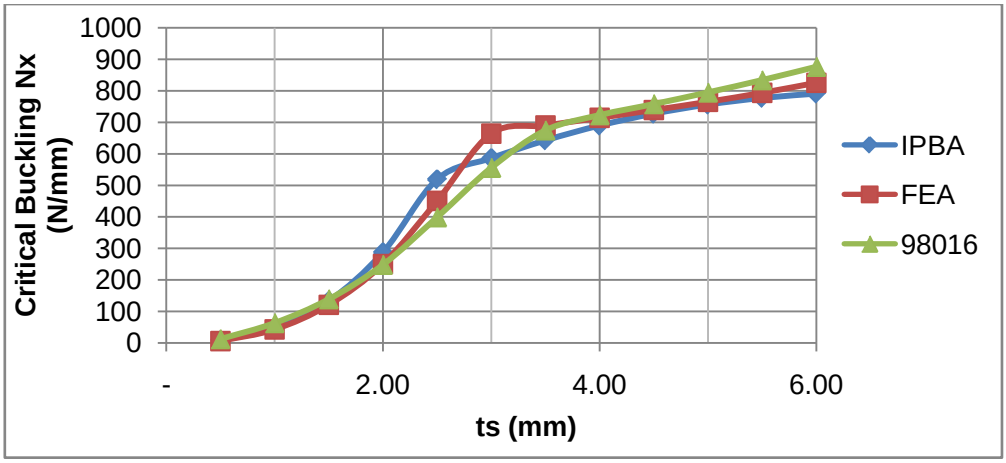

Figure 3-14 Comparison of critical buckling load

The results obtained from IPBA are very close to those from FEA and ESDU 98016 (FSM), which means that closed form equations have sufficient accuracy to predict the critical buckling load.

3.4 Isotropic Panel Optimum Design

3.4.1 Optimization Model of a Metallic Blade Stiffened Panel

The optimization problem of a metallic blade stiffened panel can be defined as:

Objective:

Minimum weight (or volume)

Design Variables:

bs, ts, tw, bw

Constraints:

(1) No local buckling happens under the given load AND

(2) No overall buckling happens under the given load AND

(3) User's geometrical dimension boundary constraint

3.4.2 Difficulties using FEM Optimization

Some commercial FE software, for example MSC.NASTRAN and Hyper Works, provide their optimization package to facilitate the optimum design process based on FE models. However, it is not efficient to optimize such a stiffened panel with geometry variables.

There are four design variables: bs, ts, bw and tw. If we keep bs (stringer pitch) fixed and just try to find other three optimum dimensions (ts, bw and tw), it is a simple sizing optimization problem, which can be solved by FEM easily. However, if we want to find the best value of bs, it is not a pure sizing optimization problem anymore. Instead it is more related to another optimization field termed topology optimization. It is because when bs changes, the number of stringers of the panel varies, which means that the basic configuration of this panel is completely changed. Thus the FE model needs to be rebuilt or updated correspondingly.

So if we want to employ FE software to achieve a stiffened panel optimum design, it must be a combination of topology optimization and sizing optimization, which will be too complicated and inefficient. Sometimes it may not be so effective to obtain a satisfying solution.

3.4.3 IPO Program Development

3.4.3.1 IPO Program Introduction

A Visual Basic program IPO (Isotropic Panel Optimization) is developed to facilitate the optimum design process. The interface of the program is shown in Figure 3-15.

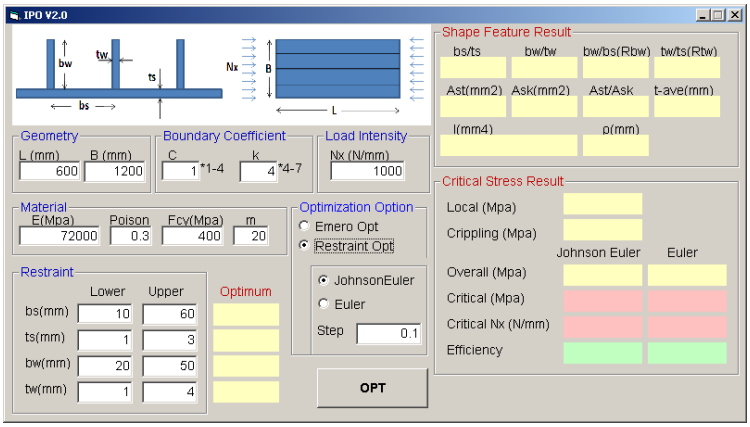

Figure 3-15 IPO program interface

IPO provides the users with two kinds of optimization modes.

(1) Emero's Opt

In this mode, the program employs Emero's method to achieve the theoretical optimum design.

(2) Restraint Opt

In this mode, IPO allows the users to define the upper and lower boundaries for each design variables: bs, ts, bw and tw. The obtained optimum design will satisfy all the boundary constraints.

IPO's optimum design flow chart is shown below.

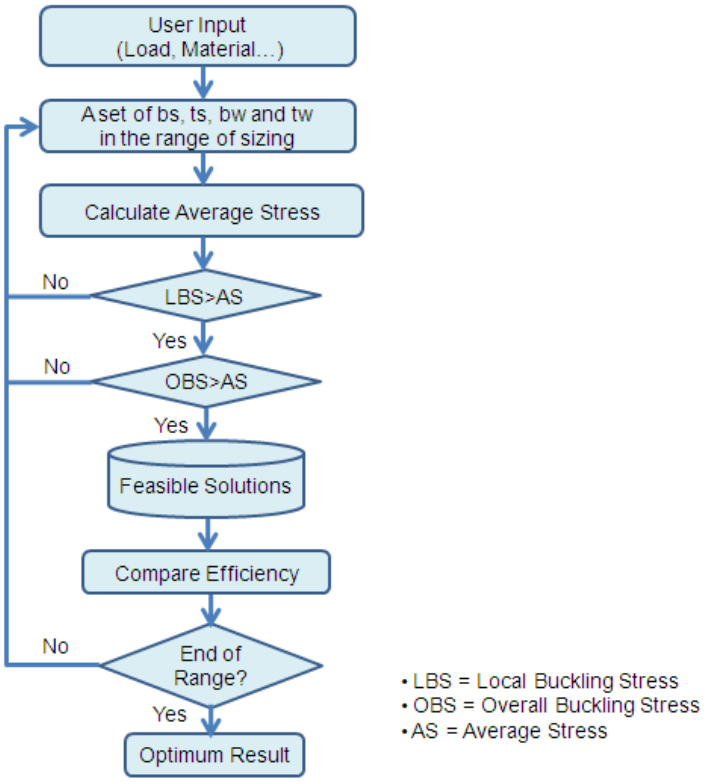

Figure 3-16 IPO program flow chart

3.4.3.2 IPO Program Validation

Two cases are carried out to validate IPO's "Restraint Opt" running mode. In the first case, the design variables (bs, bw, tw, ts) are optimized in a wide range, which makes the optimum problem like a free sizing problem; while in the second case, some design variables are limited in a small boundary, which results in a constraint sizing problem. The two cases are described below:

- Panel size: L=600mm, B=1200mm
  Load: Nx=1000 N/mm
  Design variable boundaries: bs, bw, tw, ts in the range 0.01mm~200 mm

  The optimum result given by IPO is:
  bs=56.00mm, ts=1.50mm, bw=36.87mm, tw=3.00mm

  This result is quite close to Emero's optimization result at Nx=1000 N/mm. (see Table 3-2) bs=55.41mm, ts=1.45mm, bw=36.01mm, tw=3.26mm

- Panel Size: L=600mm, B=700mm
  Load: Nx=1000 N/mm,
  Design variable boundaries: bs=100 mm, ts=4mm, bw=40mm, 1<tw<6 mm

  The optimum result given by IPO is:
  bs=100 mm, ts=4mm, bw=40mm, tw=3.08 mm

This sizing result is validated by FE analysis, see Figure 3-17. The critical buckling load given by NASTRAN is: Nx=1020.1 N/mm.

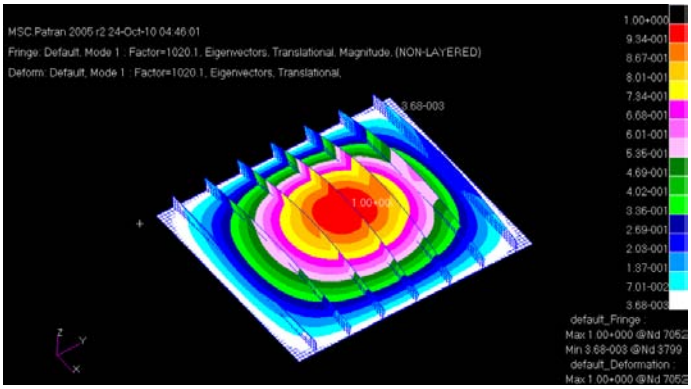

Figure 3-17 FE analysis result

The validation results show that IPO is effective to perform the optimum design process. The IPO extends the use of Emero's method to the optimum design of a blade stiffened panel under user defined variable boundaries. This feature is very useful in a practical optimum design.

3.5 Relationship between Panel Efficiency and Stringer Pitch

In the optimum design of a stiffened panel, the number of stringers is a major factor. In order to find the relationship between the stringer number (stringer pitch) and panel's efficiency, a case study is carried out, which is described as below:

Panel size: L=600mm, B=1200mm
Load: Nx=1000 N/mm
Design variable boundaries: ts, bw, tw = no constraint

bs= 10mm, 20mm, 30mm…to 300mm (Total 30 cases)

Material: E=72000Mpa, u=0.3, Fcy=400Mpa

All the optimum designs under different stringer pitches are obtained by IPO "Restraint Opt" running mode, local buckling coefficient k=4 is selected. Then these obtained designs are validated by ESDU 98016 to check the critical buckling stress. The optimum design results and validation are shown in Table 3-11 and the critical buckling stress comparison is plotted in Figure 3-18.

Table 3-11 IPO optimum sizing results at different stringer pitch

bs (mm)	Optimum Results (mm)			t_{av} (mm)	IPO σ_{cr} (MPa)			98016 (MPa)
	ts	bw	tw		Local	Overall	Critical	Critical
10	0.99	29.80	1.49	5.43	436.32	184.26	184.26	149.71
20	1.46	33.77	1.69	4.31	409.56	231.93	231.93	156.33
30	1.69	37.79	1.89	4.07	386.58	245.67	245.67	151.85
40	1.88	40.67	2.12	4.04	368.45	247.81	247.81	158.39
50	1.88	40.67	2.65	4.04	368.00	247.81	247.81	205.46
60	1.86	40.79	3.20	4.04	250.15	247.81	247.81	242.77
70	2.15	41.28	3.26	4.07	245.56	245.80	245.56	243.79
80	2.44	42.52	3.24	4.16	242.14	240.28	240.28	231.55
90	2.70	43.19	3.29	4.28	234.27	233.71	233.71	226.91
100	2.95	43.85	3.34	4.41	226.52	226.61	226.52	221.51
110	3.20	44.86	3.35	4.57	220.28	219.01	219.01	214.11
120	3.43	45.60	3.39	4.72	212.66	211.95	211.95	209.62
130	3.65	46.64	3.41	4.87	205.20	205.34	205.20	202.41
140	3.87	46.95	3.47	5.03	198.90	198.67	198.67	198.71
150	4.08	47.71	3.50	5.19	192.58	192.57	192.57	193.12
160	4.29	48.38	3.53	5.36	187.13	186.67	186.67	190.12
170	4.49	48.79	3.58	5.52	181.58	181.24	181.24	184.91
180	4.69	49.40	3.61	5.68	176.71	176.04	176.04	181.96
190	4.88	50.03	3.64	5.84	171.71	171.29	171.29	177.36
200	5.07	50.73	3.66	6.00	167.27	166.71	166.71	173.23
210	5.25	51.18	3.70	6.15	162.69	162.56	162.56	171.19
220	5.43	51.71	3.73	6.31	158.57	158.56	158.56	166.88
230	5.61	52.05	3.77	6.46	154.86	154.73	154.73	163.47
240	5.79	52.48	3.80	6.62	151.50	151.04	151.04	159.86
250	5.96	53.08	3.82	6.77	147.94	147.69	147.69	160.36
260	6.13	53.36	3.86	6.92	144.69	144.47	144.47	156.80
270	6.30	53.60	3.90	7.07	141.72	141.36	141.36	153.84
280	6.46	54.01	3.93	7.22	138.55	138.54	138.54	150.15
290	6.63	54.59	3.94	7.37	136.05	135.66	135.66	147.17
300	6.79	54.79	3.98	7.52	133.34	133.03	133.03	144.29

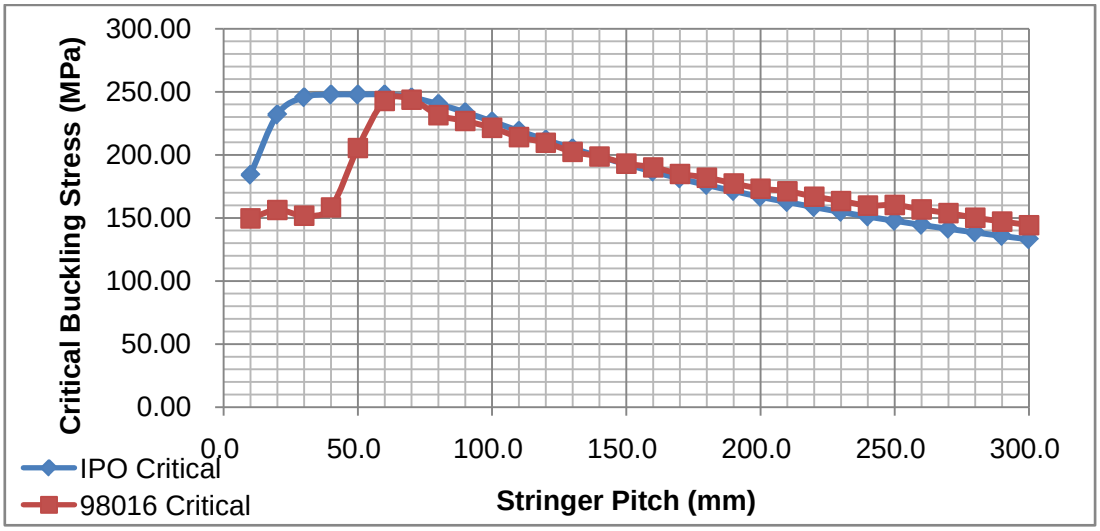

Figure 3-18 Critical buckling stress vs. stringer pitch

From Figure 3-18 we can see that for each optimum design, when bs ≥ 60 mm, the critical buckling stress obtained by IPO coincides with ESDU 98016 very well; while bs <60 mm, there exists some differences. It is because that in this range, the skin local buckling stress may exceed the material's compressive yield stress, and a plastic correction coefficient η_L is used in IPO to handle this problem. η_L is not a constant value, it varies with stress. An iteration equation from Niu's book is used in IPO to calculate η_L However ESDU 98016 can only deal with elastic problems.

Figure 3-18 also indicates that when the stringer pitch is large, the optimum design's critical buckling stress is low, which means that only relatively low efficiency can be achieved at a large stringer pitch. Then with the decrease of stringer pitch, the panel's efficiency will go up. However, when the stringer pitch reduces to a certain value, the efficiency reaches the peak point, after which the efficiency will not increase any more. It means that there exists a critical stringer pitch value at which the panel's efficiency is a maximum. It is worth mentioning here that this critical stringer pitch is exactly the optimization result obtained from Emero's method directly (Nx=1000N/mm, bs=55.41mm, see Table 3-2).

Thus Emero's method will directly give the highest panel's efficiency in the whole design space (or obtain the theoretical global optimum design), while IPO

can achieve not only the global one, but also the local optimum solutions at any specific stringer pitch values. A general curve representing the relationship between panel efficiency and stringer pitch can be drawn as below.

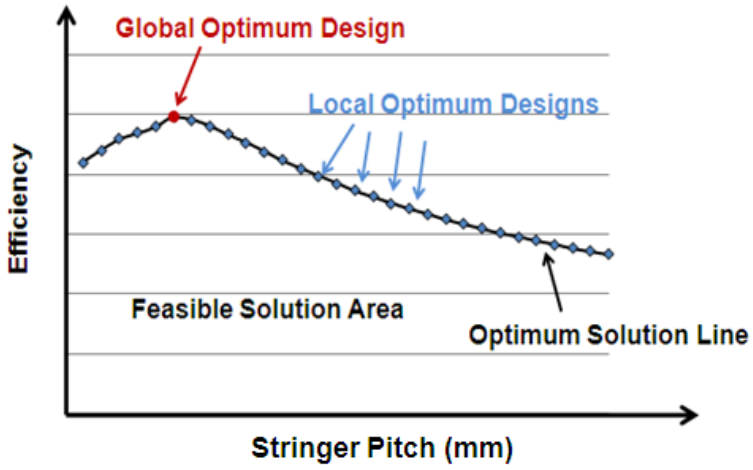

Figure 3-19 Panel efficiency vs. stringer pitch

3.6 Summary

Emero presented a set of equations and charts to facilitate the optimum design of a metallic stiffened panel under compressive load. However, the optimum result obtained from Emero's method is the global optimum solution which is too theoretical to be directly applied to a practical design on considering the manufacturability and maintainability.

In order to find an effective procedure to achieve a more practical optimum design, the blade stiffened panel is selected as the study representative for its simple construction and wide application in aircraft wing box design.

By employing appropriate CF equations, a VB program IPBA is developed to calculate the buckling stress of a stiffened panel. According to case study, the results obtained from IPBA are very close to those from FSM and FEM, which means that CF equations have sufficient accuracy. Then another VB program IPO, which enables the users to define the lower and upper boundaries for each design variable, is developed to facilitate the practical optimum design process.

Compared to Emero's method, IPO eliminates the limitations, and can give both global and local optimum solutions to satisfy specific design requirements.

Based on above study and analysis work, some conclusions can be drawn here:

(1) In the design of a metallic stiffened panel subject to axial compressive load, if the panel's length is fixed, the relationship between external load and panel's optimum configuration is:

- When the compressive load is low, small stringer pitch and thin skin configuration is efficient;
- When the compressive load is high, large stringer pitch and thick skin configuration is efficient.

(2) A panel's critical buckling stress is the smaller one between local buckling stress and overall buckling stress. High critical buckling stress is equivalent to high panel efficiency.

(3) For a stiffened panel (panel length is fixed) subject to a certain load, there exists a maximum critical buckling stress. This highest critical buckling stress can be achieved when the local buckling stress equals to the overall buckling stress, which means that the panel's highest efficiency can be obtained when the local and overall buckling modes occur simultaneously.

Still for the same panel subject to the same load, if the panel's length is not fixed (panel's length is treated as another design variable), a higher critical buckling stress (panel's efficiency) can be achieved when the panel's length becomes shorter.

(4) For a stiffened panel subject to a certain load, the relationship between panel's efficiency and stringer pitch is: The panel's efficiency can be improved by decreasing the stringer pitch, but there exists a critical stringer pitch, below which the panel's efficiency will not increase any more. This critical stringer pitch is the global optimum solution in the whole design space, while other stringer pitches will lead to local optimum designs.

4 Optimum Design of Composite Stiffened Panels

4.1 Composite Introduction

Fibre reinforced composite materials consist of fibres and matrix. Compared to conventional metallic structural materials, composite materials have many advantages, such as high strength, light weight, good fatigue and corrosion resistance. Additionally, by changing the arrangements of the fibres, the properties of composite materials can be tailored to meet a specific design requirement. Thus composite materials have been increasingly applied in aerospace industry over the last decades.

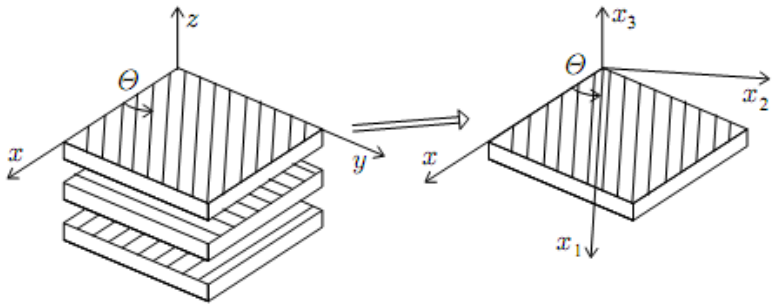

Figure 4-1 Laminate coordinate System

Composites are frequently made of plies bonded together to form a laminate, and some terms are defined below according to different ply layup strategy [37]:

(1) Symmetrical Laminate

When the laminate is symmetrical with respect to the mid-plane, it is referred to as a symmetrical laminate.

(2) Balanced Laminate

In balanced laminates, for every ply in the +θ direction there is an identical ply in the -θ direction.

(3) Cross-ply Laminate

In cross-ply laminates, fibres are only in the 0°and 90°directions. Cross-ply laminates are balanced, may be symmetrical or unsymmetrical.

(4) Angle-ply Laminate

Angle-ply laminates consist of plies in the +θ and -θ directions. Angle-ply laminates may be symmetrical or unsymmetrical, balanced or unbalanced.

(5) π/4 Laminate

π/4 Laminates consist of plies in which the fibres are in 0°, ±45° and 90° directions. The number of plies in each direction is the same (balanced). In addition, the layup is also symmetrical.

4.2 Stiffness of Thin Laminates

Thin laminates are characterized by three stiffness matrices denoted by [A], [B] and [D]. The thin laminate is subject to loading conditions illustrated below.

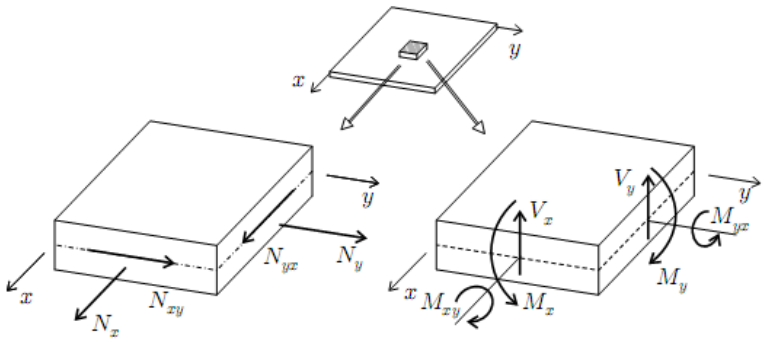

Figure 4-2 In-plane forces and moments loading condition

Kirchhoff hypothesis supposed that if the laminate is thin, the normal line to the reference surface of the laminate remains normal and straight when the laminate is extended or bent. Based on this theory, the relationship between loads and strains of thin laminate plate can be expressed as below:

$$\begin{Bmatrix} N_x \\ N_y \\ N_{xy} \\ M_x \\ M_y \\ M_{xy} \end{Bmatrix} = \begin{bmatrix} A_{11} & A_{12} & A_{16} & B_{11} & B_{12} & B_{16} \\ A_{12} & A_{22} & A_{26} & B_{12} & B_{22} & B_{26} \\ A_{16} & A_{26} & A_{66} & B_{16} & B_{26} & B_{66} \\ B_{11} & B_{12} & B_{16} & D_{11} & D_{12} & D_{16} \\ B_{12} & B_{22} & B_{26} & D_{12} & D_{22} & D_{26} \\ B_{16} & B_{26} & B_{66} & D_{16} & D_{26} & D_{66} \end{bmatrix} \begin{Bmatrix} \epsilon_x^o \\ \epsilon_y^o \\ \gamma_{xy}^o \\ \kappa_x \\ \kappa_y \\ \kappa_{xy} \end{Bmatrix}.$$

Where,

$$A_{ij} = \sum_{k=1}^{K} (\overline{Q}_{ij})_k (z_k - z_{k-1})$$

$$B_{ij} = \frac{1}{2} \sum_{k=1}^{K} (\overline{Q}_{ij})_k (z_k^2 - z_{k-1}^2)$$

$$D_{ij} = \frac{1}{3} \sum_{k=1}^{K} (\overline{Q}_{ij})_k (z_k^3 - z_{k-1}^3)$$

K is the total number of plies in the laminate. Z_k, Z_{k-1} are the distances from the reference plane to the two surfaces of the k^{th} ply (See Figure 4-3). $(\overline{Q}ij)_k$ are the elements of the stiffness matrix of the k^{th} ply.

$[\overline{Q}]$ is the stiffness matrix of the ply. The stress-strain relationship for each ply is:

$$\begin{Bmatrix} \sigma_x \\ \sigma_y \\ \tau_{xy} \end{Bmatrix} = \begin{bmatrix} \overline{Q}_{11} & \overline{Q}_{12} & \overline{Q}_{16} \\ \overline{Q}_{12} & \overline{Q}_{22} & \overline{Q}_{26} \\ \overline{Q}_{16} & \overline{Q}_{26} & \overline{Q}_{66} \end{bmatrix} \begin{Bmatrix} \epsilon_x \\ \epsilon_y \\ \gamma_{xy} \end{Bmatrix}.$$

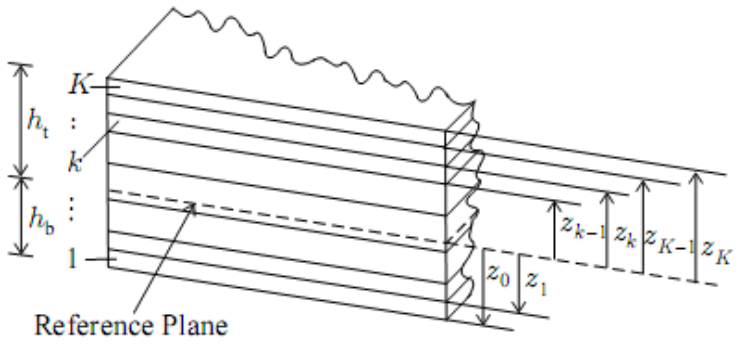

Figure 4-3 Distances from reference plane

The [A], [B], [D] matrices represent the stiffness of a laminate and describe the response of the laminate to forces and moments.

[A] is the in-plane stiffness matrix that relates the in-plane forces N_x, N_y, N_{xy} to the in-plane deformations ε_x, ε_y,γ_{xy}.

[B] is the in-plane-out-of-plane coupling stiffness matrix that relates the in-plane forces N_x, N_y, N_{xy} to the curvatures k_x, k_y, k_{xy} , and the moments M_x, M_y, M_{xy} to the in-plane deformations ε_x, ε_y,γ_{xy}. When the laminate is symmetric, [B] =0.

[D] is the out-of-plane bending stiffness matrix that relates the moments M_x, M_y, M_{xy} to the curvatures k_x, k_y, $k_{xy.}$

4.3 Layup Effects on Composite Buckling

The properties of composite laminates are designable by arranging different ply angle proportion and stacking sequence. Thus in this section, some research work is carried out to find the effects of ply layup features on buckling load.

A 600mm×700mm stiffened panel with 7 stringers is modelled in PATRAN, the dimensions of stringer pitch and stringer height are kept constant (bs =100 mm, bw = 40 mm). Apply different layup proportions and stacking sequences on skin and stringers of FE model to evaluate the influence on panel's buckling load. The buckling analysis is performed by NASTRAN. AS4/3501-6 Prepreg is selected as the material to build FE model. The properties are listed below:

Table 4-1 Properties of AS4/3501-6 prepreg

E_1 (MPa)	Young's Modulus, Longitude Direction	142,000
E_2 (MPa)	Young's Modulus, Transverse Direction	10,300
G_{12} (MPa)	Shear Modulus	7,200
u_{12}	Poisson's Ratio	0.27
XT (MPa)	Longitudinal Tensile Strength	2,280
XC (MPa)	Longitudinal Compressive strength	1,440
YT (MPa)	Transverse Tensile Strength	57
YC (MPa)	Transverse Compressive Strength	228
S (MPa)	Shear Strength	71
ρ (kg/m^3)	Density	1,600
e_{xt} (%)	Longitudinal tensile failure strain	1.5
e_{yt} (%)	Transverse tensile failure strain	0.6
t (mm)	Laminate thickness	0.25

4.3.1 Effects of Ply Angle Proportion

In order to evaluate the influence of ply angle proportion on different buckling modes (local or overall buckling), the case study is divided into four parts:

(1) Effects of skin ply angle proportion on local buckling

Strong stringer and weak skin layup is selected to make sure that the panel falls into local buckling mode. Keep the stringer's layup fixed, and only change the skin ply angle proportion. In Group A, the skin layup is unsymmetrical, while in Group B, the skin layup is symmetrical. The results are listed below.

Table 4-2 Influence of skin ply angle proportion on local buckling

Stringer	[0/-45/0/45/90/0/0/90]s		Critical Nx (N/mm)
Skin	Group A	(±45°)%	
	[45/0/0/0/0/0/0/0/0/0]	10	303.02
	[45/-45/0/0/0/0/0/0/0/0]	20	303.01
	[45/-45/45/0/0/0/0/0/0/0]	30	305.13
	[45/-45/45/-45/0/0/0/0/0/0]	40	302.99
	[45/-45/45/-45/45/0/0/0/0/0]	50	304.61
	[45/-45/45/-45/45/-45/0/0/0/0]	60	315.10
	[45/-45/45/-45/45/-45/45/0/0/0]	70	347.46
	[45/-45/45/-45/45/-45/45/-45/0/0]	80	385.98
	[45/-45/45/-45/45/-45/45/-45/45/0]	90	433.70
	Group B	(±45°)%	
	[0/0/0/0]s	0	142.65
	[45/0/0/0]s	25	207.73
	[45/-45/0/0]s	50	272.48
	[45/-45/45/0]s	75	271.53
	[45/-45/45/-45]s	100	256.99

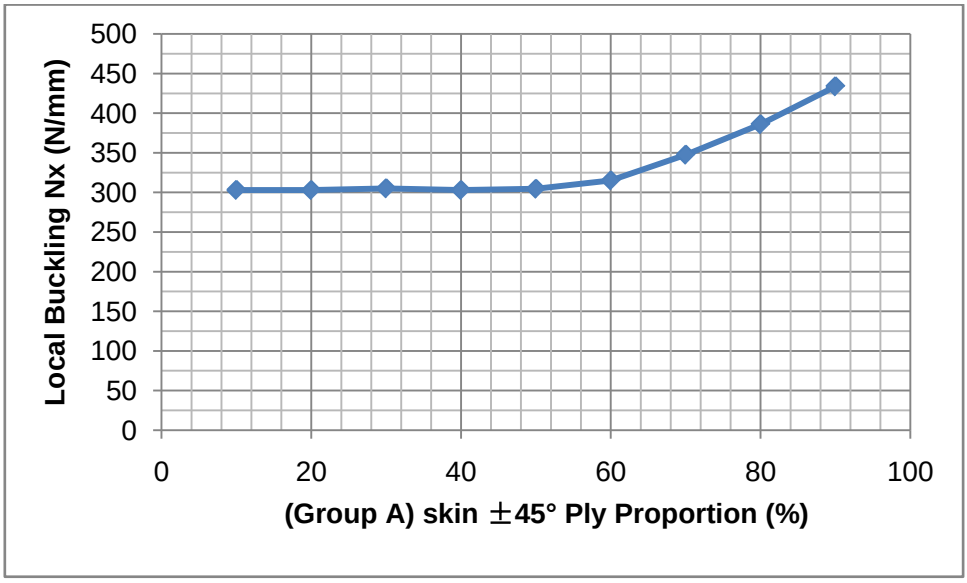

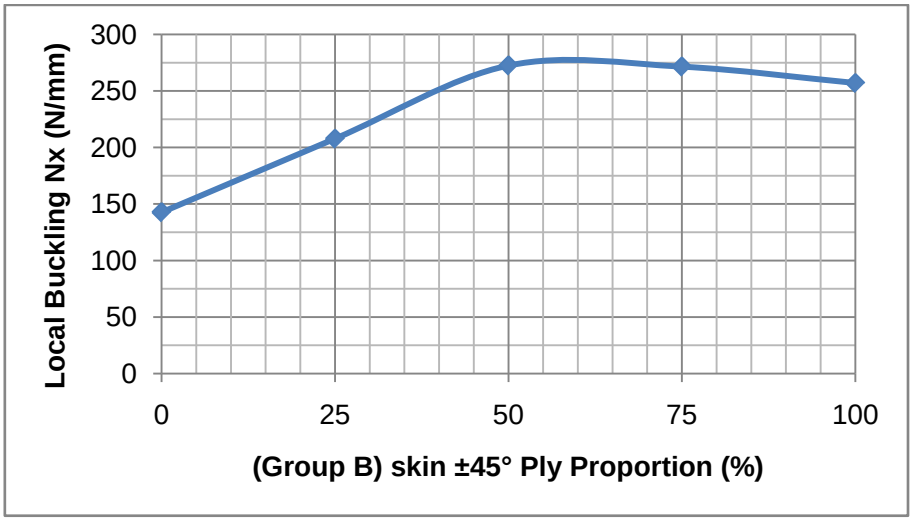

Figure 4-4 Influence of skin ply angle proportion on local buckling

The results show that no matter whether the skin layups are symmetrical or not, the skin local buckling load can be improved when the skin ±45° ply angle proportion increases. This is because the load in the skin is mainly shear force, and more ±45° can increase the shear modulus of the laminate, which will enhance the shear buckling stability of the skin.

(2) Effects of stringer ply angle proportion on local buckling

Strong stringer and weak skin layup is selected to make sure that the panel falls into local buckling mode. Keep the skin's layup fixed, and only change the stringer ply angle proportion. The results are listed below.

Table 4-3 Influence of stringer ply angle proportion on local buckling

Skin	[45/-45/0/90]		Critical Nx (N/mm)
Stringer	Layup (10 Plies)	(0°)%	
	[45/0/0/0/0/0/0/0/0/0]	90	229.68
	[45/-45/0/0/0/0/0/0/0/0]	80	233.70
	[45/-45/45/0/0/0/0/0/0/0]	70	231.50
	[45/-45/45/-45/0/0/0/0/0/0]	60	229.34
	[45/-45/45/-45/45/0/0/0/0/0]	50	227.64
	[45/-45/45/-45/45/-45/0/0/0/0]	40	227.17
	[45/-45/45/-45/45/-45/45/0/0/0]	30	226.80
	[45/-45/45/-45/45/-45/45/-45/0/0]	20	229.14
	[45/-45/45/-45/45/-45/45/-45/45/0]	10	229.31

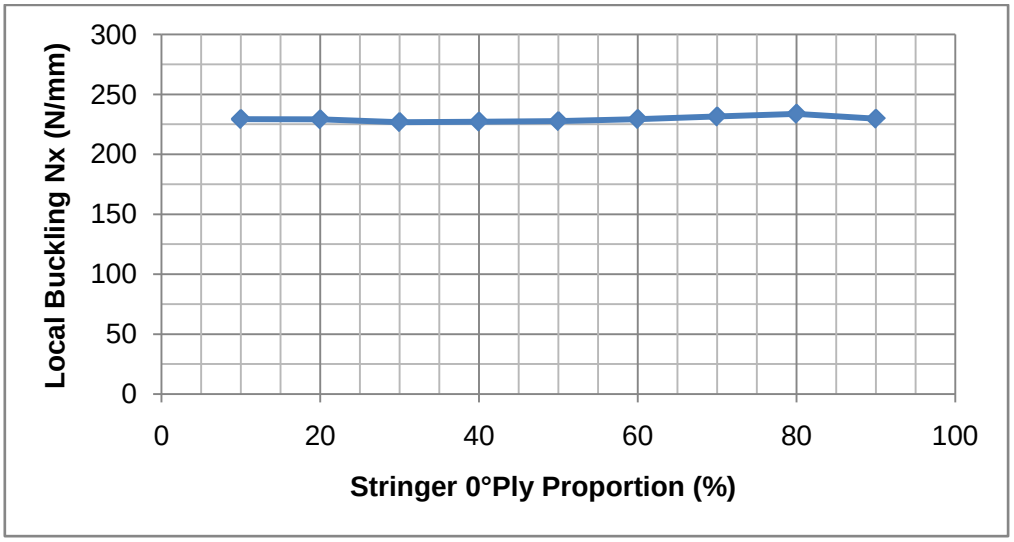

Figure 4-5 Influence of stringer ply angle proportion on local buckling

(3) Effects of skin ply angle proportion on overall buckling

Weak stringer and strong skin layup is selected to make sure that the panel falls into overall buckling mode. Keep the stringer's layup fixed, and only change the skin ply angle proportion. The results are listed below.

Table 4-4 Influence of skin ply angle proportion on overall buckling

Stringer	[45/-45]		Critical Nx (N/mm)
Skin	Layup (10 Plies)	(±45°)%	
	[45/0/0/0/0/0/0/0/0/0]	10	74.025
	[45/-45/0/0/0/0/0/0/0/0]	20	74.135
	[45/-45/45/0/0/0/0/0/0/0]	30	73.796
	[45/-45/45/-45/0/0/0/0/0/0]	40	73.521
	[45/-45/45/-45/45/0/0/0/0/0]	50	72.332
	[45/-45/45/-45/45/-45/0/0/0/0]	60	71.324
	[45/-45/45/-45/45/-45/45/0/0/0]	70	73.876
	[45/-45/45/-45/45/-45/45/-45/0/0]	80	71.432
	[45/-45/45/-45/45/-45/45/-45/45/0]	90	70.268

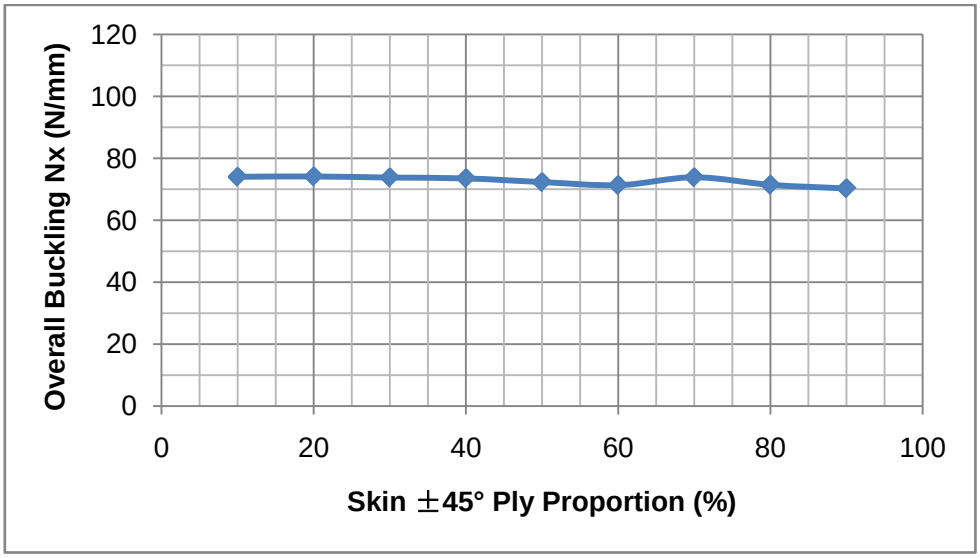

Figure 4-6 Influence of skin ply angle proportion on overall buckling

(4) Effects of stringer ply angle proportion on overall buckling

Weak stringer and strong skin layup is selected to make sure that the panel falls into overall buckling mode. Keep the skin's layup fixed, and only change the stringer ply angle proportion. The results are listed below.

Table 4-5 Influence of stringer ply angle proportion on overall buckling

Skin	[45/-45/0/45/90/-45/0/90]s		Critical Nx (N/mm)
Stringer	Layup (10 Plies)	(0°)%	
	[45/0/0/0/0/0/0/0/0/0]	90	1165.7
	[45/-45/0/0/0/0/0/0/0/0]	80	1146.0
	[45/-45/45/0/0/0/0/0/0/0]	70	1081.4
	[45/-45/45/-45/0/0/0/0/0/0]	60	1009.1
	[45/-45/45/-45/45/0/0/0/0/0]	50	922.53
	[45/-45/45/-45/45/-45/0/0/0/0]	40	828.12
	[45/-45/45/-45/45/-45/45/0/0/0]	30	723.24
	[45/-45/45/-45/45/-45/45/-45/0/0]	20	609.35
	[45/-45/45/-45/45/-45/45/-45/45/0]	10	484.17

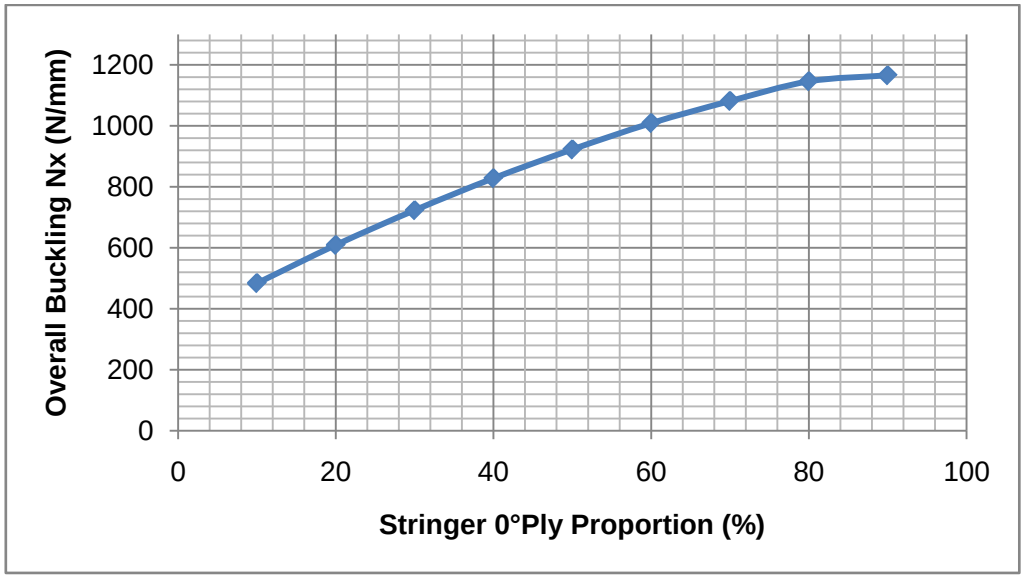

Figure 4-7 Influence of stringer ply angle proportion on overall buckling

From the case study, some conclusions can be drawn here:

(a) Critical local buckling load is more sensitive to skin ply angle proportion rather than stringer ply angle proportion;
(b) Critical overall buckling load is more sensitive to stringer ply angle proportion rather than skin ply angle proportion;
(c) In order to enhance local buckling load, it is more effective to increase ±45° plies proportion in the skin;
(d) In order to enhance overall buckling load, it's more effective to increase 0° plies proportion in the stringer.

4.3.2 Effects of Stacking Sequence

Based on above study, only the effects of skin layup sequence on local buckling mode and stringer layup sequence on overall buckling mode are investigated.

(1) Effects of skin stacking sequence on local buckling

Keep the stringer's layup fixed, just change skin stacking sequence. The results are listed below. All cases in Table 4-6 are in local buckling mode.

Table 4-6 Influence of skin stacking sequence on local buckling

Stringer	[0/-45/0/45/90/0/0/90]s		
Skin	No.	Layup	Critical Nx (N/mm)
	1	[0/0/45/-45/90/90]s	614.87
	2	[0/0/90/90/45/-45]s	626.10
	3	[45/-45/0/0/90/90]s	790.92
	4	[45/-45/90/90/0/0]s	779.47
	5	[90/90/45/-45/0/0]s	581.79
	6	[90/90/0/0/45/-45]s	603.53

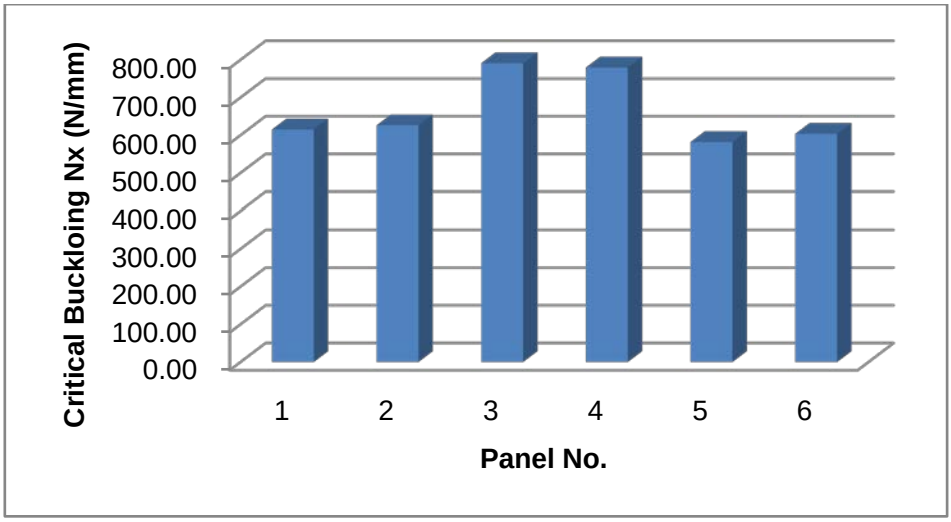

Figure 4-8 Influence of skin stacking sequence on local buckling

(2) Effects of stringer stacking sequence on overall buckling

Keep the skin's layup fixed, just change stringer stacking sequence. The results are listed below. All cases in Table 4-7 are in overall buckling mode.

Table 4-7 Influence of stringer stacking sequence on overall buckling

Skin	[45/-45/0/45/90/-45/0/90]s		
Stringer	No.	Layup	Critical Nx (N/mm)
	1	[0/0/45/-45/90/90]s	871.05
	2	[0/0/90/90/45/-45]s	869.62
	3	[45/-45/0/0/90/90]s	871.11
	4	[45/-45/90/90/0/0]s	870.10
	5	[90/90/45/-45/0/0]s	868.22
	6	[90/90/0/0/45/-45]s	867.91

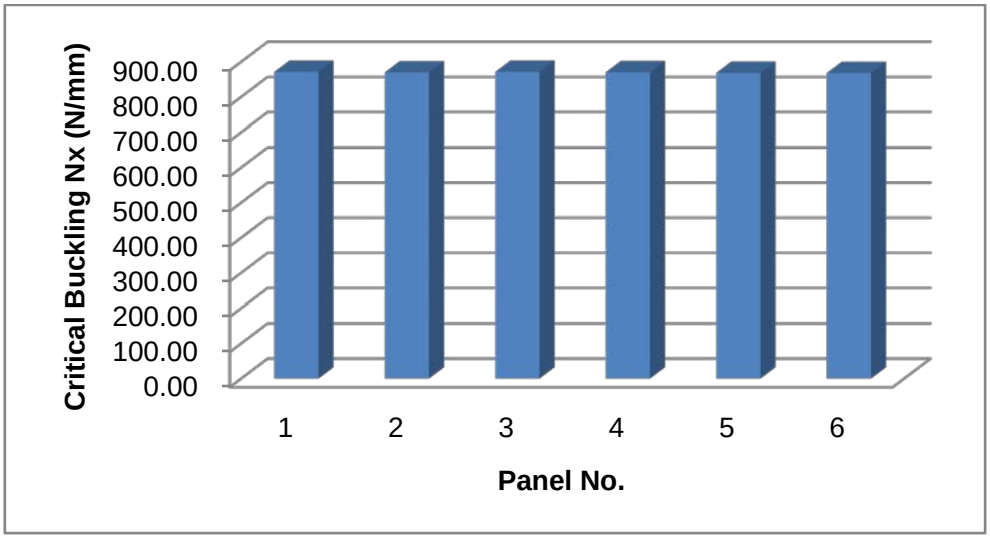

Figure 4-9 Influence of stringer stacking sequence on overall buckling

The case study results show that in order to increase critical buckling load, ±45° plies should be placed as far away as possible from the laminate mid surface.

4.4 Composite Panel Buckling Analysis

4.4.1 Composite Buckling Analysis Methods

Similar to isotropic panels, the buckling load of a composite panel can also be achieved by CF equations, FSM, or FEM.

Considerable study work has been carried out by previous researchers, and many CF equations have been developed. For example, the equation to predict the buckling load of simple supported long plates with orthotropic and symmetrical layup subject to axial compressive load is [37]:

$$\mathrm{Nxcr} = \frac{\pi^2}{\mathrm{b}^2}\left[2\sqrt{\mathrm{D}_{11}\mathrm{D}_{22}} + 2(\mathrm{D}_{12} + 2\mathrm{D}_{66})\right] \qquad \textbf{Equation 4-1}$$

Where, b is the plate width.

It is worth mentioning here that due to the complexity and diversity of laminate layup constructions, most CF equations are only suitable for some specific laminate layups.

FSM is another way to analyze the buckling load of composite panels. For example, ESDU 03001 provides a FORTRAN program which calculates initial compressive buckling loads for long flat stiffened rectangular panels based on FSM. However, the buckling analysis is only applicable to panels constructed from balanced, mid-plane symmetric layups.

4.4.2 Buckling Analysis Using Equivalent Constants

In composite structure practical design and analysis, a set of equivalent engineering elastic constants (E_x, E_y, G_{xy}, U_{xy}) are often used to study the macro mechanics of a composite component. In this way, laminates can be treated as metallic materials to simplify the analysis procedure.

There are two kinds of laminate equivalent engineering elastic constants:

(1) Equivalent membrane constants, which stand for the in-plane stiffness of the laminate, and can be calculated from [A] matrix;
(2) Equivalent bending constants: which stand for the out-of-plane stiffness of the laminate, and can be calculated from [D] matrix.

Thus by employing equivalent constants, composite stiffened panels can be simplified and transformed into metallic panels to perform buckling analysis. The next step is to investigate the accuracy of this equivalent method.

4.4.2.1 Equations Introduction

The equation for calculating local buckling stress is shown below, which is same with Equation 3-2.

$$\sigma_{crL} = \frac{K\pi^2 E}{12(1-\mu^2)}\left(\frac{t}{b}\right)^2 \qquad \textbf{Equation 4-2}$$

It is worth mentioning here that the bending equivalent Ex, not the membrane equivalent Ex, should be used to substitute E in this equation, the reasons are as following:

(1) Most developed CF equations for predicting the bucking load of a laminate plate have the expressions which are only dominated by [D] matrix, for example Equation 4-1. While equivalent constants which are determined by [D] matrix are exactly the bending equivalent modulus.

(2) From the view of buckling phenomenon, when a panel falls into local buckling mode, the skin deformation is out of its original plane. Bending equivalent modulus is more suitable to describe this out-of-plane stiffness.

Euler equation is used to predict the overall buckling load of a composite stiffened panel, see Equation 4-3. This equation accounts the effect of the transverse shear flexibility into consideration.

$$P_{cr} = \frac{P_e}{1 + \frac{P_e}{G_{xy}^{sw} A_{sw}}} \qquad \textbf{Equation 4-3}$$

Where,

$$P_e = \frac{\pi^2 \cdot EI}{L^2} \qquad \textbf{Equation 4-4}$$

P_e = Euler column buckling load (N)

G_{xy}^{sw} = Stringer web equivalent shear modulus (MPa)

A_{sw} = Stringer web area (mm^2)

EI = Panel x direction bending stiffness

L = Panel length (mm)

When using Equation 4-4, membrane equivalent Ex should be employed to calculate EI. This is because when a panel falls into overall buckling mode, the stringers' deformation is still in their original plane, and in this case, membrane equivalent modulus is more proper to present this in-plane mode.

4.4.2.2 CPBA Program Development and Case Study

By employing equivalent elastic constants and CF equations, a Visual Basic program CPBA (Composite Panel Buckling Analysis) is developed to calculate the buckling stress of a composite blade stiffened panel. The interface of the program is shown in Figure 4-10. Equivalent elastic constants of skin and stringer laminates are needed as input. Many kinds of commercial software are able to calculate equivalent modulus, and in this thesis the author employs Cranfield SOE in-house program COALA to obtain these equivalent values.

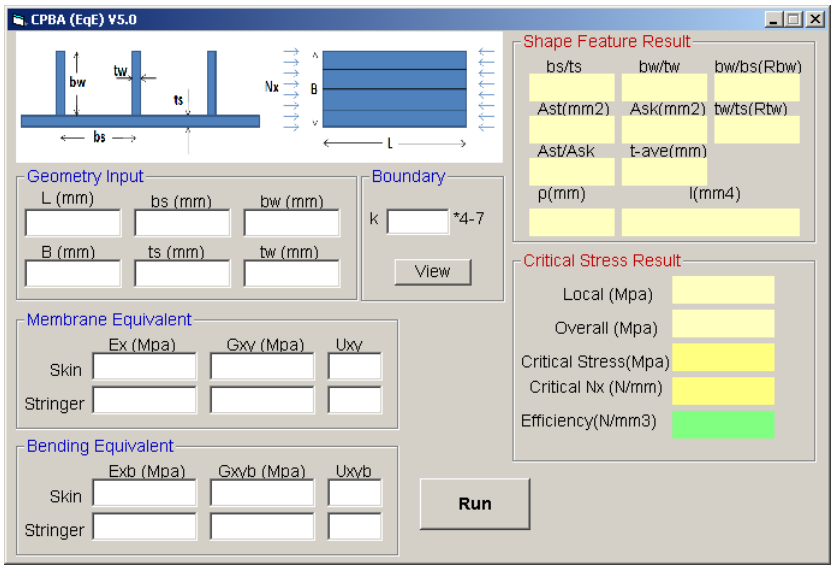

Figure 4-10 CPBA Program Interface

A case study is carried out to validate CPBA. The case study description is listed in Table 4-8. Case01 to Case08 can be treated as one group for they have the same stringer property, and Case09 to Case16 is another group. In each group, the skin thickness varies from 2.5mm to 6.0mm.

Then each case will be modelled in PATRAN using real composite layup properties, and then analyzed by NASTRAN to compare the results with CPBA.

Boundary condition Case A, which is discussed in Section 3.3.3.2, is used to build FE models. The panel's material is AS4/3501-6 (see Table 4-1). The equivalent constants obtained from COALA are listed in Table 4-9, and the

buckling results obtained from CPBA and FEA are compared in Table 4-10. All FEA post process result pictures can be found in Appendix B.

Table 4-8 Case description

Panel Length L=600 (mm) Width B=700 (mm) All cases : bs=100 (mm) bw=40 (mm)				
Case No	**Skin Layup**	**ts (mm)**	**Stringer Layup**	**tw (mm)**
	Group 1			
01	[±45/0/90/0]s	2.5	[±45/0/0/0/90/0/90]s	4.0
02	[±45/0/±45/90]s	3.0	[±45/0/0/0/90/0/90]s	4.0
03	[±45/0/±45/90/0]s	3.5	[±45/0/0/0/90/0/90]s	4.0
04	[±45/0/±45/90/0/90]s	4.0	[±45/0/0/0/90/0/90]s	4.0
05	[±45/0/±45/90/±45/0]s	4.5	[±45/0/0/0/90/0/90]s	4.0
06	[±45/0/±45/90/±45/0/90]s	5.0	[±45/0/0/0/90/0/90]s	4.0
07	[±45/0/±45/90/±45/0/90/0]s	5.5	[±45/0/0/0/90/0/90]s	4.0
08	[±45/0/±45/90/±45/0/±45/90]s	6.0	[±45/0/0/0/90/0/90]s	4.0
	Group2			
09	[±45/0/90/0]s	2.5	[±45/0/90]s	2.0
10	[±45/0/±45/90]s	3.0	[±45/0/90]s	2.0
11	[±45/0/±45/90/0]s	3.5	[±45/0/90]s	2.0
12	[±45/0/±45/90/0/90]s	4.0	[±45/0/90]s	2.0
13	[±45/0/±45/90/±45/0]s	4.5	[±45/0/90]s	2.0
14	[±45/0/±45/90/±45/0/90]s	5.0	[±45/0/90]s	2.0
15	[±45/0/±45/90/±45/0/90/0]s	5.5	[±45/0/90]s	2.0
16	[±45/0/±45/90/±45/0/±45/90]s	6.0	[±45/0/90]s	2.0

Table 4-9 Equivalent elastic constants

Layup	**Membrane Equivalent**			**Bending Equivalent**		
	Ex (MPa)	**Gxy (MPa)**	**Uxy**	**Ex (MPa)**	**Gxy (MPa)**	**Uxy**
[±45/0/90]s	56676	22040	0.29	37803	30936	0.51
[±45/0/90/0]s	73741	19072	0.29	45268	29428	0.43
[±45/0/±45/90]s	47785	26986	0.40	44889	30545	0.43
[±45/0/±45/90/0]s	61268	24160	0.39	46702	30186	0.42
[±45/0/±45/90/0/90]s	56676	22040	0.29	48634	29559	0.40
[±45/0/±45/90/±45/0]s	53804	26986	0.46	47116	29728	0.42
[±45/0/±45/90/±45/0/90]s	51521	25008	0.35	47478	29485	0.41
[±45/0/±45/90/±45/0/90/0]s	59753	23389	0.35	48001	29157	0.41
[±45/0/±45/90/±45/0/±45/90]s	47785	26986	0.40	48038	29161	0.41
[±45/0/0/0/90/0/90]s	83700	14620	0.19	71222	24136	0.24

Table 4-10 CPBA and FEA results comparison

Case No	CPBA				FEA		Critical Error %
	Local (MPa)	Overall (MPa)	Critical (MPa)	Mode	Critical (MPa)	Mode	
	Group1						
01	114.19	309.74	114.19	Local	124.24	Local	-8.09
02	163.06	258.30	163.06	Local	171.21	Local	-4.76
03	228.52	258.93	228.52	Local	232.94	Local	-1.90
04	304.76	239.23	239.23	Overall	232.46	Overall	2.91
05	381.11	223.29	223.29	Overall	215.61	Overall	3.56
06	469.40	209.63	209.63	Overall	208.02	Overall	0.78
07	574.23	205.44	205.44	Overall	205.31	Overall	0.06
08	683.91	187.12	187.12	Overall	190.03	Overall	-1.53
	Group2						
09	114.19	166.59	114.19	Local	120.34	Local	-5.11
10	163.06	139.47	139.47	Overall	134.42	Overall	3.75
11	228.52	131.06	131.06	Overall	128.47	Overall	2.01
12	304.76	118.62	118.62	Overall	119.54	Overall	-0.77
13	381.11	108.73	108.73	Overall	110.15	Overall	-1.28
14	469.40	100.57	100.57	Overall	105.12	Overall	-4.33
15	574.23	95.87	95.87	Overall	101.98	Overall	-6.00
16	683.91	87.89	87.89	Overall	96.45	Overall	-8.88

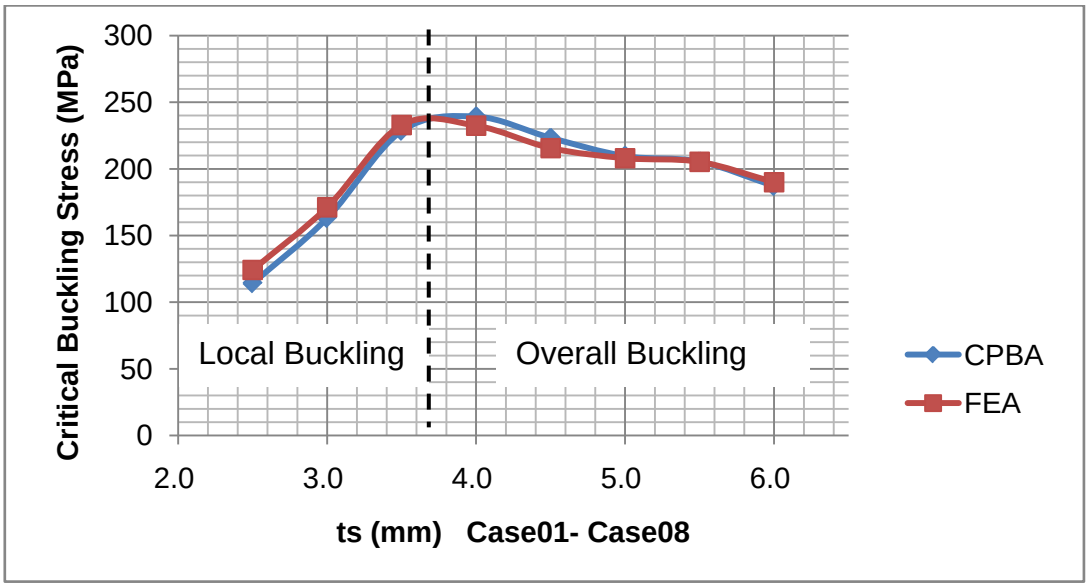

Figure 4-11 CPBA and FEA results comparison (Group1)

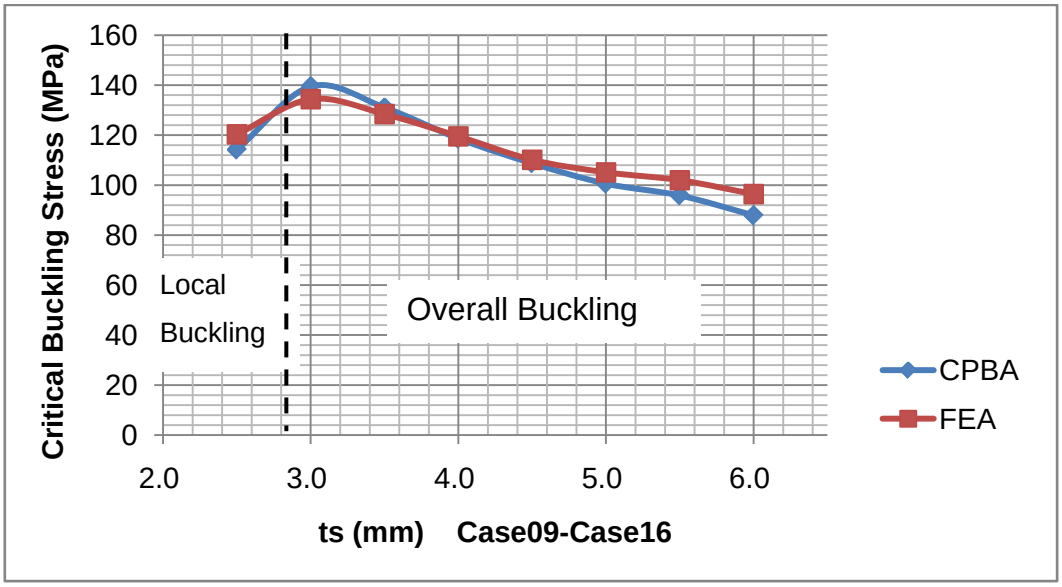

Figure 4-12 CPBA and FEA results comparison (Group2)

The results comparison shows that the buckling modes predicted by CPBA coincide with FEA, and the critical buckling stress differences between CPBA and FEA are within 10%, which means that the method of using equivalent engineering elastic constants to calculate composite panel buckling stress is feasible and effective.

4.5 Composite Panel Optimum Design

4.5.1 Optimization Model of a Composite Blade Stiffened Panel

The optimum design of a composite panel is more complicated than that of a metallic panel. The optimization problem can be defined as below:

Objective:

Minimum weight (or volume)

Design Variables:

bs, ts, tw, bw, laminate ply angle proportion, ply stacking sequence

Constraints:

(1) No local buckling happens under the given load AND

(2) No overall buckling happens under the given load AND

(3) User's geometrical dimension boundary constraint AND

(4) Ply failure index <1 AND

(5) Strain< 3500 με

4.5.2 Laminate Practical Design Guidelines

Although one advantage in composite design is that engineers can adjust the composite layups to satisfy specific loading conditions, however it does not mean that the laminate design is arbitrary. In a practical aircraft design process, some design rules should be followed in order to enhance damage tolerance features and avoid stress coupling effects [2, 38]:

(1) Laminate should be balanced to avoid shear-extension coupling;

(2) Stacking sequence should be symmetric to circumvent extension-bending coupling;

(3) In order to reduce transverse shear stress and minimize edge splitting, stacking of more than 4 plies of the same orientation should be avoided;

(4) It is recommended to have at least 10% of the fibres in each direction, and the maximum of any single orientation is 70% in either 0° or 90°, and 80% in the ±45°, which can help to achieve good damage tolerance characteristics;

(5) At least put one set of ±45° plies on the outside of the laminate to take damage tolerance and maximize panel shear buckling;

(6) If the laminate is to be assembled by mechanical fastened joints, at least 40% of ±45° plies are needed to maximize the bearing strength.

4.5.3 CPO Program Development

Compared to metallic panels, the optimum design of a composite stiffened panel is more complicated, because more design variables (ply angle proportion and stacking sequences) are involved, and some design variables (skin and stringer thickness) fall into discrete problems due to constant ply thickness.

Moreover, if a feasible practical optimum result is required, ply stacking guidelines listed in Section 4.5.2 should also be satisfied, which makes the optimization problem more difficult.

Due to the reason that the panel's buckling load will be influenced by ply angle proportion or stacking sequence, and a practical laminate design has to obey many layup rules, a "Practical Laminate Database" (PLDB) concept is introduced by the author to facilitate the optimum design. By employing PLDB and equivalent elastic constants, an efficient optimum design process for composite panels can be achieved.

4.5.3.1 Program Architecture

Two Visual Basic programs, named PLDBM (Practical Laminate Database Management) and CPO (Composite Panel Optimization) are developed to perform the optimum design, and these two programs should be used together.

The main function of PLDBM is to help users to establish and maintain the practical laminate database (PLDB), which will play an important role in the optimum design process. The interface of PLDBM is shown in Figure 4-13.

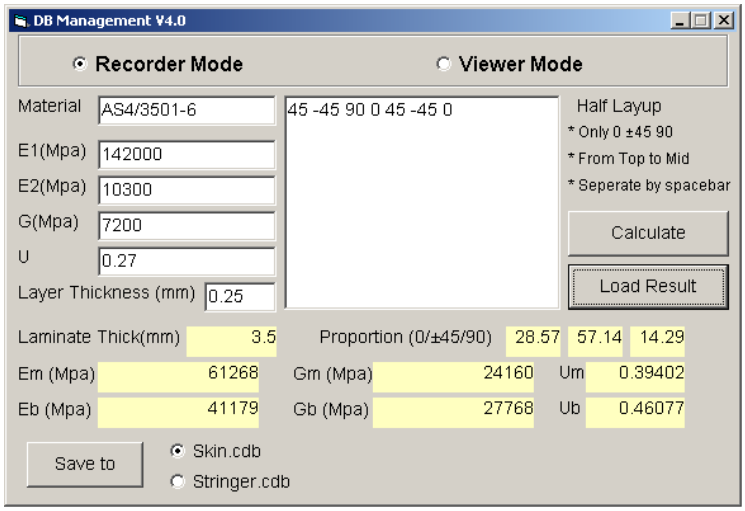

Figure 4-13 PLDBM Program Interface

To insert a new record into PLDB, the users are required to input the ply properties (E1, E2, G, Poisson's ratio, ply thickness) and the layup stacking

sequence. Then PLDBM will employ COALA to calculate the equivalent elastic constants, and the obtained results will be saved to PLDB as a piece of record automatically. There are two separate databases named “Skin.cdb” and “Stringer.cdb” to store skin and stringer candidate layups respectively.

It’s important that the users must make sure the records saved to PLDB are feasible layups according to either the practical layup guidelines or their own engineering experience. It seems that it is such onerous work to establish PLDB because so many records need to be input. But in fact, the layup solutions for different thicknesses are limited due to practical stacking guidelines.

The next step is to obtain the optimum design of a composite stiffened panel. This process is performed by program CPO. The interface of CPO is shown in Figure 4-14. The users are required to input the values of panel’s geometry, compressive load, and define the boundaries of each design variables (bs, ts, bw, tw). Then CPO will carry out the optimum design and present the results.

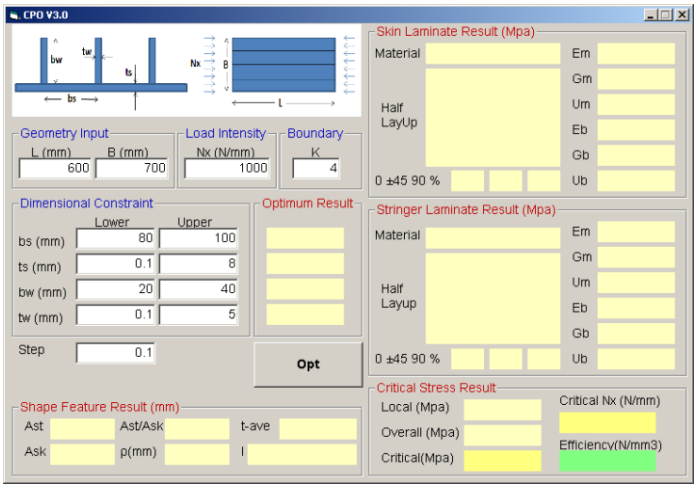

Figure 4-14 CPO Program Interface

In the optimum design process, CPO will keep communicating with PLDB to obtain possible skin and stringer layups. Due to the reason that all the laminate layups are derived from PLDB directly, the final optimum design is definitely to be a practical solution. The dimensional optimum results (bs, ts, bw, tw) and the

layup stacking sequence can be obtained by CPO simultaneously. The whole program architecture is illustrated in Figure 4-15.

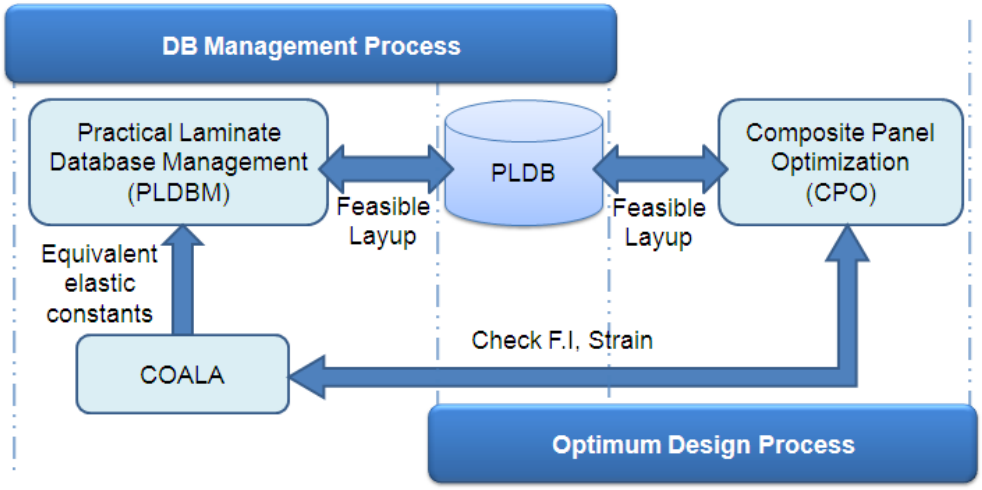

Figure 4-15 Optimum program architecture

4.5.3.2 Optimization Strategy

Optimization is an iterating process. Two factors, namely the design space area and iteration step length will influence the optimization efficiency. Design space area is determined by the upper and lower boundaries of each design variable. In order to achieve a high efficiency, a multi-level and step-length-adjustable strategy is applied in program CPO, which is introduced below:

Step1, a long step length (for example step=1mm) is selected in the first round iteration, CPO will search the whole design space area for a rough optimum solution. If this solution is found, go to next step; if not, adjust the step length to a smaller one, and repeat this process until obtaining the rough solution. For clarity, the rough solution obtained in this round is called Solution1 (bs1, ts1, bw1, tw1).

Step2, the obtained rough Solution1 will be set as the new starting point to iterate. In this round, a narrowed down area which is around Solution1 will be focused on instead of the original whole design area. A new step length which is smaller than that in Step1 will be chosen (for example step=0.5 mm) to carry out a new round iteration to find a more accurate solution, here say it Solution2.

Step3, Solution2 will be selected as the new starting point. A new round iteration will be performed in a further narrowed down design space around Solution 2 at a new step length. Thus in such a way, after several rounds of iteration, the final optimum design solution which satisfies the accuracy requirement will be found.

By using this optimization strategy, CPO works effectively and efficiently. The optimum design flow chart is shown in Figure 4-16.

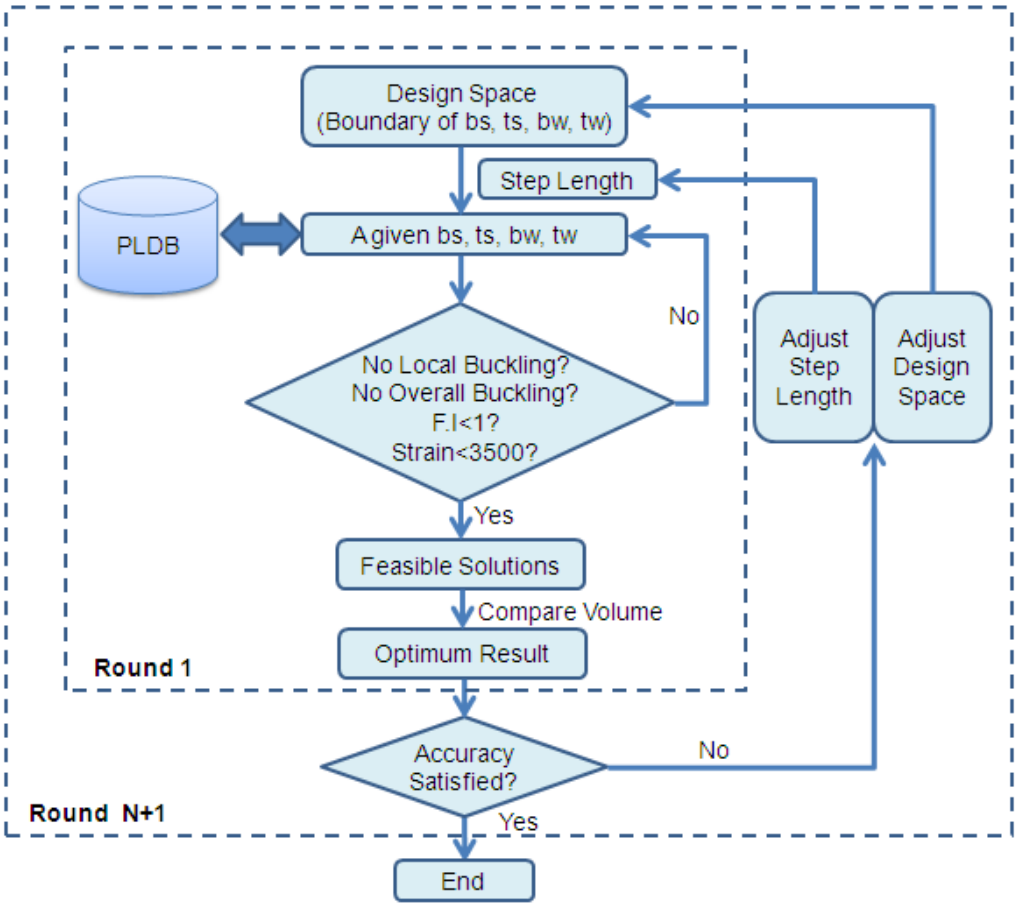

Figure 4-16 CPO program flow chart

4.6 Summary

Compared to metallic panels, the optimum design of a composite stiffened panel is more complicated, because more design variables are involved, and some of them are discrete variables.

Case study shows that ply angle proportion and stacking sequences exert significant influence on the stability characteristics of composite stiffened panels. Local buckling stability is dominated by skin laminate layups, while overall buckling stability is more sensitive to stringer's construction, and some useful conclusions are obtained:

(1) More ±45° plies in the skin will increase local buckling stability;

(2) More 0° plies in the stringers can enhance overall buckling stability;

(3) To increase critical buckling load, it is beneficial to put ±45° plies as far away as possible from the laminate mid surface.

By employing laminate equivalent membrane and bending engineering constants, the composite panels can be treated as metallic panels, which will greatly simplify the analysis process. Based on CF equations and equivalent modulus, a VB program CPBA is developed to perform buckling analysis. The results obtained by CPBA are very close to FE analysis, which proves that the equivalent method is feasible and effective.

Based on the concept of combining a practical laminate data base (PLDB), a VB program CPO is developed to solve the composite panel optimum design problem using a multi-level and step-length-adjustable optimization strategy. There are some advantages of CPO:

(1) All the records in PLDB are feasible layup candidates which can be directly applied to a practical design. CPO will select some appropriate layups from PLDB to achieve the optimum design, which guarantees that the final result given by CPO is definitely a practical solution.

(2) Compare to other researchers' two level or three level optimization strategies, CPO can obtain all the design variables optimum values (geometrical dimensions, ply angle proportion, ply stacking sequence) at one level, which greatly simplifies the optimization process.

5 Outer Wing Box Optimum Design

5.1 GDP Wing Box Introduction

Flying Crane is a new generation130-seat civil aircraft. CCAR 25 is used as the airworthiness standard during the design. The design philosophy is a combination of strength, stiffness, weight, cost, reliability and maintainability.

The wing box is a two spar configuration. The front spar locates at 15% wing chord, while the rear spar is at 65% wing chord. Advanced composite material AS4/3501-6 is used for both inner and outer wing design. All the stringers are parallel to outer rear spar with a constant pitch on considerations of load transfer efficiency, manufacturability and maintainability. In this chapter, the optimum design work will focus on the outer wing stiffened skin panel, which starts from wing station 7467mm to wing tip. The outer wing skin panel is naturally divided into 14 sections by ribs, see Figure 5-1.

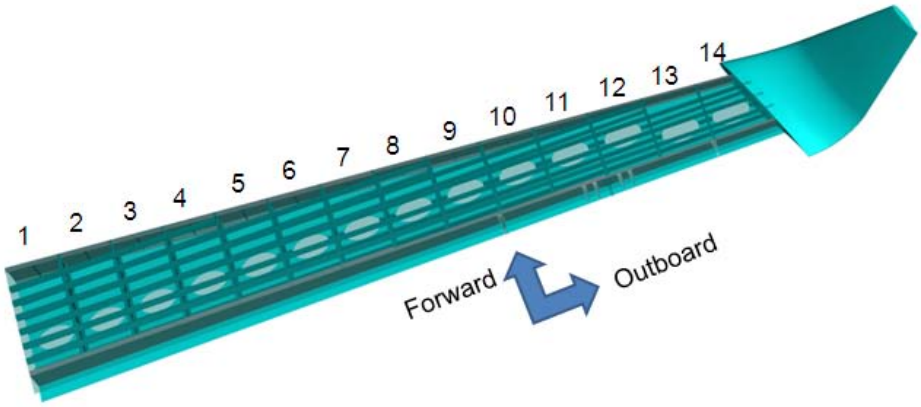

Figure 5-1 Flying Crane outer wing box

5.2 Initial Sizing Results

According to the structure layout, the geometry of each wing box section is determined by the location of spars and ribs. Based on loading calculation [39], the max bending moment, torque and shear force under ultimate load in each box section are obtained, the loading data are listed below:

Table 5-1 Outer wing box loading results [39]

Box No.	BM max (Nm)	SF max (N)	T max (Nm)
1	1289365.83	290471.18	164179.39
2	1137627.48	263688.77	146488.86
3	994057.89	237888.90	129886.78
4	858346.75	219792.58	114288.48
5	730202.65	207445.65	99681.51
6	589826.26	193746.77	83946.97
7	476958.02	182562.76	71487.62
8	336610.50	168410.25	56229.98
9	239561.98	152735.92	45877.75
10	156241.62	123533.55	36475.62
11	83412.96	86755.22	26613.83
12	41161.86	57085.14	19179.15
13	18937.76	30785.51	12516.80
14	4510.08	12816.68	5870.82

The initial sizing process uses the approach introduced in Ref [40].

(1) Skin Thickness Sizing

Firstly, the equivalent skin thickness t_e should be obtained. Equivalent skin thickness is an average thickness where the stringers' area is merged into skin thickness. Two loading conditions, which are overall torsion and overall bending moment, need to be considered to evaluate equivalent skin thickness.

Equivalent skin thickness due to overall torsion can be determined by the following equation:

$$t_q = \frac{T}{2A\sigma_s} \qquad \textbf{Equation 5-1}$$

Where,

T = Applied ultimate torque

A = Wing box cross section area

σ_s = Allowable shear stress

Equivalent skin thickness due to overall bending moment is determined by the following formula:

$$t_b = \frac{M}{hw\sigma_b} \qquad \textbf{Equation 5-2}$$

Where,

M = Applied ultimate bending moment

h = Mean depth of the wing box cross section

w = Distance between front and rear spars

σ_b = Allowable proof stress, it can be defined as

$$\sigma_b = \bar{A}\left(\frac{P}{wL}\right)^{0.5} F_B \qquad \textbf{Equation 5-3}$$

Where,

$\bar{A}$ = Function of material

F_B = Stringer configuration coefficient

P = Effective end load, which equals to M/h

L = Rib pitch

Then the larger value between t_q and t_b is equivalent skin thickness t_e. The skin thickness can be approximately determined by t_s=0.65 t_e.

(2) Stringer Dimensional Sizing

The sizing of stringer is performed by Dr. Guo's program TWpanles, which is based on Niu's design guidelines.

Based on above methods, the initial sizing results for each upper skin panels are obtained. Then according to the achieved skin and stringer dimensions, the normal load intensity and shear load intensity in each panel can be calculated. These results are summarized below.

Table 5-2 Initial sizing results and load intensity

Panel No.	L (mm)	B (mm)	bs (mm)	ts (mm)	bw (mm)	tw (mm)	Nx (N/mm)	Nxy (N/mm)
1	677	1558	206	8	75	5	1924.7	364.5
2	677	1503	206	7	75	5	1844.1	480.4
3	677	1449	206	7	75	5	1727.3	418.7
4	677	1395	206	7	75	5	1640.3	386.6
5	677	1341	206	7	75	5	1514.3	335.4
6	677	1286	206	6	75	5	1406.1	585.7
7	677	1232	206	6	75	5	1241.7	517.4
8	677	1178	206	6	60	4	968.2	400.4
9	677	1124	206	6	60	4	736.9	323.5
10	686	1070	206	5	60	4	582.8	567.4
11	686	1015	206	5	45	3	362.1	387.4
12	686	960	206	4	45	3	199.4	227.4
13	686	905	206	4	45	3	104.6	115.2
14	645	850	206	3	45	3	60.5	111.6

5.3 Optimum Design

From a physical point of view, the thickness of skin stiffened panel is usually small compared to the depth of the wing box, which means that the contribution to the overall stiffness of the wing box is primarily dominated by the depth between the upper and lower wing skin panels, and the contribution made by the skin panel itself in plane stiffness is relatively small. Thus in the following optimum design process, the axial load intensity for each panel is assumed to be the same with the initial sizing results to simplify the load calculation.

Two kinds of optimum design are performed: free sizing and constraint sizing. Only axial compressive load Nx is considered in the optimization process. CPO is employed to obtain the optimum solution, and the available laminate layup records in PLDB are listed in Appendix C.

5.3.1 Free Sizing Optimum Design

Each panel will be optimized without any dimensional constraints to obtain the optimum design. The sizing results are listed in Table 5-3.

Table 5-3 Free sizing optimum results

Panel No.	bs (mm)	ts (mm)	bw (mm)	tw (mm)	Skin (layup)	Stringer (layup)
1	52.15	2.5	50.00	2.5	[45/-45/0/90/0]s	[45/-45/0/0/90]s
2	54.19	2.5	49.71	2.5	[45/-45/0/90/0]s	[45/-45/0/0/90]s
3	55.46	2.5	48.80	2.5	[45/-45/0/90/0]s	[45/-45/0/0/90]s
4	56.48	2.5	48.10	2.5	[45/-45/0/90/0]s	[45/-45/0/0/90]s
5	58.11	2.5	47.03	2.5	[45/-45/0/90/0]s	[45/-45/0/0/90]s
6	59.68	2.5	46.08	2.5	[45/-45/0/90/0]s	[45/-45/0/0/90]s
7	62.44	2.5	44.53	2.5	[45/-45/0/90/0]s	[45/-45/0/0/90]s
8	68.51	2.5	41.65	2.5	[45/-45/0/90/0]s	[45/-45/0/0/90]s
9	56.71	2.0	37.53	2.5	[45/-45/0/90]s	[45/-45/0/0/90]s
10	59.71	2.0	40.00	2.0	[45/-45/0/90]s	[45/-45/0/90]s
11	72.98	2.0	35.54	2.0	[45/-45/0/90]s	[45/-45/0/90]s
12	93.00	2.0	30.74	2.0	[45/-45/0/90]s	[45/-45/0/90]s
13	122.82	2.0	26.58	2.0	[45/-45/0/90]s	[45/-45/0/90]s
14	156.65	2.0	22.65	2.0	[45/-45/0/90]s	[45/-45/0/90]s

The geometrical dimension variation trends are plotted as below.

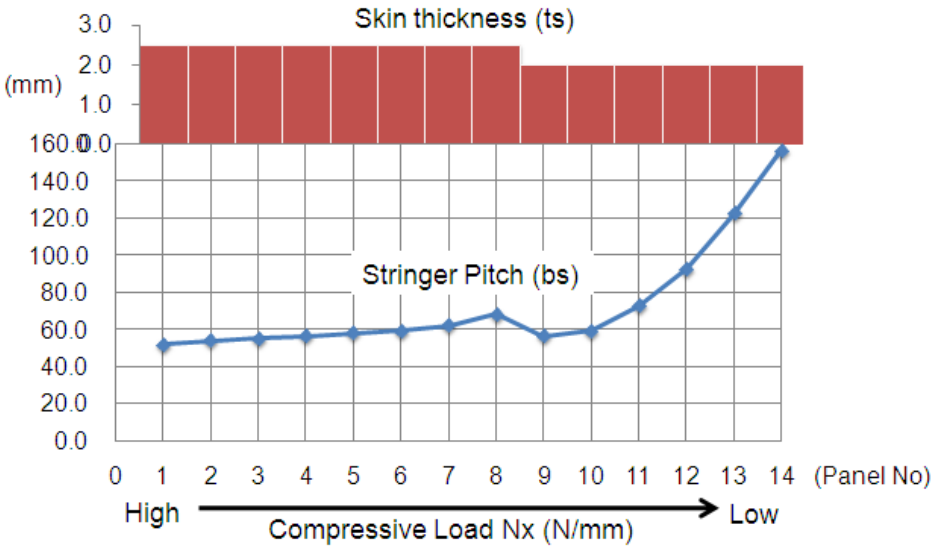

Figure 5-2 Optimum results of skin thickness and stringer pitch

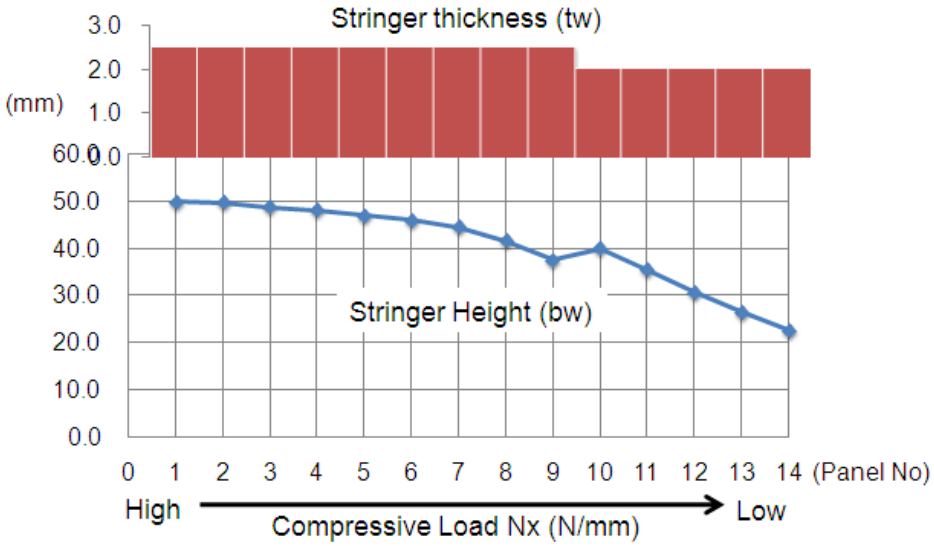

Figure 5-3 Optimum results of stringer thickness and stringer height

Figure 5-2 and 5-3 show that with the decrease of compressive load, skin thickness, stringer thickness and stringer height all drops, but stringer pitch rises up. The trend in Figure 5-2 is different from that of a metallic panel (see Figure 3-3). The discussion about this issue is presented in Chapter 6.

The weight saving of free sizing optimum design is summarized below.

Table 5-4 Free sizing weight saving

Panel No.	Initial (mm^3)	Optimum (mm^3)	Save (%)
1	10358211.74	5165117.30	50.14
2	8975018.58	4877351.49	45.66
3	8652562.82	4610360.84	46.72
4	8330107.06	4371765.26	47.52
5	8007651.31	4106525.77	48.72
6	6808602.15	3857112.21	43.35
7	6522704.39	3572222.38	45.23
8	5714169.20	3205855.38	43.90
9	5452229.36	2780861.72	49.00
10	4525268.93	2451486.66	45.83
11	3937756.55	2070742.42	47.41
12	3065820.58	1752477.73	42.84
13	2890174.61	1510372.94	47.74
14	2004040.05	1255042.77	37.37
Total	85244317.33	45587294.87	46.52

From Table 5-4, a considerable weight saving of 46.52% is achieved after optimization. But this optimum design result is not practical, because each panel has different stringer pitches, which means that the stringers are not continuous along wing spanwise. This situation is totally unacceptable in a practical design. Thus the free sizing optimum result is a theoretical solution, which realizes the global optimum design but not a practical one.

5.3.2 Constraint Sizing Optimum Design

In order to obtain a more practical design, a constraint sizing process is performed. In this optimization case, all the stringer pitches of each panel are constrained to use the same value bs= 206mm, which is the same with initial layout, to make sure that the stringers of the final optimum design can be continuous along spanwise. Under this constraint, the optimum design of each panel is obtained by CPO. The optimum design results and weight saving are summarized in Table 5-5 and Table 5-6 respectively.

Table 5-5 Constraint sizing optimum results

Panel No.	bs (mm)	ts (mm)	bw (mm)	tw (mm)	Skin (layup)	Stringer (layup)
1	206	7.5	60.13	3.5	[±45/90/0_2/±45/90/0/±45/90/±45/0]s	[±45/0_3/90/0]s
2	206	7.0	61.73	4.5	[±45/0/±45/90/±45/0/±45/0/90/0]s	[±45/0_3/±45/90/0]s
3	206	7.0	57.82	3.5	[±45/0/±45/90/±45/0/±45/0/90/0]s	[±45/0_3/90/0]s
4	206	7.0	56.69	3.5	[±45/0/±45/90/±45/0/±45/0/90/0]s	[±45/0_3/90/0]s
5	206	7.0	59.28	3.0	[±45/0/±45/90/±45/0/±45/0/90/0]s	[±45/0_3/90]s
6	206	6.5	55.90	3.5	[±45/90/0/±45/0/±45/90/±45/0]s	[±45/0_3/90/0]s
7	206	6.5	55.51	3.0	[±45/0/±45/90/±45/0/±45/90/0]s	[±45/0_3/90]s
8	206	6.0	51.16	3.0	[±45/0/±45/90/±45/0/±45/90]s	[±45/0_3/90]s
9	206	5.5	46.00	3.0	[±45/0/±45/90/±45/0/90/0]s	[±45/0_3/90]s
10	206	5.0	47.64	2.5	[±45/0/±45/90/±45/0/90]s	[±45/0_2/90]s
11	206	4.5	40.25	2.5	[±45/0/±45/90/±45/0]s	[±45/0_2/90]s
12	206	3.5	38.19	2.0	[±45/0/±45/90/0]s	[±45/0/90]s
13	206	3.5	30.36	2.0	[±45/0/±45/90/0]s	[±45/0/90]s
14	206	2.5	24.26	2.0	[±45/0/90/0]s	[±45/0/90]s

Table 5-6 Constraint sizing weight saving

Panel No.	Initial (mm^3)	Optimum (mm^3)	Save (%)
1	10358211.74	8988321.59	13.23
2	8975018.58	8494827.92	5.35
3	8652562.82	7830497.92	9.50
4	8330107.06	7520546.27	9.72
5	8007651.31	7138752.83	10.85
6	6808602.15	6485922.58	4.74
7	6522704.39	6095671.72	6.55
8	5714169.20	5379216.68	5.86
9	5452229.36	4694975.28	13.89
10	4525268.93	4094477.58	9.52
11	3937756.55	3473422.38	11.79
12	3065820.58	2549138.70	16.85
13	2890174.61	2355899.16	18.49
14	2004040.05	1499756.50	25.16
Total	85244317.33	76601427.14	10.14

The results show that under the constraint of bs=206 mm, the total weight saving of optimum design is only 10.14%, which is a huge decrease compared to the 46.52% weight saving of free sizing optimum design. However, this optimum design is more practical.

5.3.3 FEA Validation

Both the initial sizing results and the constraint optimum design results are modelled and analysed by NASTRAN to check whether they can satisfy the strength and stiffness design requirements, and to demonstrate the comparison between the initial design and optimum design. The FE model is half of the whole wing box which includes both inner wing and outer wing. The description of the modelling process can be seen in Appendix D.

The initial design FEA results are shown in Figure 5-4 to Figure 5-6.

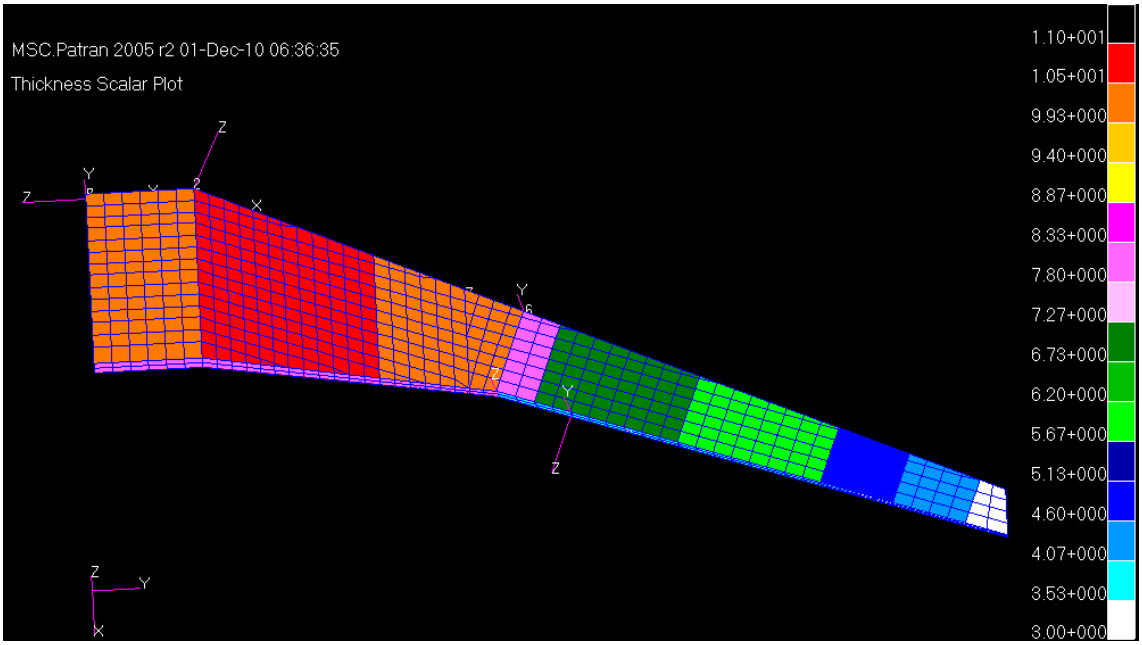

Figure 5-4 Initial design skin thickness

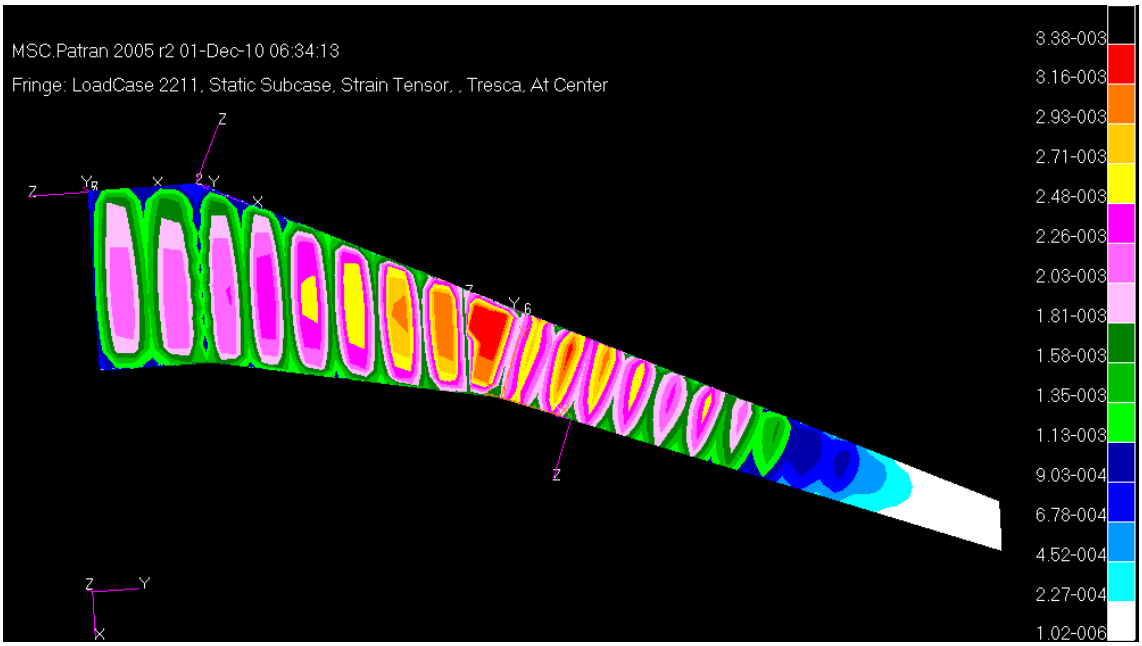

Figure 5-5 Initial design strain

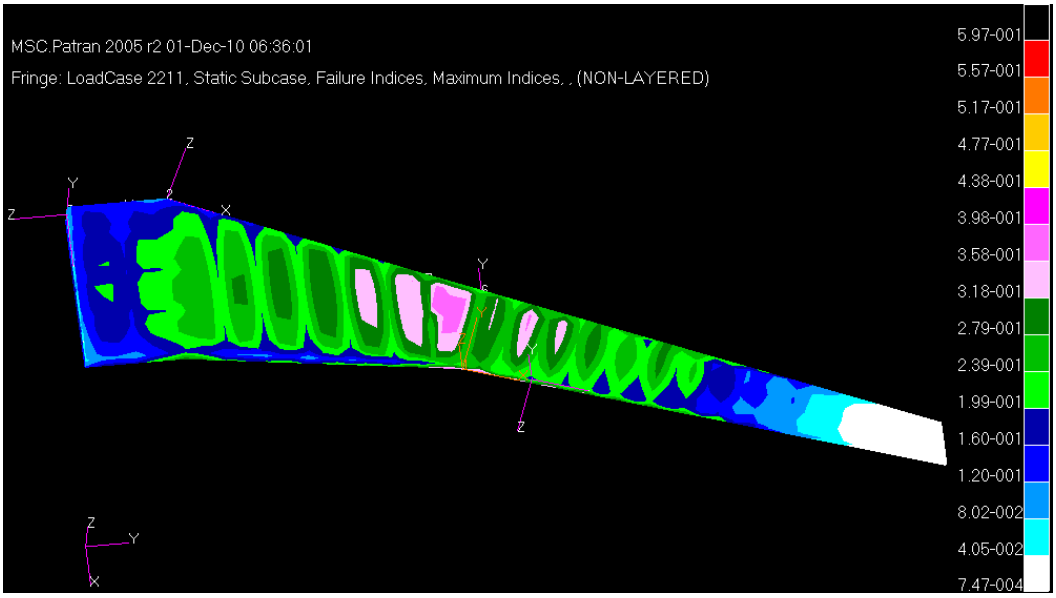

Figure 5-6 Initial design max Hoffman failure index

According to the constraint optimum sizing results listed in Table 5-5, the optimum design FE model is built up. Compared to the initial design FE model, the outer wing skin panel parameters are modified, while the inner wing is not changed. It needs to be mentioned here that the outer wing lower skin panel is also modelled using the same optimum parameters as outer upper skin panel. The optimum design FEA results are illustrated in Figure 5-7 to Figure 5-9.

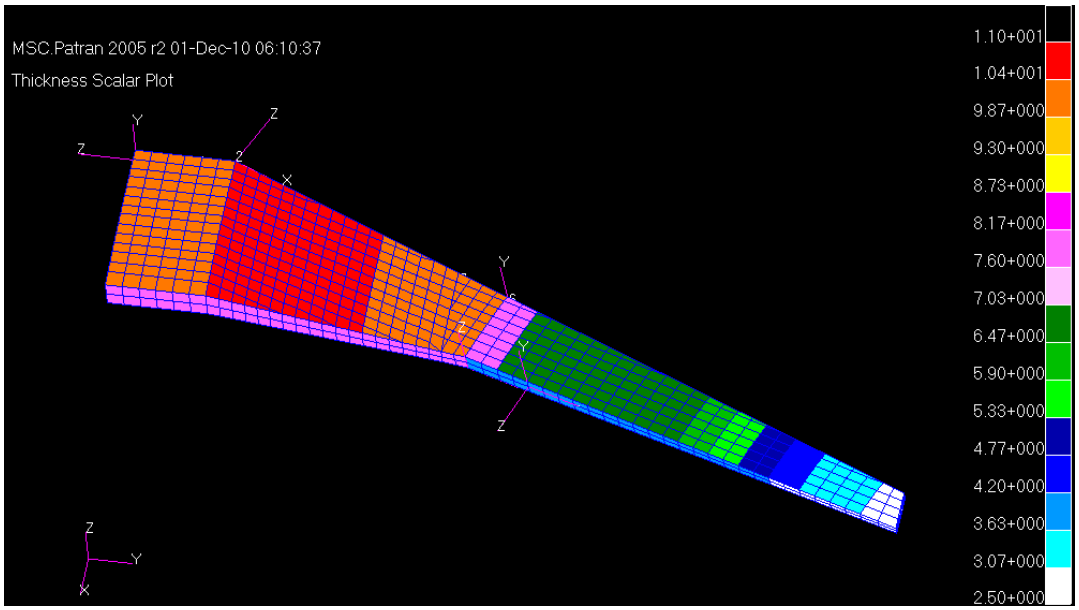

Figure 5-7 Optimum design skin thickness

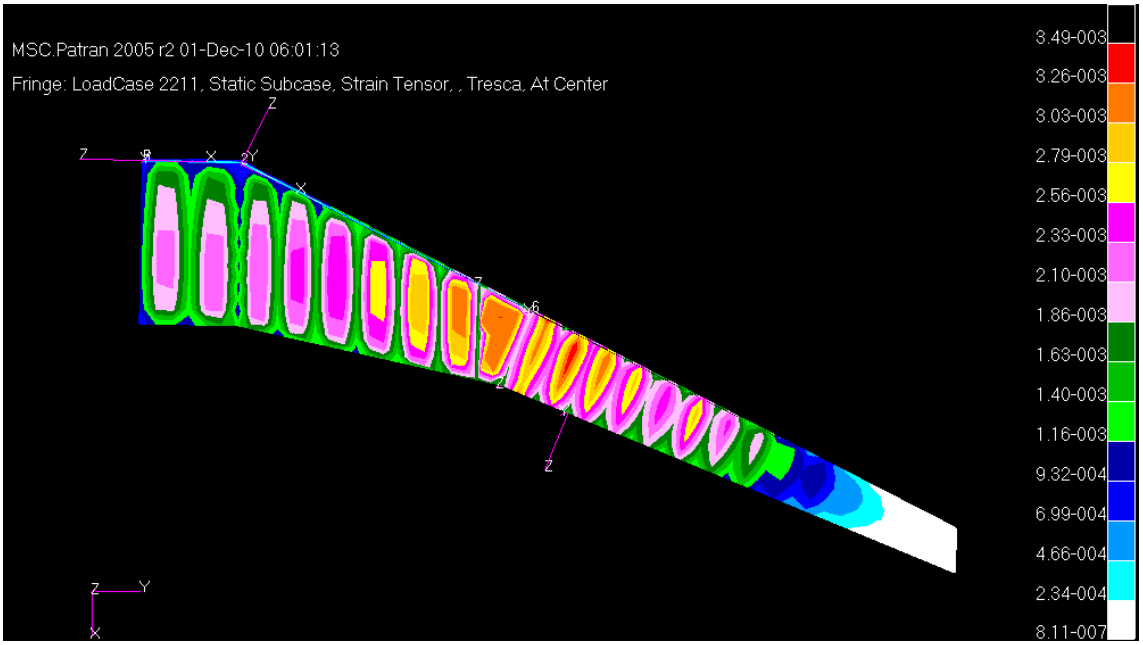

Figure 5-8 Optimum design stain

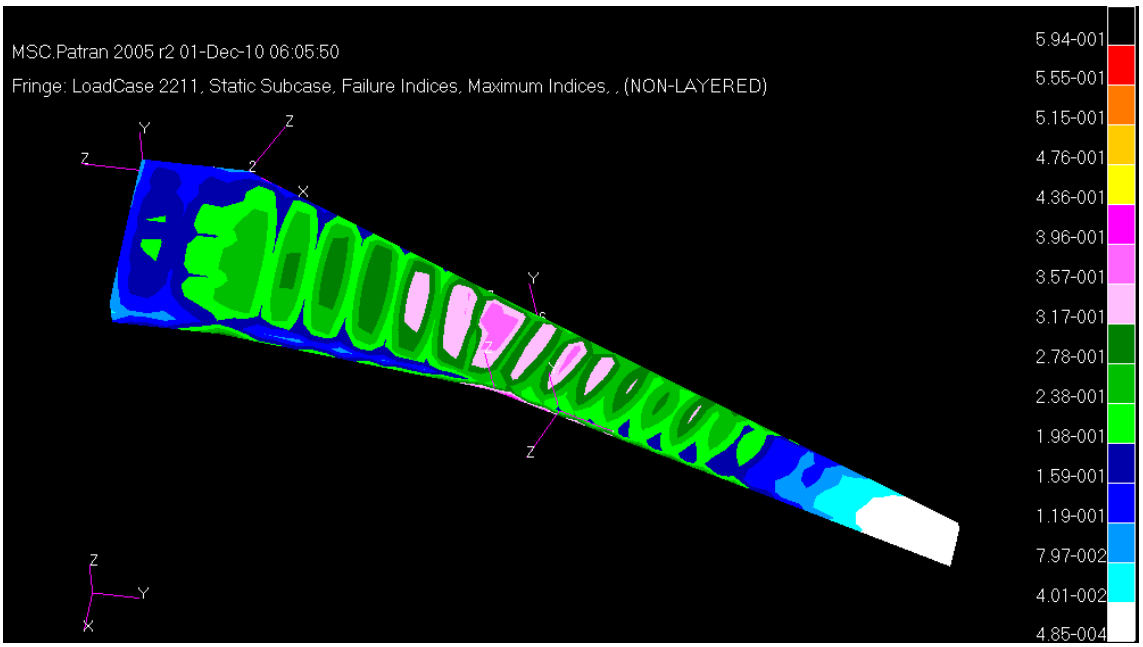

Figure 5-9 Optimum design max Hoffman failure index

The FE analysis result shows that the optimum design still satisfies the stiffness and strength design requirements. The maximum strain is below 3500 με, and the laminate failure indices are under 1.0.

The FEA results of initial design and optimum design are summarized in Table 5-7.

Table 5-7 Results comparison

	Outer Wing Upper Panel		Whole Wing Box	
	Initial	**Optimum**	**Initial**	**Optimum**
Max Strain (με)	3152 [(a)]	3312 [(a)]	3380 [(b)]	3490 [(c)]
Max FI (Hoffman)	0.376 [(a)]	0.380 [(a)]	0.597 [(b)]	0.594 [(b)]

(a) Occurs in outer wing box 02 upper panel

(b) Occurs in inner wing box 07 lower panel

(c) Occurs in outer wing box 02 lower panel

6 Discussion

Flying Crane's outer wing box optimum design shows that a significant weight saving of 46.52% can be obtained from the theoretical point of view. However, when taking practical design requirements (stringers should be continuous) into consideration, the weight saving is just 10.14%, which means that in a practical design, the best solution is usually not the global theoretical optimum result, instead it is more likely to be some local optimum solutions to satisfy or compromise with other design constraints.

Based on the study of Emero's method, the relationship between theoretical optimum panel configuration and compressive load for a length fixed metallic panel (see Figure 3-3 and Figure 3-4) is obtained as below:

(1) Small stringer pitch and thin skin is better when the load is at lower level;
(2) Large stringer pitch and thick skin is preferred when the load is high.

This trend is reasonable because when the load is low, thin skin is abundant to take the load. But thin skin may fall into buckling problem easily, thus close stringer configuration is needed to enhance skin stability, and vice versa. Thus, for a metallic wing box with constant rib pitch (each skin panel section has the same length), the theoretical optimum design of the wing upper skin panel along spanwise can be drawn as Figure 6-1.

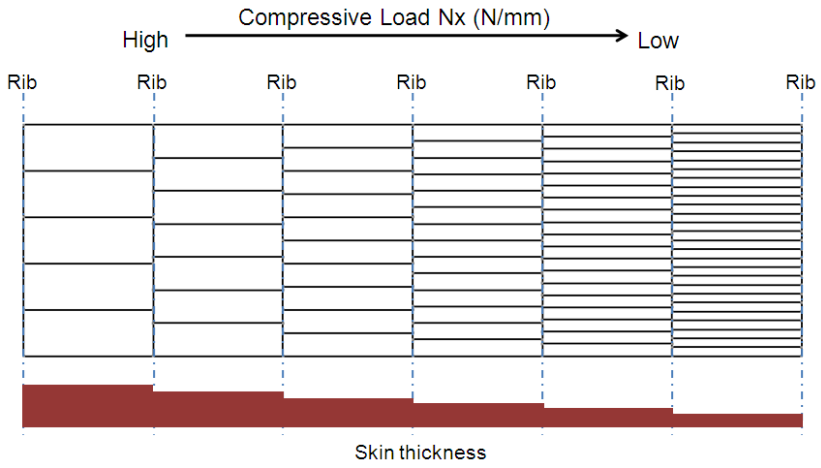

Figure 6-1 Metallic wing panel theoretical optimum design concept

With the decreases of compressive load from inboard to outboard, the stringers become closer and closer along spanwise, and the skin thickness is getting thinner and thinner gradually. The variation trend of wing panel configuration along spanwise is continuous and smooth.

However, according to Section 5.3.1(see Figure 5-2 and Figure 5-3), the theoretical optimum design of a composite wing skin panel along spanwise will not follow this trend. Instead, it can be demonstrated as Figure 6-2.

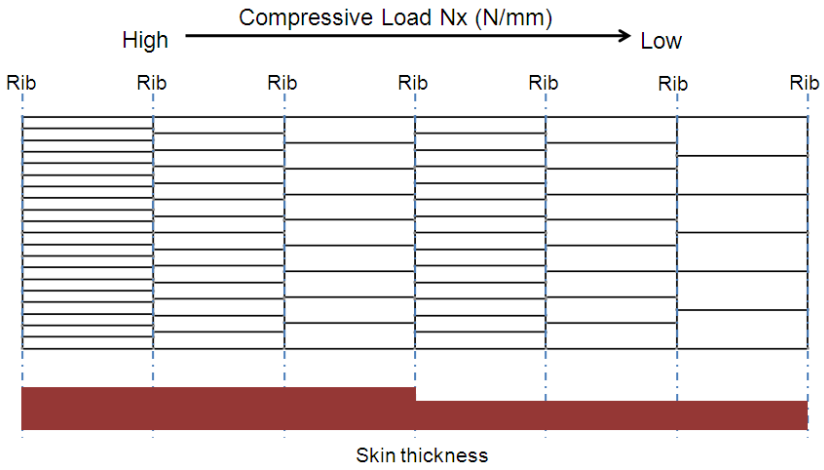

Figure 6-2 Composite wing panel theoretical optimum design concept

With the decrease of compressive load, the stringer pitch is becoming larger where the skin thickness is constant. When the skin thickness changes to another value, it causes a sudden change in the movement of stringer pitch correspondingly. The variation trend of wing panel configuration along spanwise is stepped.

The reason of this phenomenon is that the thickness of laminate is discrete variable due to constant ply thickness. To make it clear, imagine that the inboard first panel in Figure 6-2 is an optimum design and the skin thickness is 4mm. Then the compressive load becomes lower in the second panel, maybe a 3.98 mm skin thickness is efficient, but there is no such a thickness, thus the 4mm laminate has to be used again in the second panel. However, the load in the second panel is lower than that in the first panel, thus the stringer pitch can

be a little larger in the second panel to achieve a high efficiency. For the same reason, when there is a skin thickness change between the third and fourth panel, it will result in a step change in the stringer pitch movement.

Additionally, it can be predicted that if the skin thickness is also constrained to some specific values (skin thickness is not continuous variable) for a metallic wing box, the optimum design will look like Figure 6-2 as well.

Only blade section stiffened panels are used as representatives to demonstrate the study work in this thesis. However the developed optimum method and procedures are general solutions which can be applied to other stringer section panels.

7 Conclusion and Future Work

7.1 Conclusion

The aim of this thesis is to identify an effective way to optimize composite wing structure, especially the stiffened skin panels for minimum weight subject to stiffness and strength constraints. In this thesis, blade stiffened panels under compressive load are selected as representatives to demonstrate the research work.

Firstly, metallic stiffened panels are selected as the starting point. Based on the study of Emero's method and case study of different critical buckling load calculation methods, a VB program IPO, which employs closed form equations, is developed to facilitate the optimum design process. IPO eliminates the limitations of Emero's method, and it is able to give both global and local optimum solutions to satisfy specific practical optimum design requirements.

Then the optimum design method for composite stiffened panels is studied. Case study shows that by employing laminate equivalent membrane and bending engineering modulus, composite panels can be treated as metallic panels to perform buckling analysis, and this equivalent method can give very close results compared to FE analysis. By combining equivalent modulus, closed form equations and a practical laminate database, a VB program CPO is developed to achieve the optimum design of a composite stiffened panel. A multi-level and step-length-adjustable strategy is applied in CPO, which makes the optimum design process effective and efficient.

Lastly, CPO is employed to optimize Flying Crane's outer wing box, and the results are validated by FE analysis. The results show that a theoretical optimum solution can save weight up to 46.52%. However a more practical optimum design will only achieve a weight saving of 10.14%.

Based on the research work in this thesis, some conclusions are obtained and they are listed as follows:

(1) In the design of a metallic stiffened panel subject to axial compressive load, if the panel's length is fixed, the relationship between compressive load and panel's optimum configuration is:

- When the compressive load is low, small stringer pitch and thin skin configuration is efficient;
- When the compressive load is high, large stringer pitch and thick skin configuration is efficient.

  However, if (a) the metallic panel's skin thickness is constrained to some specific values or (b) for a composite stiffened panel optimum design, this trend is not applicable because skin thicknesses are discrete variables.

(2) The optimum design given by Emero's method is the theoretical optimum solution, in other words, it is the global optimum design in the whole design space.

(3) The minimum value between local buckling stress and overall buckling stress is the critical buckling stress. High critical buckling stress is equivalent to high panel efficiency. The highest critical buckling stress can be achieved when local buckling stress equals to overall buckling stress, which means that the panel's highest efficiency can be obtained when the local and overall buckling modes occur simultaneously.

(4) For a metallic stiffened panel (panel length is fixed) subject to a certain compressive load, the panel's efficiency can be improved by decreasing the stringer pitch, but there exists a critical stringer pitch, below which the panel's efficiency will not increase any more.

(5) For a stiffened panel subject to a certain load, if the panel's length is adjustable (panel's length is treated as a design variable), a higher efficiency (critical buckling stress) can be achieved when the panel's length becomes shorter.

(6) Ply angle proportion and stacking sequence exert significant influence on the stability characteristics of composite stiffened panels. Local buckling

stability is dominated by skin laminate layups, more ±45° plies in the skin can increase local buckling stability; while overall buckling stability is more sensitive to stringer's construction, and more 0° plies in the stringers can increase the overall buckling stability.

(7) In order to improve critical buckling load, it is effective to put ±45° plies as far away as possible from laminate mid surface.

To summarize, the optimum design methods for metallic and composite stiffened panels are studied and the optimum design process is established. Four VB programs (IPBA, IPO, CPBA and CPO) are developed to facilitate the optimum design. FE validation results indicate that the methods and procedures presented in this thesis are effective to solve the optimum design problems.

The objectives of the research project have been achieved.

7.2 Recommendation for Future Work

Although all the stated objectives have been achieved, there are a few items which can be further investigated in the area.

(1) Only compressive load is considered in this thesis. For a more accurate optimum design, it should take shear load into account as well.

(2) Although CPO is able to achieve the practical optimum design which satisfies the requirement of stringers' continuity, it ignores the manufacturing constraints of the blending of skin laminate stacking sequence between panels. This subject should be further studied.

(3) Due to time limit, the optimum design work mainly focuses on skin panels, and the panel's length is fixed during optimization process. However, from the whole wing box perspective, the number of ribs can be optimized as well, which means that the length of the skin panel should be treated as a design variable. A more comprehensive wing box optimum design should consider both skin panels and ribs as a whole.

(4) More panel configurations with other stringer sections can be extended into the developed programs.

(5) The results given by the optimization programs can be validated by real test data or existing published data, then some revision can be added to mature these programs.

REFERENCES

1. AVIC GROUP1. (2008), “Flying Crane Conceptual Design Specification”, SOE, Cranfield University.

2. Niu, M.C. (1999), “Composite Airframe Structures”, Conmilit Press Ltd, Hong Kong.

3. S. P. Timoshenko. (1961), “Theory of Elastic Stability”. 2nd edition. McGraw-Hill Book Company, New York.

4. Gerard, G and Becker, H. (1957), "Handbook of Structural Stability: part 2 - Buckling of Compression Elements", NACA TN 3782, NACA, Washington, D.C.

5. Gerard, G and Becker, H. (1957), "Handbook of Structural Stability: part 5 - Compressive Strength of Flat Stiffened Panels", NACA TN 3785, NACA, Washington, D.C.

6. Gerard, G and Becker, H. (1957), "Handbook of Structural Stability: part 6 – Strength of Stiffened Curved Plates and Shells", NACA TN 3786, NACA, Washington, D.C.

7. Rothwell, A. (1968), “Coupled Modes in the Buckling of Panels with Z-Section Stringers in Compression”, Journal of The Royal Aeronautical Society, Feb, 1968

8. Boughan, and Baab. (1944), “Charts for Calculating the Critical Compressive Stress for Local Instability of Idealized T Stiffened Panels”, NACA, WRL-204.

9. Catchpole. E.J. (1954), “The Optimum Design of Compression Surfaces Having Unflanged Integral Stiffeners”, Journal of The Royal Aeronautical Society, Nov, 1954

10. Wittrick, W.H. (1968), “A Unified Approach to the Initial Buckling of Stiffened Panels in Compression”, Aero Quarterly, Vol XIX.

11. Emero, D.H, and Spunt, L. (1965), “Optimization of Multirib and Multiweb Wing Box Structures Under Shear and Moment Loads”, AIAA 6th Structures and Materials Conference, New York.

12. Niu, M.C. (1999), “Airframe Stress Analysis and Sizing (2nd edition)”, Conmilit Press Ltd, Hong Kong.

13. Schmit, L.A and Farshi, B. (1973), “Optimum laminate design for strength and stiffness”. International journal for numerical methods in engineering, Vol. 7, pp.519-536.

14. Schmit, L.A and Farshi, B. (1977), “Optimum design of laminated fiber composite plates”. International journal for numerical methods in engineering, Vol. 11, pp.623-640.

15. Nemeth, M.P. (1992), “Buckling behavior of long symmetrically laminated plates subjected to combined loadings”. TP 3195, NASA.

16. Nemeth, M.P. (1997), “Buckling behavior of long symmetrically laminated plates subjected to shear and linearly varying axial edge loads”. TP 3659, NASA.

17. Agarwal.B and Davis.R.C. (1974), “Minimum Weight Designs for Hat Stiffened Composite Panels under Uniaxial Compression”. NASA TN D-7779, Langley Research Centre, Hampton.

18. Grosset.L, Riche.R.L. and Haftka.R.T. (2004), “A Double-Distribution Statistical Algorithm for Composite Laminate Optimization”, AIAA Journal, AIAA 2004-1910

19. Liu, B., Haftka, R.T. and Akgün, M.A. (2000), “Two-Level Composite Wing Structural Optimization Using Response Surfaces”, Structural Multidisciplinary Optimization, Vol. 20, 2000

20. Herencia. J.E, Weaver, P.M and Friswell, M.I, (2007), “Optimization of Long Anisotropic Laminated Fiber Composite Panels with T-Shaped Stiffeners”, AIAA Journal, Vol. 45, No.10.

21. Liu.W and Butler.R, (2007), “Optimum Buckling Design of Composite Wing Cover Panels with Manufacturing Constraints”, AIAA Journal, AIAA 2007-2215.

22. Liu. D, Toropov. V.V, Querin. O.M and Barton. D.C, (2009), “Bi-level Optimization of Blended Composite Panels” AIAA Journal, AIAA 2009-2182.

23. Emero, D.H, and Spunt, L, (1965), “Wing box optimization under combined Shear and bending”, AIAA 6th Structures and Materials Conference.

24. Seresta. O, Gürdal. Z, Adams. D.B, Watson. L.T, (2004), “Optimal Design of Composite Wing Structures with Blended Laminates”, AIAA journal, 10th AIAA/ISSMO Multidisciplinary Analysis and Optimization Conference.

25. Butler, R., (1995), “Optimum Design of Composite Stiffened Wing Panels - a Parametric Study,” Aeronautical Journal, Vol.99, No.985, pp.169-177.

26. Schuhmacher. G, Murra. I, and Wang. L, (2002), “Multidisciplinary Design Optimization of A Regional Aircraft Wing Box”, AIAA journal, AIAA 2002-5406, 9th AIAA/ISSMO Symposium on Multidisciplinary Analysis and Optimization.

27. Weck. O.D, Agte. J, and Jaroslaw.S., (2007), “State-of-the-Art and Future Trends in Multidisciplinary Design Optimization”, AIAA journal, AIAA 2007-1905, 48th AIAA/ASME/ASCE/AHS/ASC Structures, Structural Dynamics, and Materials Conference.

28. Rajagopal. S, Ganguli. R, (2009), “Multidisciplinary Design Optimization of a UAV Wing using Kriging based Multi-Objective Genetic Algorithm”, AIAA journal, AIAA 2009-2219, 50th AIAA/ASME/ASCE/AHS/ASC Structures, Structural Dynamics, and Materials Conference.

29. Chiba. K, and Oyama. A., (2007), “Multidisciplinary Design Optimization and DataMining for Transonic Regional Jet Wing”, Journal of Aircraft, Vol.44, No.4, 2007

30. Fletcher .R., (1987), “Practical Methods of Optimization”, John Wiley & Sons, New York

31. Rao.S., (1996), “Engineering Optimization Theory and Practice (Third Edition)”, John Wiley & Sons, New York

32. http://en.wikipedia.org/wiki/Genetic_algorithm

33. Nagendra, S.,Haftka,R.T.,and Gürdal,Z., (1993), “Design of a Blade Stiffened Composite Panel by Genetic Algorithm,” AIAA Paper 1993-584.

34. Adams D. B., Watson, L. T., Gürdal, Z., and Anderson-Cook C. M., (2004), “Genetic Algorithm Optimization and Blending of Composite Laminates by Locally Reducing Laminate Thickness”, Advances in Engineering Software.

35. ESDU No. 72012, “Information on the use of data Items on the buckling of plates and compression panels manufactured from isotropic materials”, Engineering Science Data Unit International plc

36. ESDU No. 98016, “Elastic buckling of flat isotropic stiffened panels and struts in compression”, Engineering Science Data Unit International plc

37. Kollar. L.P and Springer. G.S, (2003), “Mechanics of Composite Structures”, Cambridge University Press.

38. Guo. S, (2010),”Design and Analysis of Composite Structures”, MSc Course Note, SOE, Cranfield University.

39. Zhou. S. (2009), “130-seat Civil Airliner Flying Crane Outer Wing Preliminary Design”, SOE, Cranfield University.

40. Howe. D. (2004),”Aircraft Loading and Structural Layout”, Professional Engineering Publishing, Bury St Edmunds.

APPENDIX A

FE Boundary Condition Case Study

A-1 Boundary Condition Case A

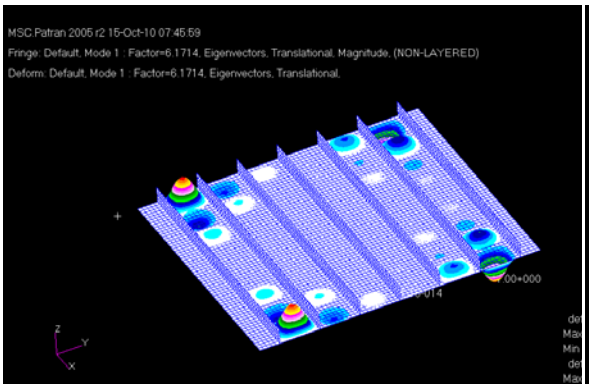

(a) ts=0.5mm

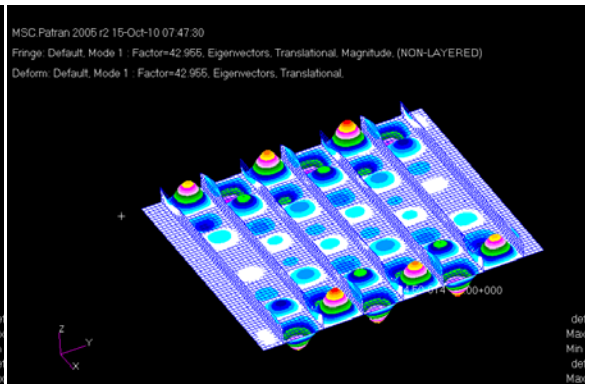

(b) ts=1.0mm

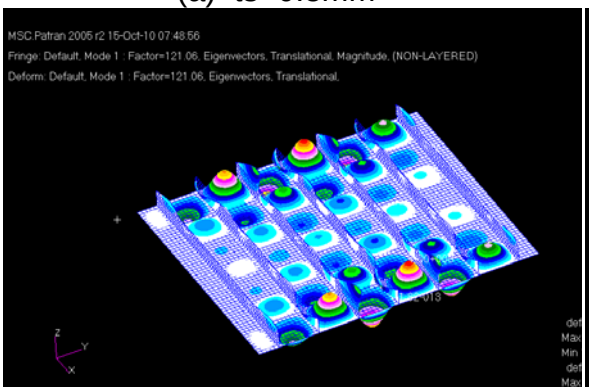

(c) ts=1.5mm

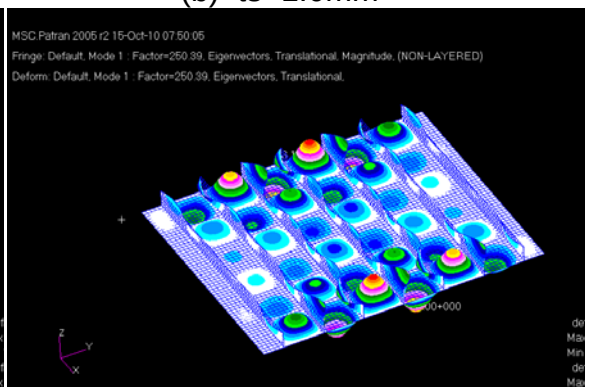

(d) ts=2.0mm

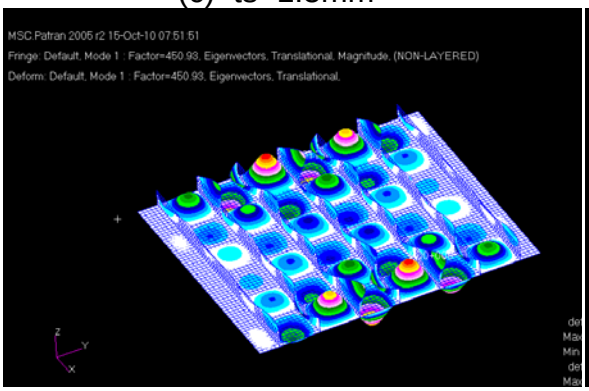

(e) ts=2.5mm

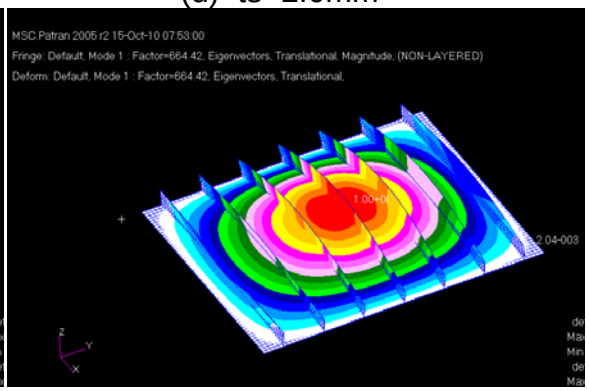

(f) ts=3.0mm

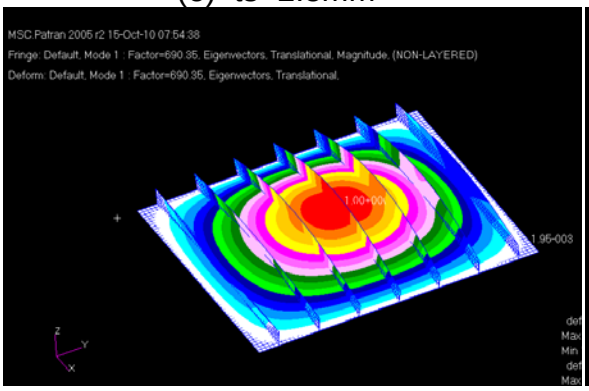

(g) ts=3.5mm

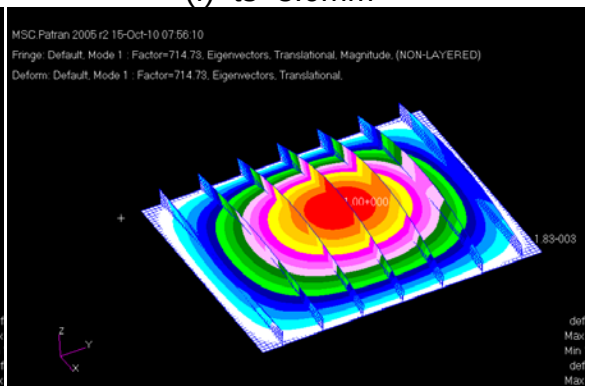

(h) ts=4.0mm

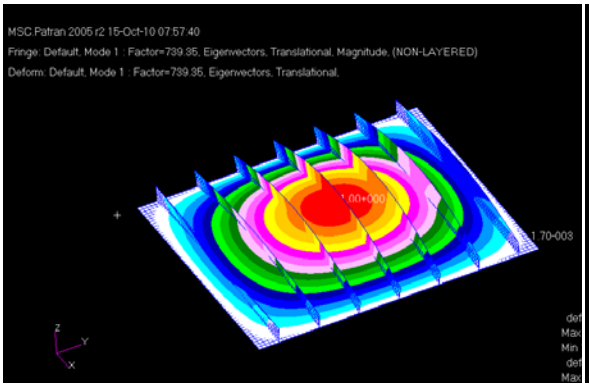

(i) ts=4.5mm

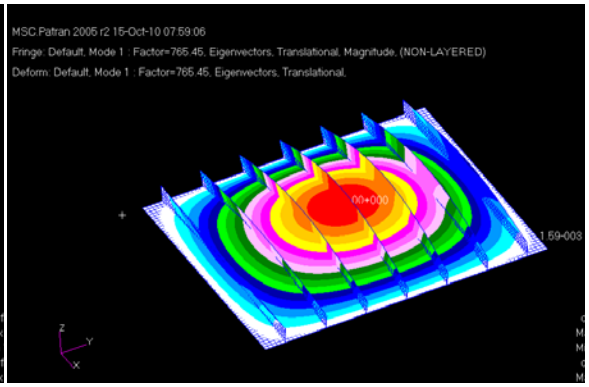

(j) ts=5.0mm

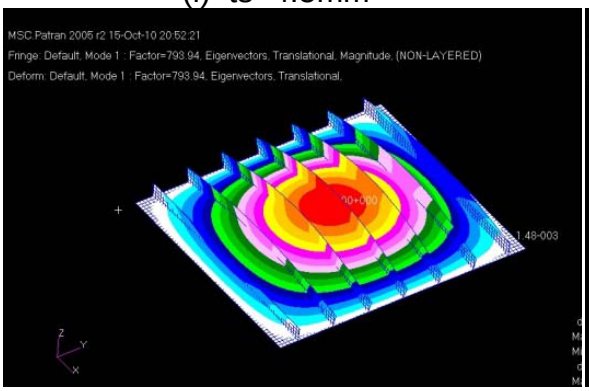

(k) ts=5.5mm

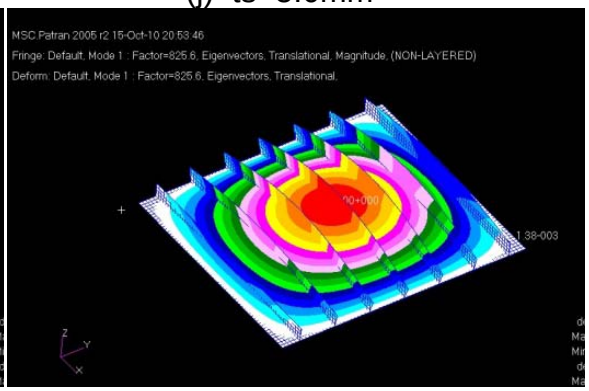

(l) ts=6.0mm

A-2 Boundary Condition Case B

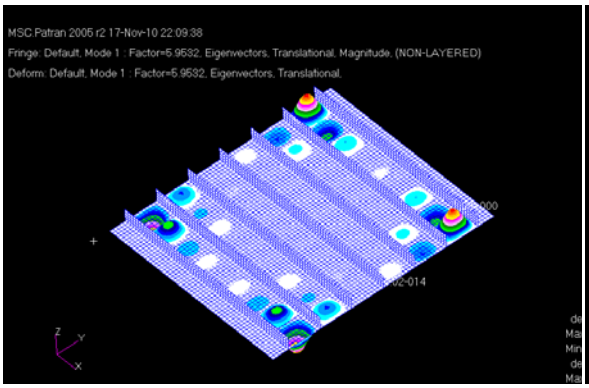

(a) ts=0.5mm

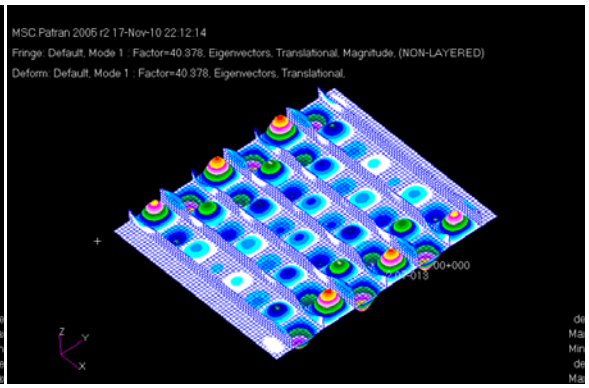

(b) ts=1.0mm

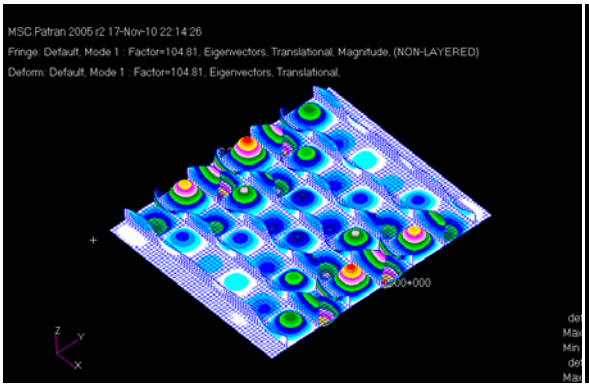

(c) ts=1.5mm

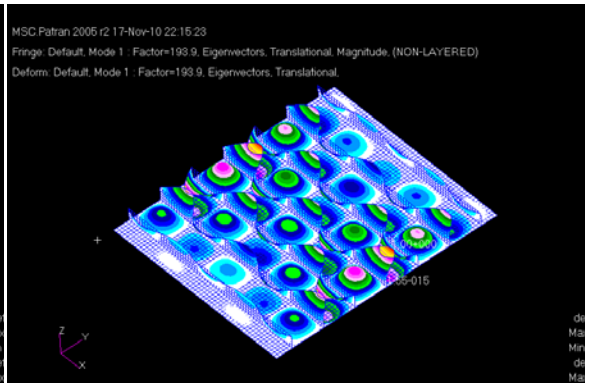

(d) ts=2.0mm

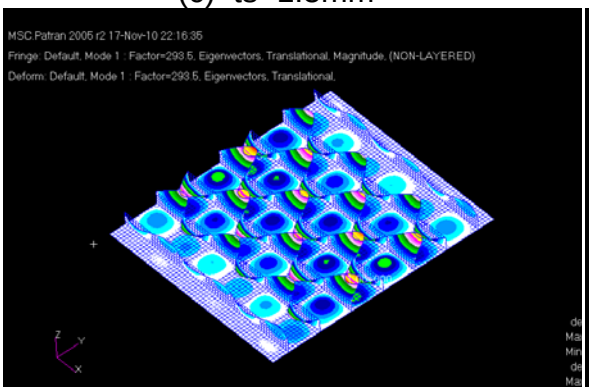

(e) ts=2.5mm

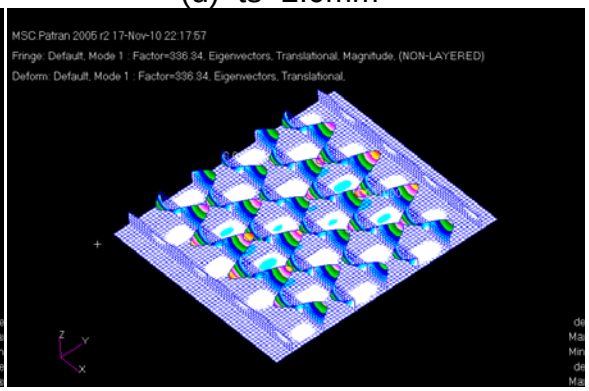

(f) ts=3.0mm

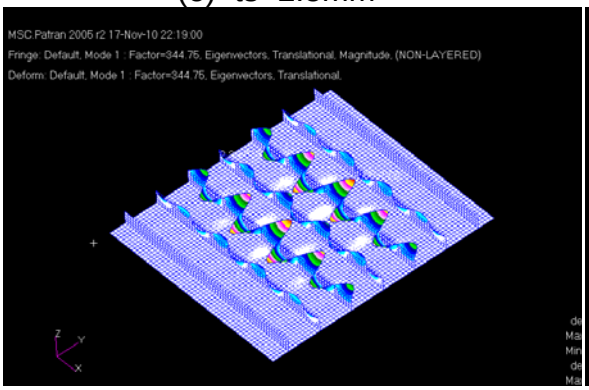

(g) ts=3.5mm

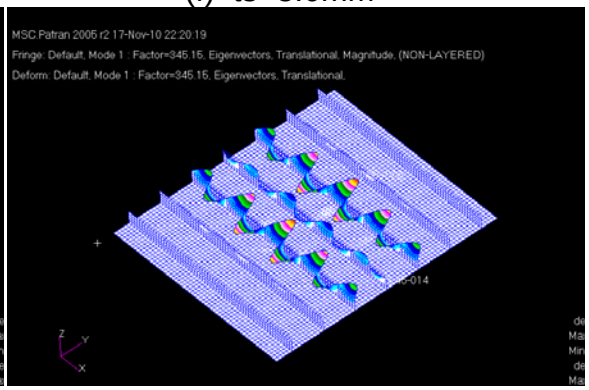

(h) ts=4.0mm

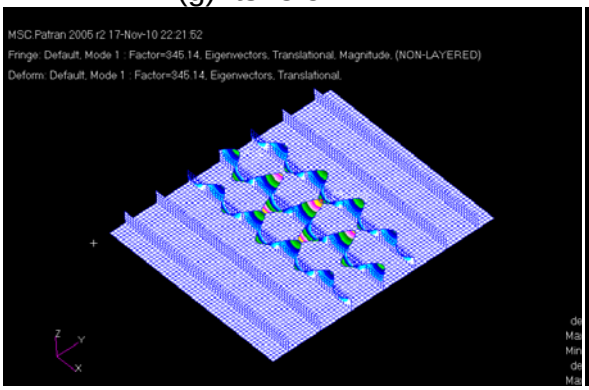

(i) ts=4.5mm

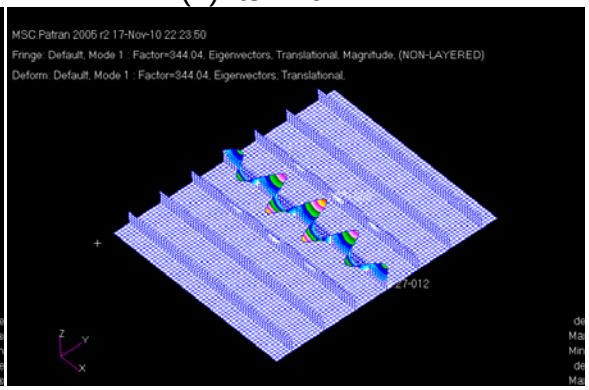

(j) ts=5.0mm

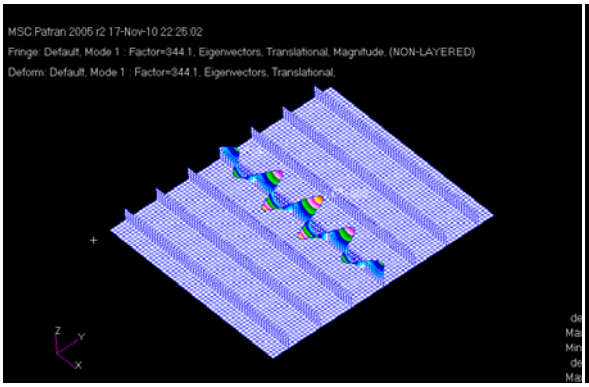

(k) ts=5.5mm

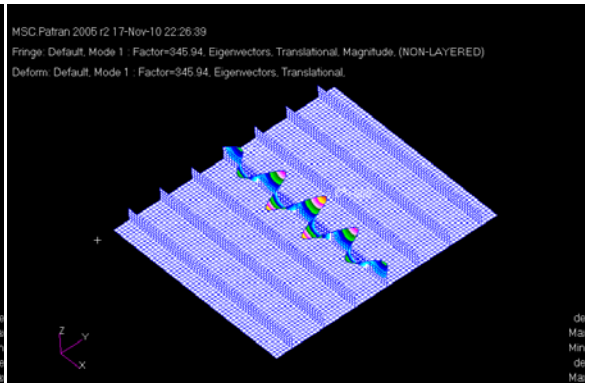

(l) ts=6.0mm

A-3 Boundary Condition Case C

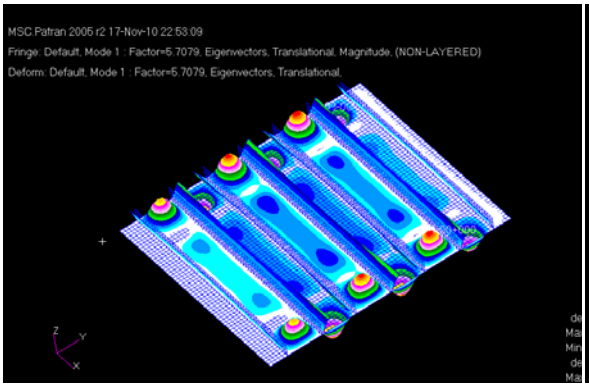

(a) ts=0.5mm

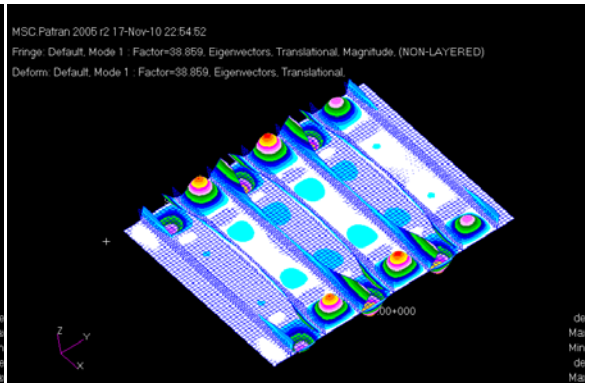

(b) ts=1.0mm

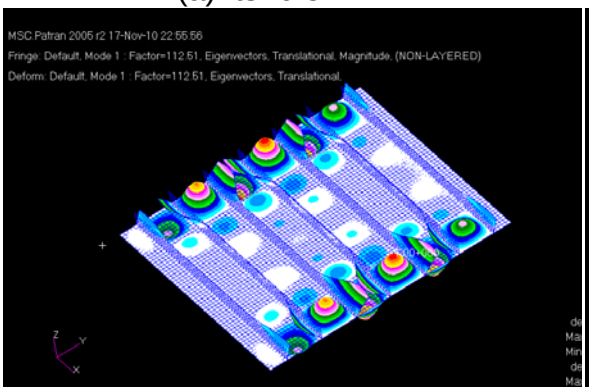

(c) ts=1.5mm

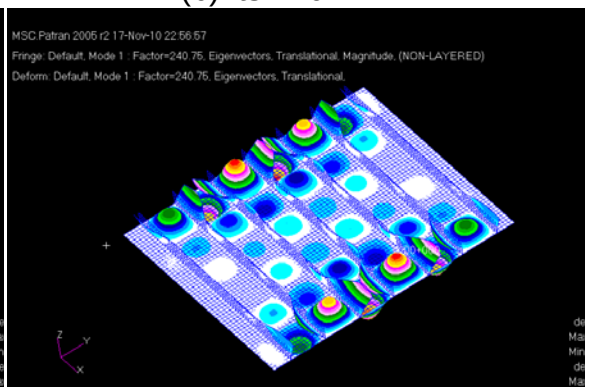

(d) ts=2.0mm

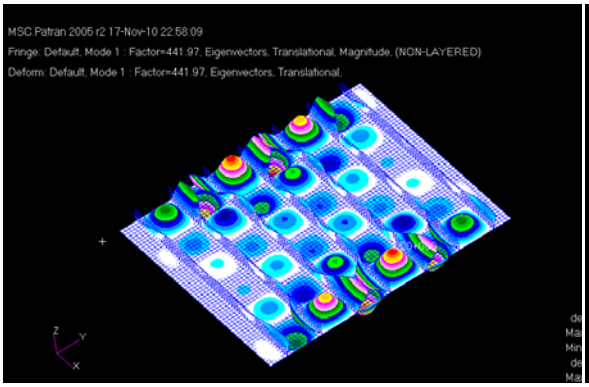

(e) ts=2.5mm

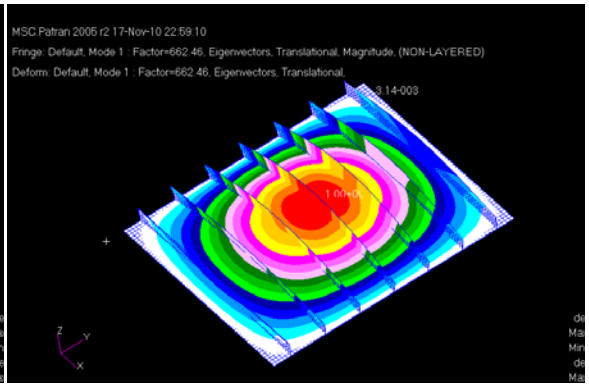

(f) ts=3.0mm

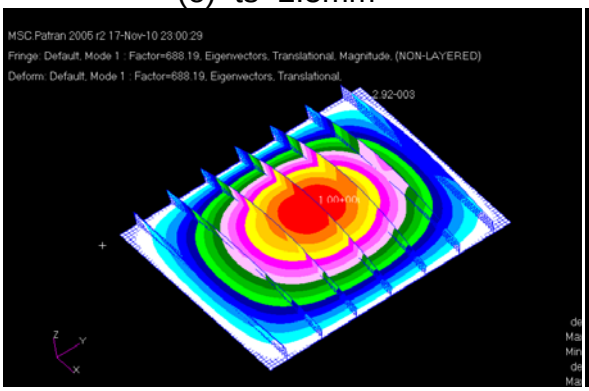

(g) ts=3.5mm

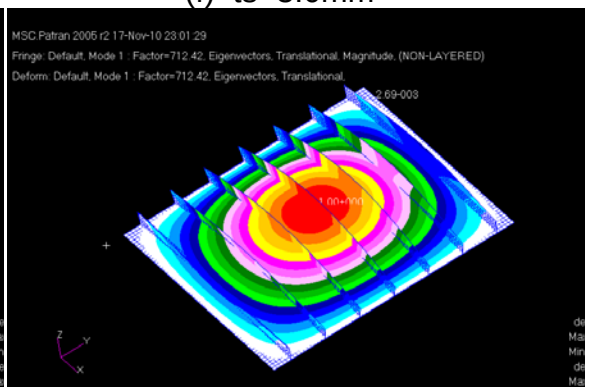

(h) ts=4.0mm

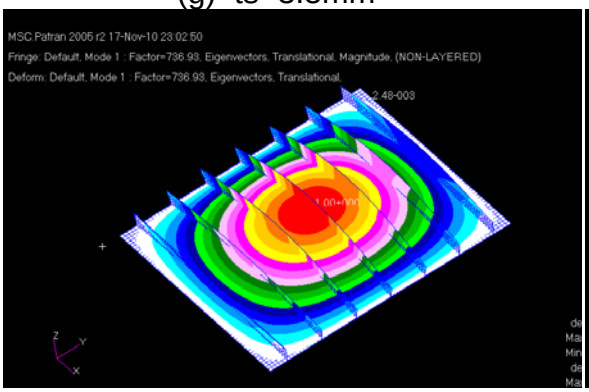

(i) ts=4.5mm

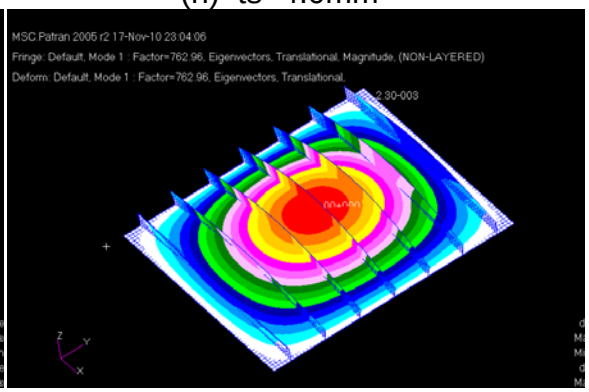

(j) ts=5.0mm

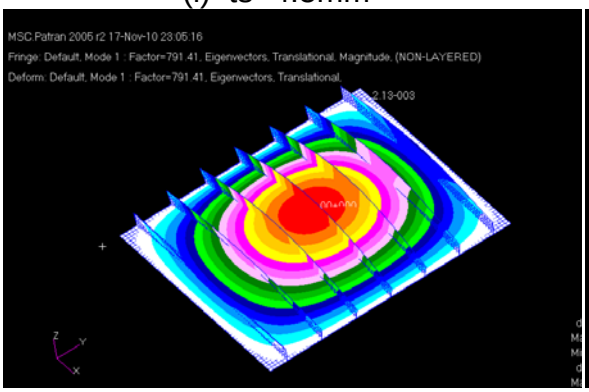

(k) ts=5.5mm

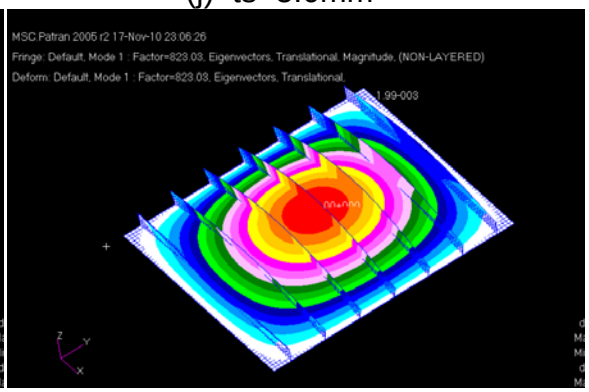

(l) ts=6.0mm

A-4 Boundary Condition Case D

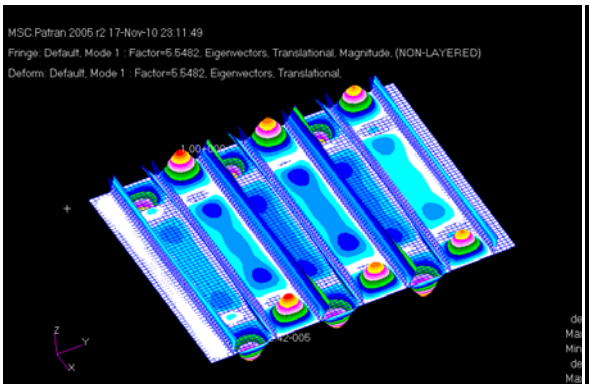

(a) ts=0.5mm

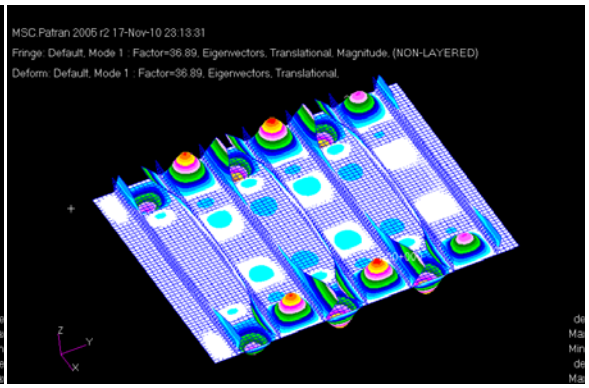

(b) ts=1.0mm

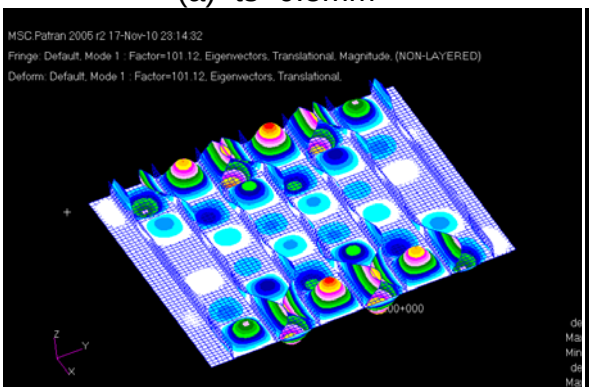

(c) ts=1.5mm

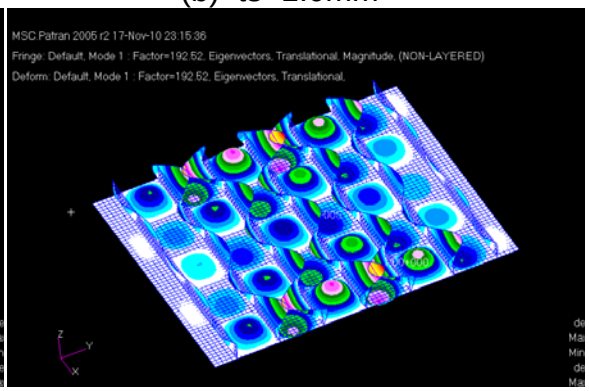

(d) ts=2.0mm

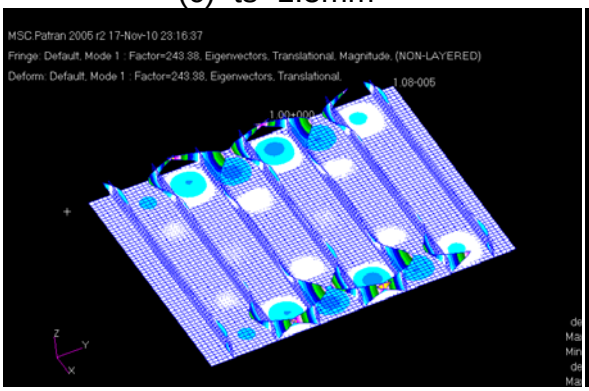

(e) ts=2.5mm

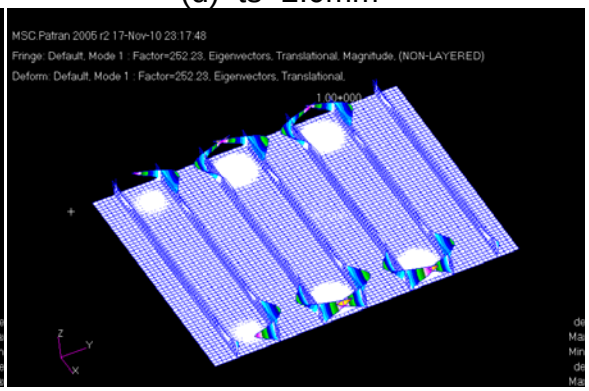

(f) ts=3.0mm

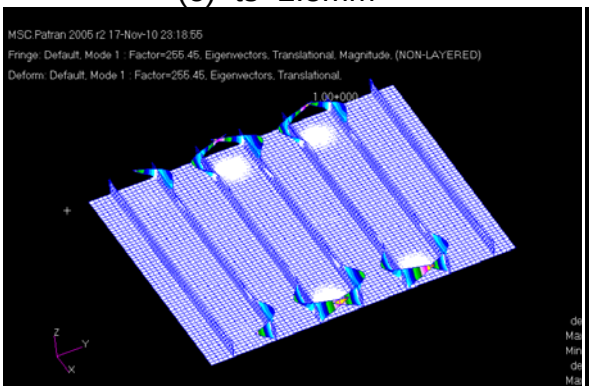

(g) ts=3.5mm

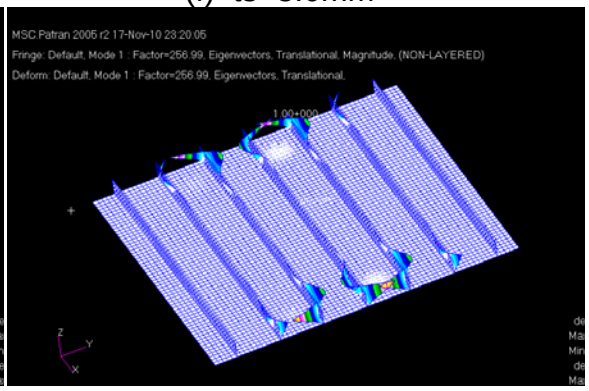

(h) ts=4.0mm

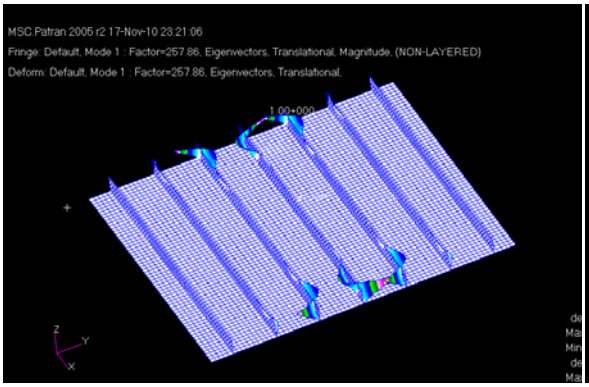

(i) ts=4.5mm

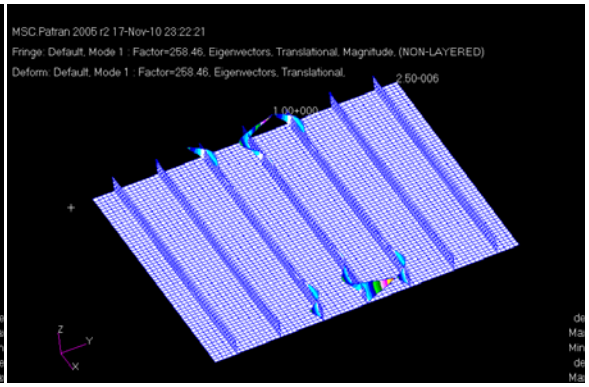

(j) ts=5.0mm

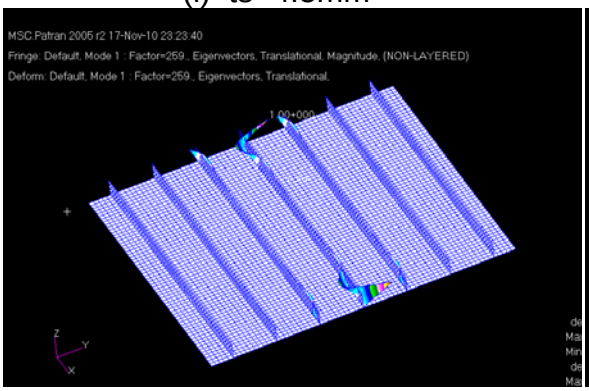

(k) ts=5.5mm

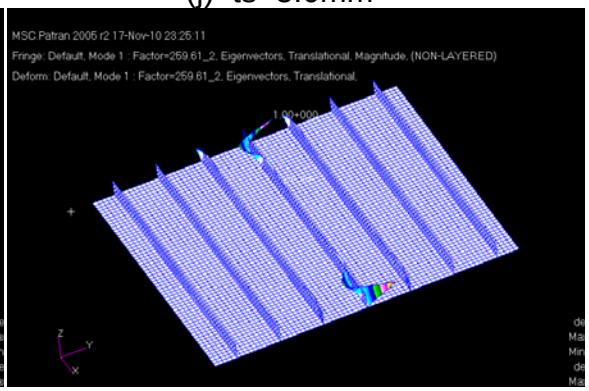

(l) ts=6.0mm

APPENDIX B

Composite Panel Buckling FEA Case Study

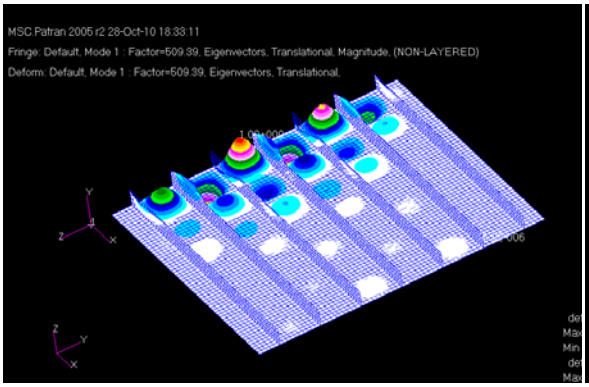

Case 01

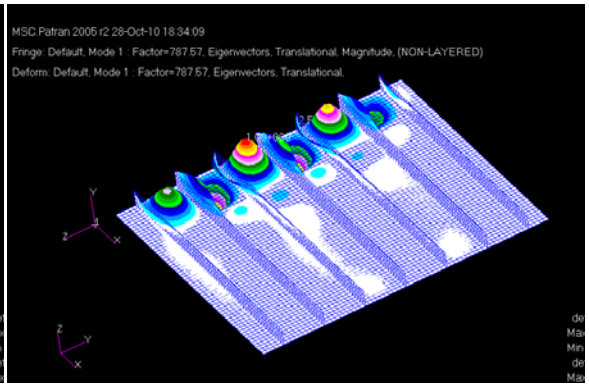

Case 02

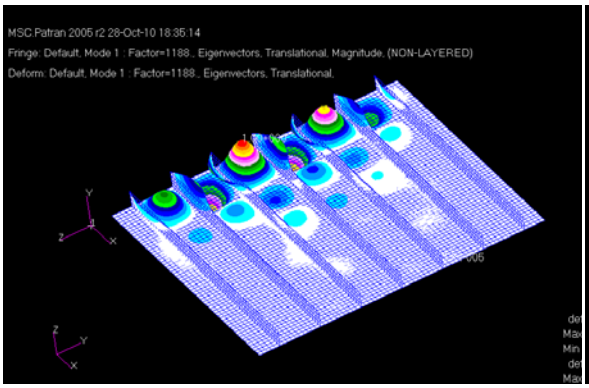

Case 03

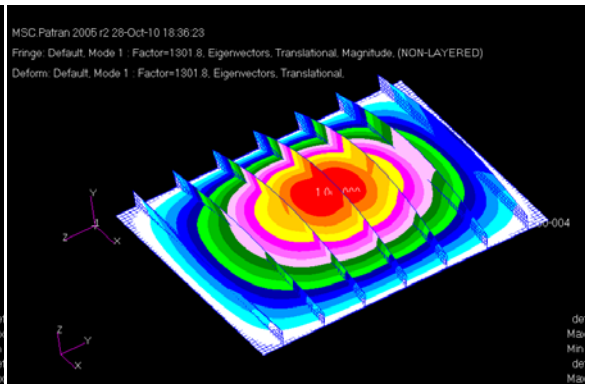

Case 04

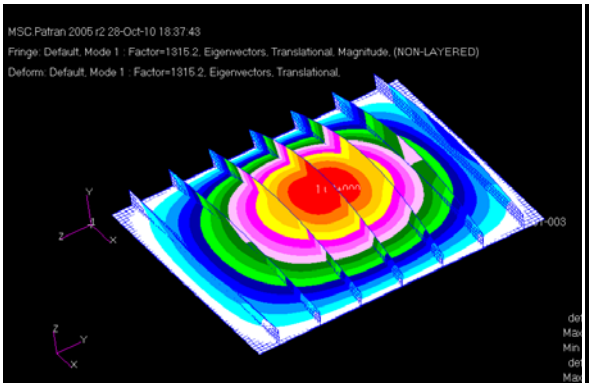

Case 05

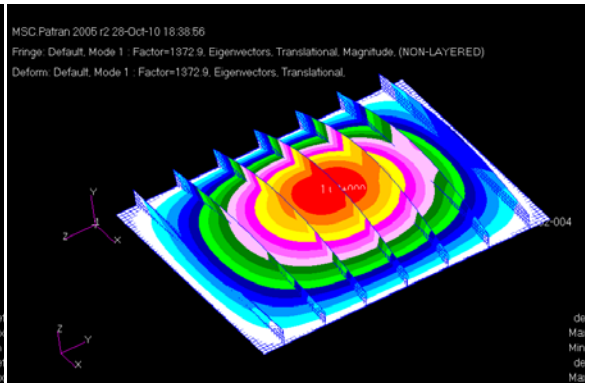

Case 06

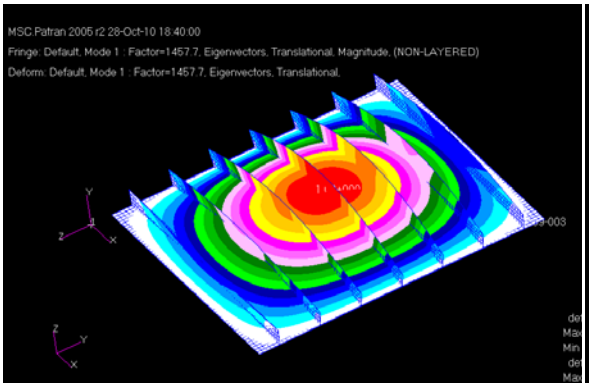

Case 07

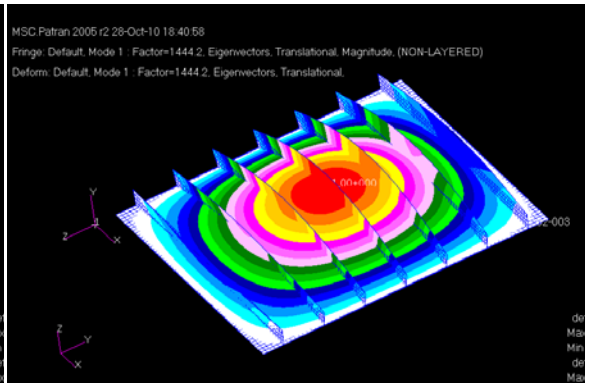

Case 08

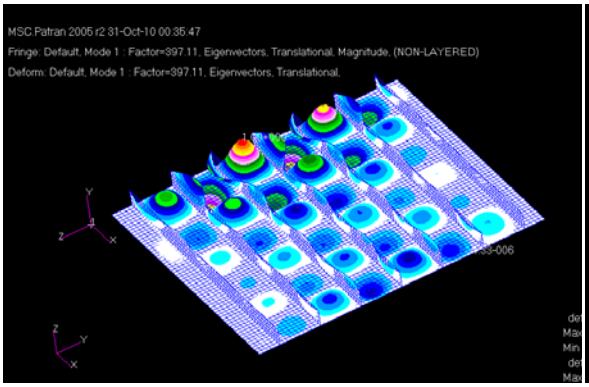

Case 09

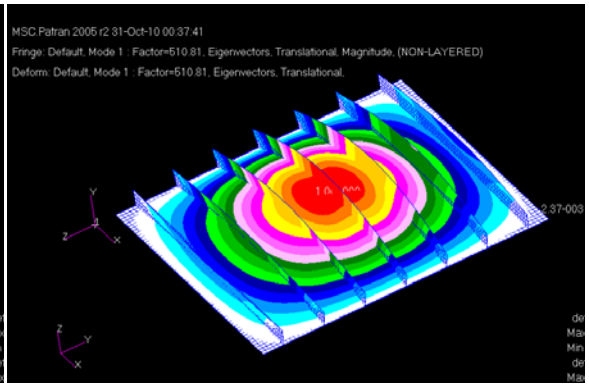

Case 10

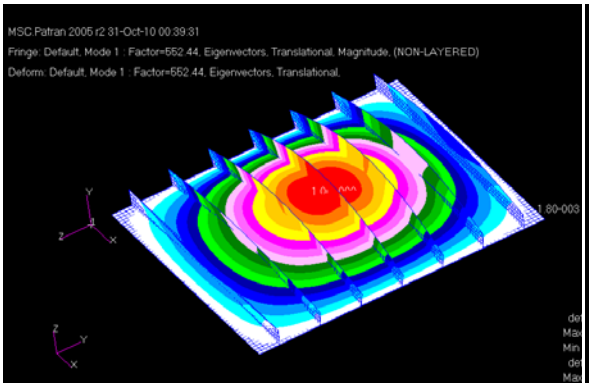

Case 11

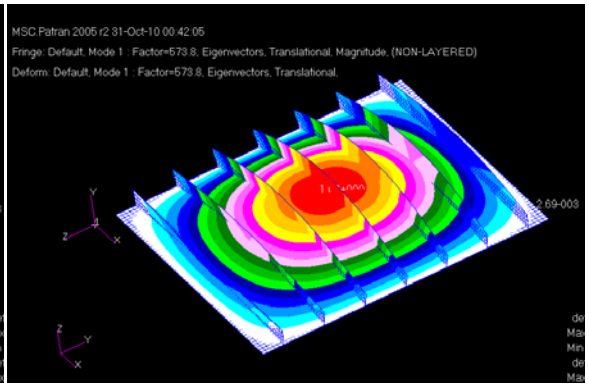

Case 12

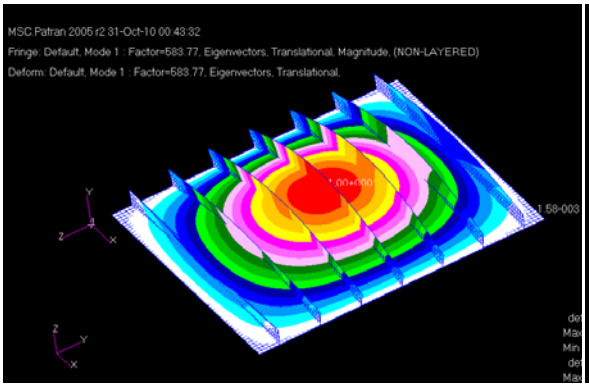

Case 13

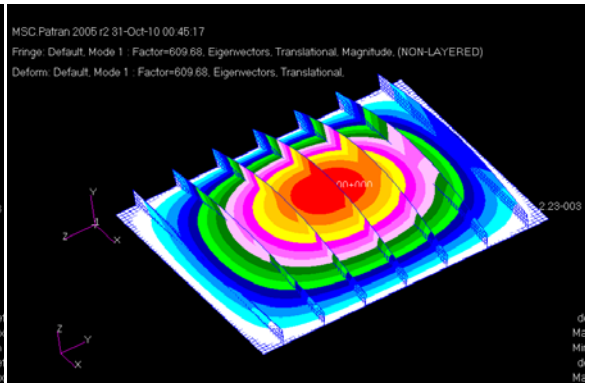

Case 14

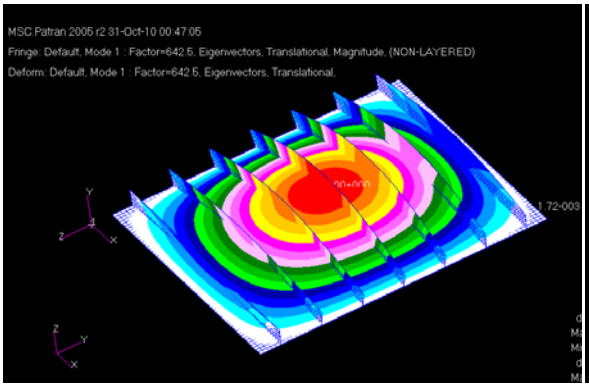

Case 15

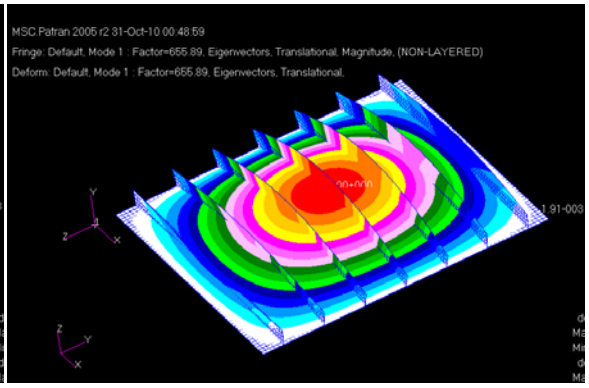

Case 16

The description of the panel’s geometrical dimensions and laminate layups can be found in Table 4-8.

APPENDIX C

Practical Laminate Database Introduction

Two separate databases “Skin.cdb” and “Stringer.cbd” are established to store practical laminate layup information for skin and stringer respectively.

Each record in the database contains the following information:

ID- Unique identification for different layups
Layup- Feasible layup construction (Stacking sequence)
Thickness- Laminate thickness (mm)
Material- Ply material name, AS4/3501-6 is used for all the records here
Em- Membrane equivalent Young’s modulus (MPa)
Gm- Membrane equivalent shear modulus (MPa)
Um- Membrane equivalent Poisson's ratio
Eb- Bending equivalent Young’s modulus (MPa)
Gb- Bending equivalent shear modulus (MPa)
Ub- Bending equivalent Poisson's ratio

Table C-1 Records in skin PLDB

ID	Layup	t (mm)	Em (MPa)	Gm (MPa)	Um	Eb (MPa)	Gb (MPa)	Ub
1	[±45/0/90]s	2.0	56676	22040	0.29	37803	30936	0.48
2	[±45/0/90/0]s	2.5	73741	19072	0.29	45268	29428	0.42
3	[±45/0/±45/90]s	3.0	47785	26986	0.40	44889	30545	0.42
4	[±45/0/±45/90/0]s	3.5	61268	24160	0.39	46702	30186	0.42
5	[±45/0/±45/90/0/90]s	4.0	56676	22040	0.29	48634	29559	0.40
6	[±45/0/±45/90/±45/0]s	4.5	53804	26986	0.46	47116	29728	0.42
7	[±45/0/±45/90/±45/0/90]s	5.0	51521	25008	0.35	47478	29485	0.41
8	[±45/0/±45/90/±45/0/90/0]s	5.5	59753	23389	0.35	48001	29157	0.40
9	[±45/0/±45/90/±45/0/±45/90]s	6.0	47785	26986	0.40	48038	29161	0.40
10	[±45/0/±45/90/±45/0/±45/90/0]s	6.5	55046	25464	0.40	48246	29004	0.40
11	[±45/0/±45/90/±45/0/±45/0/90/0]s	7.0	61268	24160	0.39	49015	28806	0.40
12	[±45/0/±45/90/±45/0/±45/90/±45/0]s	7.5	51442	26986	0.43	48229	28779	0.40
13	[±45/90/0/±45/0/±45/90/±45/0]s	6.5	55046	25464	0.40	49402	26368	0.38
14	[±45/90/0/±45/90/0/±45/90/±45/0]s	7.0	53046	24160	0.33	47688	25281	0.38
15	[±45/90/0/0/±45/90/0/±45/90/±45/0]s	7.5	58979	23029	0.33	57465	23337	0.30
16	[±45/90/0/0/±45/90/0/±45/90/0/±45/0]s	8.0	64170	22040	0.33	58396	23062	0.29

Table C-2 Records in stringer PLDB

ID	Layup	t (mm)	Em (MPa)	Gm (MPa)	Um	Eb (MPa)	Gb (MPa)	Ub
1	[±45/0_3/90/0/90]s	4.0	83700	14620	0.19	71222	24136	0.24
2	[±45/0/90]s	2.0	56676	22040	0.29	37803	30936	0.48
3	[±45/0_2/90]s	2.5	73741	19072	0.29	49395	29361	0.38
4	[±45/0_3/90]s	3.0	85118	17093	0.28	59280	27465	0.31
5	[±45/0_3/90/0]s	3.5	93244	15680	0.28	66104	25701	0.27
6	[±45/0_2/45/0/-45/90]s	4.0	71379	22040	0.39	64196	26245	0.28
7	[±45/0_3/±45/90]s	4.0	71379	22040	0.39	68419	25480	0.26
8	[±45/0_3/±45/90/0]s	4.5	79242	20391	0.39	70497	24910	0.25
9	[±45/0_3/90/±45/90/0]s	5.0	73741	19072	0.29	72381	23180	0.23
10	[±45/0_2/90/0_2/±45/0]s	5.0	85532	19072	0.38	73443	22319	0.22
11	[±45/0_3/90/0_2/±45/0]s	5.5	90677	17993	0.38	80717	21104	0.19
12	[±45/0_2/90/±45/90/±45/0]s	5.5	59753	23389	0.35	61686	24424	0.28
13	[±45/0_3/90/0_2/±45/90/0]s	6.0	85118	17093	0.28	81837	20586	0.18
14	[±45/0_2/90/0_2/±45/0/90/0]s	6.0	85118	17093	0.28	76406	21302	0.20
15	[±45/0/90/0]s	2.5	73741	19072	0.29	45268	29428	0.42
16	[±45/0_2/90/0]s	3.0	85118	17093	0.28	56962	27499	0.33
17	[±45/90/0_3/90]s	3.5	75363	15680	0.19	49544	25759	0.37
18	[±45/90/0_3/90/0]s	4.0	83700	14620	0.19	54845	24172	0.32

APPENDIX D

Flying Crane Inner Wing Detail Design

D-1 Introduction

D-1.1 Background

Flying Crane is a three-year cooperative project between Cranfield University and Aviation Industry Corporation of China (AVIC). As a part of AVIC MSc program, the Flying Crane project consists of three phases: conceptual design, preliminary design, and detail design. Based on previous two cohorts' work, the author is involved in the last detail design phase as the designer of central and inner wing structure.

Flying Crane is a new generation 130-seat airliner, which mainly focuses on Chinese domestic market to replace the current Boeing 737 and Airbus A320 aircrafts. It is designed with new technological features and equipped with new generation systems to achieve the design philosophy: more comfortable, more economical and environmental friendliness.

D-1.2 Scope

The central and inner wing box extends from the centreline of the aircraft to the rear spar kink. Based on the preliminary design, the detailed design and analysis of inner wing contains the following contents:

- Loading review
- Wing layout
- Material and manufacturing consideration
- Major component design (Including skin panels, spars, ribs, wing root joint, main landing gear support beam and attachment)
- Global component finite element analysis
- Local detail stress analysis
- Damage tolerance and fatigue analysis
- Mass and CG estimation
- Airworthiness Compliance

D-1.3 Specifications and Requirements

The specifications and requirements relevant to wing design are quoted below in Figure D-1 and Table D-1. In addition, Flying Crane is designed to satisfy the requirements of CCAR 25.

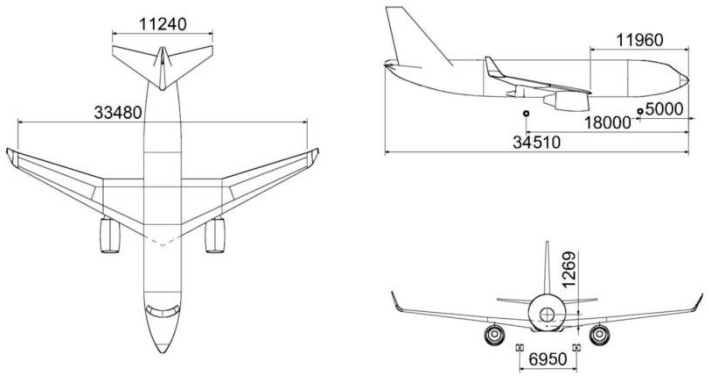

Figure D-1 Three-view of Flying Crane (Unit: mm)

Table D-1 Parameters of Flying Crane

Weight & Capacity	
Maximum take-off weight	64,582 kg
Maximum landing weight	60,707 kg
Operating empty weight	37,844 kg
Performance Requirements	
Range	2000 nautical miles
Cruise Speed	Mach 0.78
Cruise Altitude	12,000 m
Wing Geometry	
Wing Span (excluding winglet)	33.48 m
Wing area (reference)	118 m^2
Leading Edge Sweep angle	28°
Aspect Ratio	9.5
1/4 Chord Line Sweep	25°
Root Chord	7.46 m
Tip Chord	1.63 m
Aerodynamic Mean Chord	3.865 m
Wing-body Incidence Angle	3.5°
Wing Twist Angle	3°
Wing Dihedral Angle	6°

D-2 Loading Review

D-2.1 Flight Manoeuvre and Gust Envelop

Flying Crane flight maneuver and gust envelope (n-V diagrams) are derived from five different masses and five different altitudes as listed in Table D-2, which result in the construction of total 25 maneuver and gust envelopes.

Table D-2 Flying Crane aircraft mass and altitude envelopes

Altitudes (m)	0m	Sea level
	6000	VD becomes Mach limited
	8000	VC becomes Mach limited
	10000	Cruise level
	13000	Maximum achievable altitude
Masses (kg)	64582	Maximum Take off Mass
	60707	Maximum Landing Mass (MLM)
	37844	Operating Empty Mass (OEM)
	58502	1/2 Payload Mass (1/2 PM)
	54844	Maximum Zero Fuel Mass

D-2.2 Load Cases

The design loading diagrams are considered for the combination of five different masses and five different altitudes conditions. The involved cases and manoeuvres are:

- Symmetric manoeuvres
  (Steady rotary motion and pitching manoeuvres);
- Symmetric gusts;
- Asymmetric manoeuvres
  (Steady roll, roll acceleration and combined pitch and roll);
- Asymmetric gusts;
- Manoeuvring load factor of 2.0 with flaps for take-off and landing configuration.

In preliminary design, total 3990 load cases were calculated, from which 16 cases are picked out as critical load cases for FE analysis. These 16 cases, summarized in Table D-3, will lead to either maximum or minimum values of shear force, bending moment or torque at different wing small segment stations. In order to apply the load to the FE model, each load case is pre-processed to obtain the load distribution on each rib. Details of this work can be seen in the author's GDP report.

Table D-3 Critical Load Cases

Case No.	Manoeuvre	n	Mass(kg)	Altitude(m)
1	Symmetric SRM,V_{S1}	2.5	64582	0
21	Symmetric SRM,V_{S1}	2.5	64582	13000
76	Symmetric SRM,V_{S1}	2.5	54844	0
130	Symmetric SRM,V_D	-1	64582	0
135	Symmetric SRM,V_D	-1	64582	6000
205	Symmetric SRM,V_D	-1	54844	0
879	Symmetric pitching,V_D	-1	60707	0
1505	Symmetric pitching,V_{S1}	2.5	64582	0
2104	Steady Roll, SRM,V_D	0	64582	0
2211	Steady Roll, SRM,V_C	1.67	64582	8000
2218	Steady Roll, SRM,V_C	1.67	64582	13000
2963	Roll ac, SRM,V_C	1.67	37844	0
3363	Roll ac & pitching, SRM,V_C	0	60707	8000
3634	Asymmetric, +' ve Gusts, +' ve roll ac. V_C	2.15	64582	0
3685	Asymmetric, +' ve Gusts, +' ve roll ac. V_C	2.33	54844	0
3981	Symmetric SRM,V_{FL}	2	64582	0

D-3 Wing Layout

The inner wing box layout is decided based on considerations of load transfer, strength, stiffness, minimum weight and lower manufacturing cost. In addition, other components related to the wing box such as the high lift devices and the system devices are also taken into account. Figure D-2 shows the overall layout of semi wing.

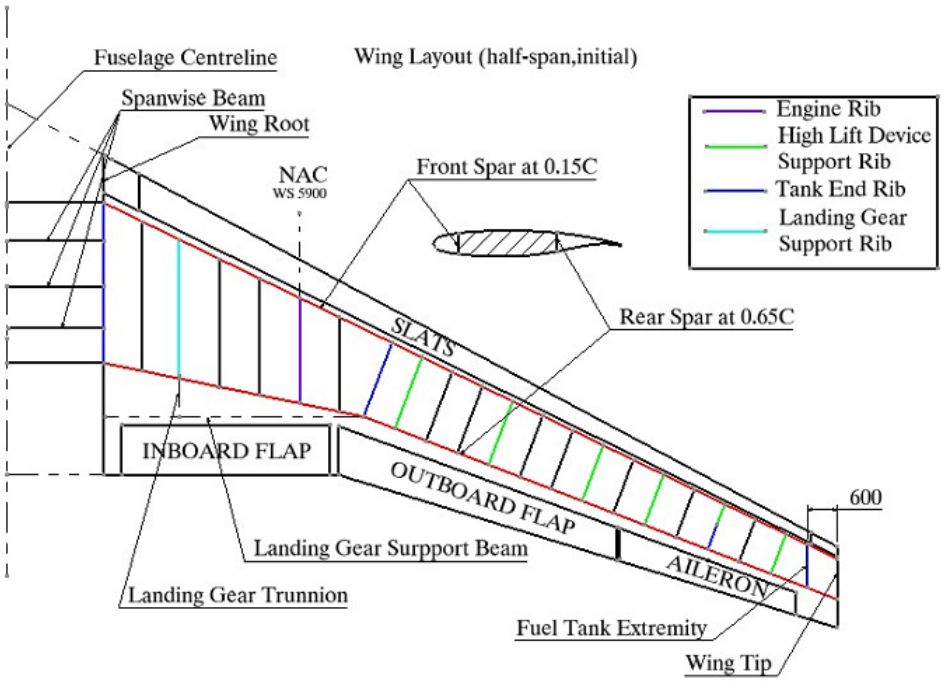

Figure D-2 Semi wing layout

D-4 Materials

High strength carbon-epoxy prepreg AS4/5301-6 is used for the design of entire wing box, except for the wing root joint and main landing gear support beam and attachment, where Ti-6Al-4V is applied.

D-5 Manufacturing Consideration

The manufacturing of the structure must be kept in mind in order to ensure the final design will be produced properly and cost effectively. Manufacturing process and procedure are the controlling elements of the cost of a composite component. Therefore, it is mandatory that they should be an integral part of the design process.

As far as Flying Crane is concerned, the manufacturing process is as follows:

- A tape laying machine is to be used to make the layup of the skin, and then cure the skin in an autoclave;
- Assemble the upper and lower skin panels by bounding the stringers onto

the cured skin using an adhesive, then co-curing the stringers to the skin;

- Co-cure the spar webs, spar stiffeners and spar caps to make one-piece spar;
- Co-cure the rib webs, rib stiffeners and rib caps to make one-piece rib;
- Upper skin panel, lower skin panel, spars and ribs are assembled together by a co-bonded process by putting the entire semi wing into an autoclave and curing.

D-6 Environmental Effects Consideration

Some environmental effects on composite materials, such as humidity, lighting strike, hail and foreign objects impact damage, have been taken into consideration during the design.

D-6.1 Lighting Strike Protection

Aircraft protruding tips, leading edges, and trailing edge are the exterior line or surfaces most likely to be primary lighting strike zones. Exposure of an unprotected carbon laminate to direct lighting strike can result in severe laminate damage. The lighting protection system for advanced composite applications should satisfy the following requirements:

- The system design provide for the prevention of electrical arcing when dissipating high-impulse, short duration and high-current electrical energy.
- A conductive surface-to-metallic-substructure joint is required to provide for electrical grounding.
- The lighting protection conductive surface design should provide adequate shielding from electromagnetic interference.
- The surface protective material should be repairable and require a minimum of maintenance.
- Wings for carrying fuel will either have to use bladders or other means to prevent metal fastener arcing inside the wing.

In Flying Crane inner wing design, aluminium wire mesh is chosen to provide lighting protection. It has the following advantages:

- Minimum shape constraint
- Lightest weight system
- Repairable
- Low maintenance
- Lowest cost system, because mesh is co-cured with laminate.

D-6.2 Moisture Effects

Composite materials are sensitive to moisture in service environment exposure. The epoxy resin systems absorb moisture from the surrounding atmosphere, which causes the matrix to swell. Edge sealing and application of face protection will minimize moisture effects.

D-6.3 Foreign Object Impact

Impact damage in composite is of great importance because of the tendency towards delamination, even when the impact has low energy and does not appear to cause any damage. In Flying Crane inner wing detail design, the following precautions have been taken:

- Whenever possible, maintain a homogeneous stacking sequence and avoid grouping of too many plies of the same orientation to minimize edge splitting.
- Use continuous ±45° plies at the exterior surface.
- All laminates should contain a minimum of 10% fibres in the 0, ±45, and 90 directions.

D-7 Component Detail Design

D-7.1 Wing Root Joint Design

Wing root joint is one of the most critical design areas in aircraft structures as it locates at the connection area of wing to fuselage, where the load transfer is complicated. The design requirements of wing root joint are as following:

- This joint should connect the wing and fuselage reliably, and keep the integrity of structure.
- The load transfer path should be direct and not cause stress concentration.
- Apply fatigue and damage tolerance design.

Due to light weight and reliability, the spliced plate configuration is chosen for the wing root joint of Flying Crane. As the attachment of the wing root joint is very critical, a mature technology which leads to lower risk and higher reliability will be the first choice. Therefore, the method of mechanical fastening has been chosen for the root joint attachment. The joint is shown in Figure D-3. Detailed sizing process and results can be seen in GDP report.

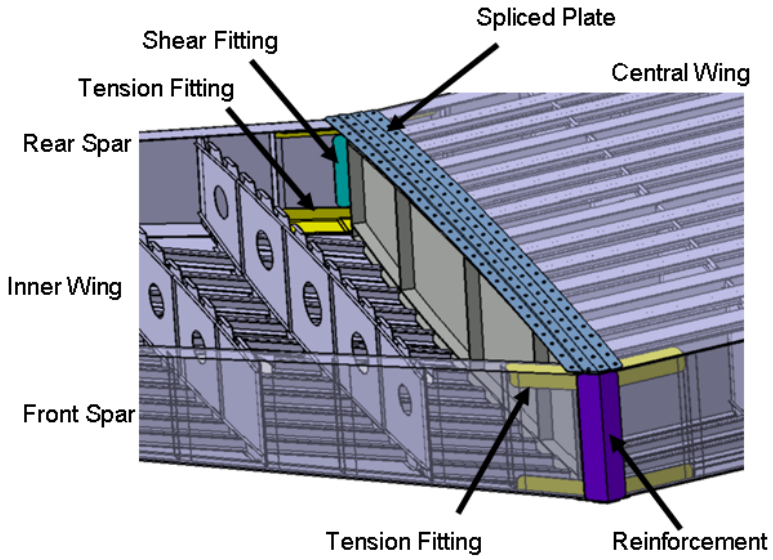

Figure D-3 Wing root joint (skin hidden)

D-7.2 MLG Beam and Attachment Design

Flying Crane's main landing gear is mounted between the rear spar of inner wing and the main landing gear support beam at the pivot points, which will undertake the majority of vertical forces and drag.

In preliminary design, support beam configuration is selected as the layup of main landing gear attachment. The author continued this concept and detailed the design. The final structure is shown in Figure D-4. The MLG support beam is manufactured by forging, and the material is Ti-6Al-4V.

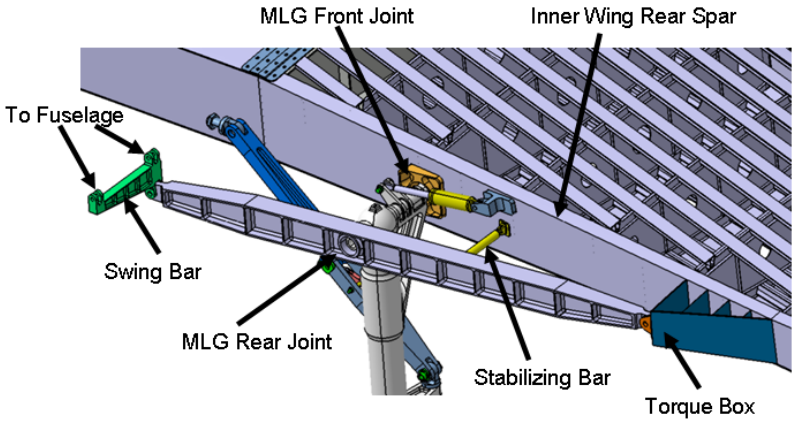

Figure D-4 MLG attachment

On one end of the support beam, a small section of torque box is constructed between rib 6 and rib 7 at the rear of inner wing. This area is not only for attaching the joint of main landing gear beam, but also for the pylon rear joint and inner flap track attachment. On the other end of the support beam, a swing bar is introduced to link the support beam and fuselage. The function of the swing bar is to release the freedom of Y-direction of the support beam end, which is beneficial to the fatigue of support beam.

The front joint of main landing gear strut is at the rear spar of inner wing, where a fitting is placed. The rear joint of main landing gear strut is mounted in the middle of the support beam, and it is assembled into the beam by the supporting of a ball bearing. The reason of using ball bearing is that the characteristic of self aligning makes the assembly much easier, so that the axial lines of the rear spar fitting and support beam hole don’t need to coincide exactly.

Also a short bar, called stabilizing bar, is included in the space between the inner wing rear spar and MLG beam to enhance stability of the MLG support beam.

According to the load provided by the landing gear designer, FE analysis has been carried out to check the stress in the MLG support beam. The load is summarized below.

Table D-4 MLG maximum loading (ultimate load)

	X (KN)	Y (KN)	Z (KN)
MLG Front Joint	-221.7	108.54	843.16
MLG Rear Joint	0	-3.08	-1013.37

The FE analysis is performed by using CATIA. The results can be seen in Figure D-5 and D-6. The maximum Von Misses stress is 901 MPa under ultimate load, and the maximum displacement is 73.4 mm under limit load.

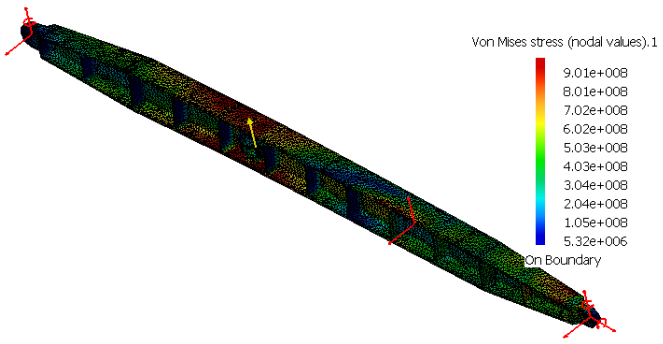

Figure D-5 MLG beam stress (ultimate load)

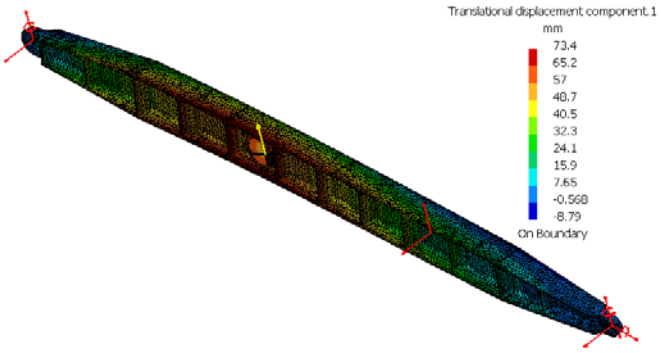

Figure D-6 Displacement of MLG beam (limit Load)

A detailed stress analysis of the MLG support beam male lug, bush and bolt has been carried out, which is presented in GDP report.

D-7.3 Cut-out Design

Cut-outs are essential in airframe structures due to the following reasons:

- Lightening holes in webs are frequently used to save structural weight in cases of minimum gage thickness requirements.
- Passages for wires, cables, tubes, control linkages, hydraulic lines etc.
- Accessibility for assembly and maintenance.

The inner wing lower cover includes 7 inspection access holes, and there are lightening holes in each rib except for the root rib and Rib 8, which are used as the end ribs of tank. The cut-out design is shown in Figure D-7.

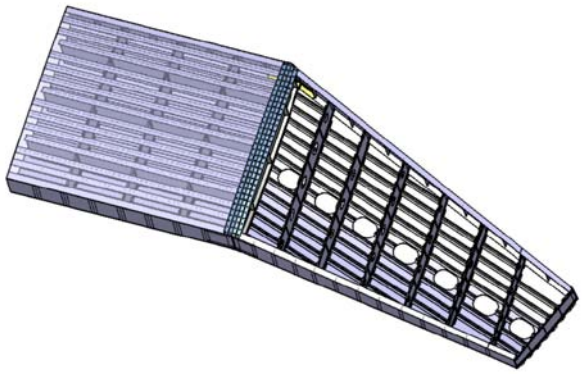

Figure D-7 Inner wing inspection access holes

The holes are located along the same line so that only one stringer is broken. The panel size is 450mm×300mm for a man's head and both arms. Non-stressed panels are used. O-section rubber and dome nuts are selected for the sealing.

D-8 FE Analysis

A semi wing box FE model is built to perform static strength and stiffness analysis.

D-8.1 Element and Coordinate

All the stringers are simplified using ROD elements, which will only transfer axial load; Spar flanges, rib flanges, stiffeners are modelled in BEAM elements, which can carry both axial load and bending moment; Skins, spar webs and rib webs are treated as SHELL elements, which will take the combination of bending flexure and membrane action. CQUAD4 elements are used to build shell meshes except for some edge areas and kink areas, which are meshed by CTRIA3. An aspect ratio is kept below 3 when using CQUAD4 elements.

In order to arrange the laminate ply orientations of different component, seven additional coordinate systems are introduced into the model.

Table D-5 Coordinate systems

No.	Zone
Coord0	global
Coord1	local for skin
Coord2	local for front spar web
Coord3	local for inner rear spar web
Coord4	local for outer rear spar web
Coord5	local for inner, tip and central rib web
Coord6	local for outer rib web
Coord7	local for central spar web

D-8.2 Boundary Condition

Due to the reason that the FE model is semi span, the boundary condition of this symmetric model should be able to represent the wing's real attachment and restraint.

The constraints are illustrated in Figure D-8. All the nodes on the symmetry plane are constrained in y-axial displacement and x-axial rotation. Two nodes, one on front spar and the other on rear spar at the wing to fuselage attachment position are constrained in x, y and z axial displacements.

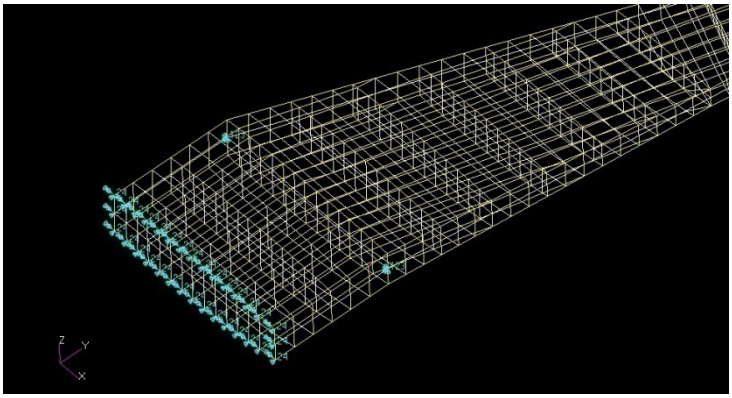

Figure D-8 FE model constraints

16 critical load cases are multiplied by 1.5 to obtain the ultimate load, and then the ultimate load at different wing station is applied on 40% cord position of corresponding rib. RBE3 elements are employed to distribute the load to the nodes around the rib. Figure D-9 shows the use of RBE3 elements for load distribution.

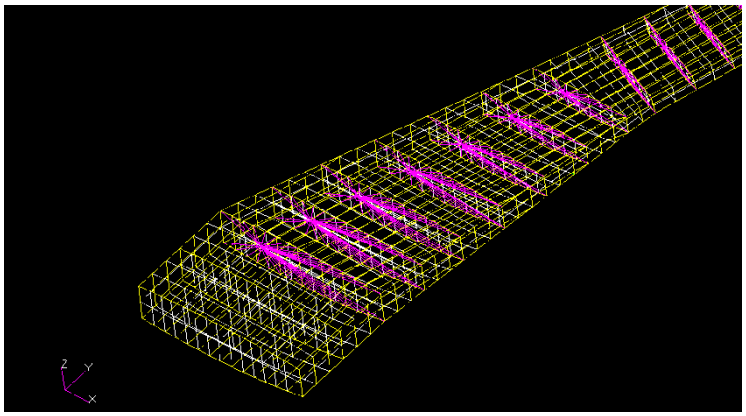

Figure D-9 Load distribution by RBE3

D-9 Fatigue and Damage Tolerance Analysis

Damage tolerance consideration for aircrafts is defined as the ability of structure to tolerate a reasonable level of damage or defects that might be encountered during manufacture or in service. The Flying Crane airframe design life is 90,000 flight hours (30 calendar years).

Metal fatigue typically occurs by mechanism of crack initiation and propagation, but crack propagation is not an issue for composite materials which are more sensitive to impact damage.

D-9.1 Metal Crack Propagation

The Titanium plate at the wing root joint is selected for the crack propagation analysis. The fatigue spectrum is provided by the spectrum calculation group, and the life estimation is analyzed by using “AFGROW” program which calculates crack growth life by the method of linear elastic fracture mechanism. A scatter factor of 4 is chosen to allow loading uncertainties and scatter in results. The crack length growth is obtained and shown in Figure D-10. More details about the calculation process are presented in GDP report.

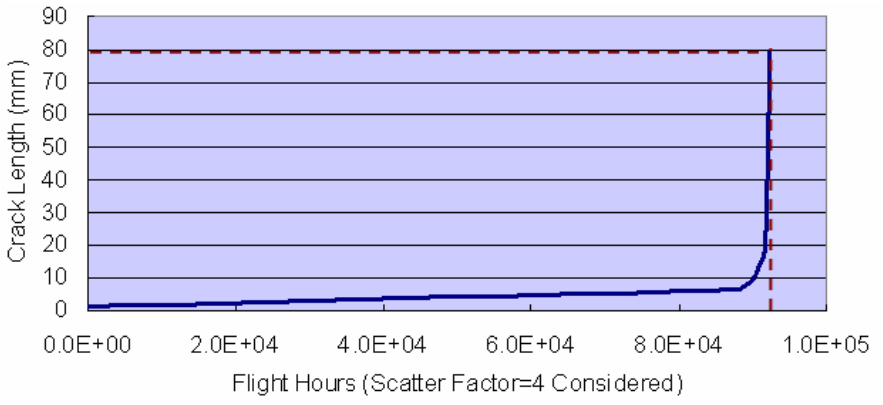

Figure D-10 Crack growth

The AFGROW calculation shows that the theoretic life of the plate (scatter factor =4 considered) is 92248 hours, which satisfies the Flying Crane’s design requirement of 90,000 flight hours.

D-9.2 Composite Impact Damage

Damage sources for composite structures can be related to manufacturing, assembly, and in-service use. Of these sources of damage, in-service impact is considered to be the most severe loading condition. In order to improve the ability of the structure to tolerate damage or defects, as for the composite

structure, the laminate strain must be restrained to a reasonable level. In this thesis, the maximum laminate design strain is 3500 micro-strains.

D-10 Mass and CG

A detailed inner wing 3D CATIA model is built according to the sizing and analysis result, the mass and CG of each component is obtained from the model. The total inner wing box mass is 3113 kg, which consists of the mass of central wing box, inner wing box (both half), wing root attachment (both half), MLG support beam and attachment (both half). The mass of standard fasteners, paint and system equipments are not included.

Table D-6 Mass and CG

Component Name	Mass （kg）	CG(X) （mm）	CG(Y) （mm）	CG(Z) （mm）
Central wing	685.05	15574.714	-8.748	-1055.488
Inner wing (R)	765.511	16498.582	4396.037	-771.316
Inner wing (L)	765.511	16498.582	-4396.037	-771.316
Wing root (R)	315.912	15559.256	1934.591	-1052.072
Wing root (L)	315.912	15559.256	-1934.591	-1052.072
MLG beam (R)	132.558	18203.772	3818.112	-794.939
MLG beam (L)	132.558	18203.772	-3818.112	-794.939
Total	3113.012			

The mass of the central and inner wing box is 3113.012kg. Together with outer wing box, flaps and ailerons, the total mass of wing component is 4689kg, which is lighter than the design target of 5905 kg.

D-11 Airworthiness Compliance

Flying Crane is designed to satisfy the requirements of CCAR 25. Based on the airworthiness requirement matrix for inner wing design, which was provided by the airworthiness control designer, the author followed and satisfied all the requirement items in the matrix. More details about airworthiness compliance are presented in GDP report.

D-12 Conclusion

CCAR-25 has been used as the airworthiness standard of the central and inner wing box detail design. The primary design target is to achieve the minimum structure weight. At the same time, manufacturability, maintainability and cost are taken into consideration as well.

Based on loading review and structure refine from preliminary design work, 16 load cases are selected as critical load input for detail design, and a semi-wing box FE model is built to carry out static analysis. According to preliminary structure layout, the design of central and inner wing box is detailed in this stage, for example, wing root joint design, main landing gear support beam and attachment design, lightening hole and inspection hole cut-out design. Detailed local stress analysis, buckling analysis and fatigue analysis are involved to make sure that the design is able to meet the CCAR 25 requirement. According to the analysis result, the inner wing satisfies the design requirement of strength, stiffness, stability, fatigue, and damage tolerance.

The application of composite materials provides a significant weight saving to the design.